Nagra
Nationale
Genossenschaft
für die Lagerung
radioaktiver Abfälle

Cédra
Société coopérative
nationale
pour l'entreposage
de déchets radioactifs

Cisra
Società cooperativa
nazionale
per l'immagazzinamento
di scorie radioattive

TECHNICAL REPORT 85-33

Nuclide Release from the Near-Field of a L/ILW Repository

Lars-Gunnar Karlsson
Lars Olof Höglund
Karin Pers

December 1986

KEMAKTA Konsult AB, Stockholm, Sweden

Parkstrasse 23 5401 Baden/Schweiz Telephon 056/20 55 11

Nagra
Nationale
Genossenschaft
für die Lagerung
radioaktiver Abfälle

Cédra
Société coopérative
nationale
pour l'entreposage
de déchets radioactifs

Cisra
Società cooperativa
nazionale
per l'immagazzinamento
di scorie radioattive

TECHNICAL REPORT 85-33

Nuclide Release from the Near-Field of a L/ILW Repository

Lars-Gunnar Karlsson
Lars Olof Höglund
Karin Pers

December 1986

KEMAKTA Konsult AB, Stockholm, Sweden

Parkstrasse 23 5401 Baden/Schweiz Telephon 056/20 55 11

Der vorliegende Bericht wurde im Auftrag der Nagra erstellt. Die Autoren haben ihre eigenen Ansichten und Schlussfolgerungen dargestellt. Diese müssen nicht unbedingt mit denjenigen der Nagra übereinstimmen.

Le présent rapport a été préparé sur demande de la Cédra. Les opinions et conclusions présentées sont celles des auteurs et ne correspondent pas nécessairement à celles de la Cédra.

This report was prepared as an account of work sponsored by Nagra. The viewpoints presented and conclusions reached are those of the author(s) and do not necessarily represent those of Nagra.

Summary

For Project Gewähr 1985, the release of nuclides from a repository for low- and intermediate-level radioactive waste is calculated. The calculations are made for a reference design repository located in the marl host rock at the Oberbauen Stock reference site. The results are limited to the release of the nuclides from the waste through the engineered barriers into the surrounding host rock and will, therefore, constitute a source term for the far-field and biosphere calculations.

The most probable nuclide transport mechanism is diffusion and releases are thus influenced by the nuclide diffusivities in the barriers, nuclide sorption and nuclide solubility limits. Degradation of the engineered concrete barriers is taken into account. The effects of convective flow through the barriers are described elsewhere.

A near-field release model is presented. It consists of a set of computer programs suited to handle different repository designs, solubility limitations and the different waste categories.

The release calculations were made for a base case in which best estimates of the parameters were used. Sensitivity to the choice of the most important parameters was tested by parameter variations. The numerical models used were checked by comparative calculations with different codes and similar data.

The results of the base case calculations show that near-field barriers will cause both a delay of the release to the far-field and a reduced rate of release.

The sorbed nuclides, comprising the actinides and some activation and fission products, will be delayed by 10'000 years and have a maximum release rate of less than 10^{-3} Ci/a each. The non-sorbed nuclides are delayed by only about 100 years and the maximum release rate is less than 10^{-2} Ci per year and nuclide.

The parameter variations and the design model tests gave only limited deviations from the base case results.

ZUSAMMENFASSUNG

Die Radionuklidfreisetzung aus einem Endlager für schwach- und mittelaktive Abfälle wird für Projekt Gewähr 1985 berechnet. Die Berechnungen werden für ein Referenzendlager im Wirtgestein Valanginienmergel am Sondierstandort Oberbauenstock durchgeführt. Die Ergebnisse beschränken sich auf die Abfallnuklid-freisetzung durch die technischen Barrieren ins umgebende Wirtgestein und bilden damit einen Quell-term für die Fernfeld- und Biosphären-Berechnungen.

Die Diffusion ist der wahrscheinlichste Transportmechanismus für die Radionuklide, der somit durch die Nukliddiffusivitäten in den Barrieren, die Nuklidsorption und die Löslichkeitsgrenzen der verschiedenen Nuklide beeinflusst wird. Der allmähliche Zerfall der technischen Betonbarrieren wird berücksichtigt. Die Einwirkungen des konvektiven Flusses durch die Barrieren werden nicht behandelt.

Ein Modell für die Nahfeldfreisetzung wird präsentiert. Es besteht aus einem Satz von Computer-programmen, die verschiedene Endlagerkonzepte, Löslichkeitsbegrenzungen und verschiedene Abfall-kategorien zu berücksichtigen vermögen.

Die Freisetzungsberechnungen wurden für einen Basis-fall durchgeführt, abgestützt auf die bestmöglichen Schätzungen der Parameter. Die Sensitivität der Wahl der wichtigsten Parameter wurde mit Parametervaria-tionen getestet. Die numerischen Modelle wurden durch vergleichende Berechnungen mit verschiedenen Codes und ähnlichen Daten geprüft.

Die Ergebnisse der Basisfall-Berechnungen zeigen, dass die Nahfeldbarrieren sowohl eine Verzögerung der Freisetzung ins Fernfeld als auch eine Reduktion der Freisetzungsraten verursachen.

Die sorbierenden Nuklide, d.h. die Actinide und manche Aktivierungs- und Spaltprodukte, werden um 10,000 Jahre verzögert und haben je eine maximale Freisetzungsrate von weniger als 10^{-3} Ci/a. Die nichtsorbierenden Nuklide werden nur um ca. 100 Jahre verzögert, die maximale Freisetzungsrate beträgt weniger als 10^{-2} Ci pro Jahr und Nuklid.

Die Parametervariationen und die Modelltests ergaben nur kleine Abweichungen von den Basisfall-Ergebnissen.

RESUME

Le relâchement de radionucléides hors d'un dépôt final pour déchets de faible et moyenne radioactivité est calculé pour le projet Garantie 1985. Ces calculs sont réalisés pour un dépôt final-référence aménagé dans les marnes valanginiennes, roche d'accueil du site de sondage de l'Oberbauenstock. Les résultats se limitent au relâchement des nucléides à partir du déchet à travers les barrières ouvragées, jusque dans la roche d'accueil environnante, et constituent ainsi un terme source pour les calculs du champ éloigné du dépôt et de la biosphère.

La diffusion est le mécanisme de transport le plus vraisemblable pour les nucléides; les relâchements sont donc influencés par les diffusivités des nucléides dans les barrières, la sorption des nucléides et les limites de solubilité des nucléides. On tient compte de la dégradation progressive des barrières ouvragées en béton. Les effets du flux convectif à travers les barrières ne sont pas abordés.

Un modèle est présenté pour le relâchement dans le champ proche du dépôt. Il consiste en un ensemble de programmes d'ordinateur susceptibles de traiter différents concepts de dépôt final, différentes limites de solubilité et les diverses catégories de déchets.

Les calculs de relâchement ont été réalisés pour un cas de référence se basant sur les meilleures estimations possibles des paramètres. La sensibilité des résultats au choix des paramètres les plus importants a été testée avec des variations de paramètre. Les modèles numériques utilisés ont été contrôlés à l'aide de calculs comparatifs avec différents codes et des données similaires.

Les résultats des calculs du cas de référence montrent que les barrières du champ proche du dépôt entraînent tant un retard du relâchement dans le champ éloigné du dépôt qu'une réduction des taux de relâchement.

Les nucléides sorbants, c.-à-d. les actinides et certains produits d'activation et de fission, sont retardés d'environ 10'000 ans et ont chacun un taux de relâchement maximum inférieur à 10^{-3} Ci/an. Les nucléides non sorbants ne sont retardés que d'environ 100 ans et les taux de relâchement maximum sont de moins de 10^{-2} Ci par an et nucléide.

Les variations de paramètres et les tests de modèles n'ont donné que des déviations limitées par rapport aux résultats du cas de base.

LIST OF CONTENTS

LIST OF TABLES

LIST OF FIGURES

List of Figures continued

List of Figures continued

0. INTRODUCTION

One section of Project Gewähr deals with the final disposal of low- and intermediate level radioactive waste. Oberbauen Stock is selected as a reference site and a reference design consisting of almost 5 km of tunnels located in marl is defined for the repository.

This report is focused on the release and transport of the radionuclides from the waste drums and containers through the engineered barriers in the repository into the surrounding host rock. The results serve as input data for the far-field transport calculations which are presented elsewhere.

The release calculations are based on the reference design of the repository and on the extensive waste inventory worked out for Project Gewähr. Barrier property data are, to a large extent, obtained from literature studies.

The main nuclide transport mechanism is diffusion. The diffusivities in the different concrete barriers are therefore important. Also, the extent to which these diffusivities change as a consequence of degradation of the concrete is significant. Also relevant is the retardation of nuclides caused by sorption or by limited solubility. Radionuclide transport through the technical barriers by way of convection is described in /NGB 85-08/.

The repository design and its surrounding environment are summarized in Chapter 1. The waste inventory and a 'short list' of nuclides are discussed in Chapter 2. The third Chapter deals with the input data to be used - diffusivities, distribution coefficients for describing sorption and solubility limits.

The phenomenology and the computer models used are described in Chapter 4. In Chapter 5, the results are presented for a base case and a number of parameter and model variations. Finally, the results are discussed in Chapter 6.

Most of the results were used in /NGB 85-08/. This report is, however, more detailed and contains some improvements to be used in future development work. One is the modelling of barrier degradation, another the effect of solubility limitation.

1. DESCRIPTION OF THE REPOSITORY

1.1 General

The type B repository at Oberbauen Stock, used as a reference site in "Project Gewähr", is located in a Valanginian marl formation. The repository is designed as a system of tunnels where low- and intermediate-level waste will be stored.

Most of the waste is contained in steel drums and solidified with concrete. The drums are placed in containers surrounded by a concrete backfill. The containers are piled in the tunnels and the space between them and the tunnel lining is also backfilled with concrete.

The radionuclides in the waste drums have to pass through all these consecutive barriers to reach the surrounding host rock.

The water chemistry will be characterized by reducing conditions and a high pH which will slowly decrease.

1.2 Repository location and design

The repository is located in a Valanginian marl formation surrounded by limestone layers and shales, as presented in Figure 1-1. Figure 1-2 shows a schematic presentation of the repository and the aecess tunnel in the host rock.

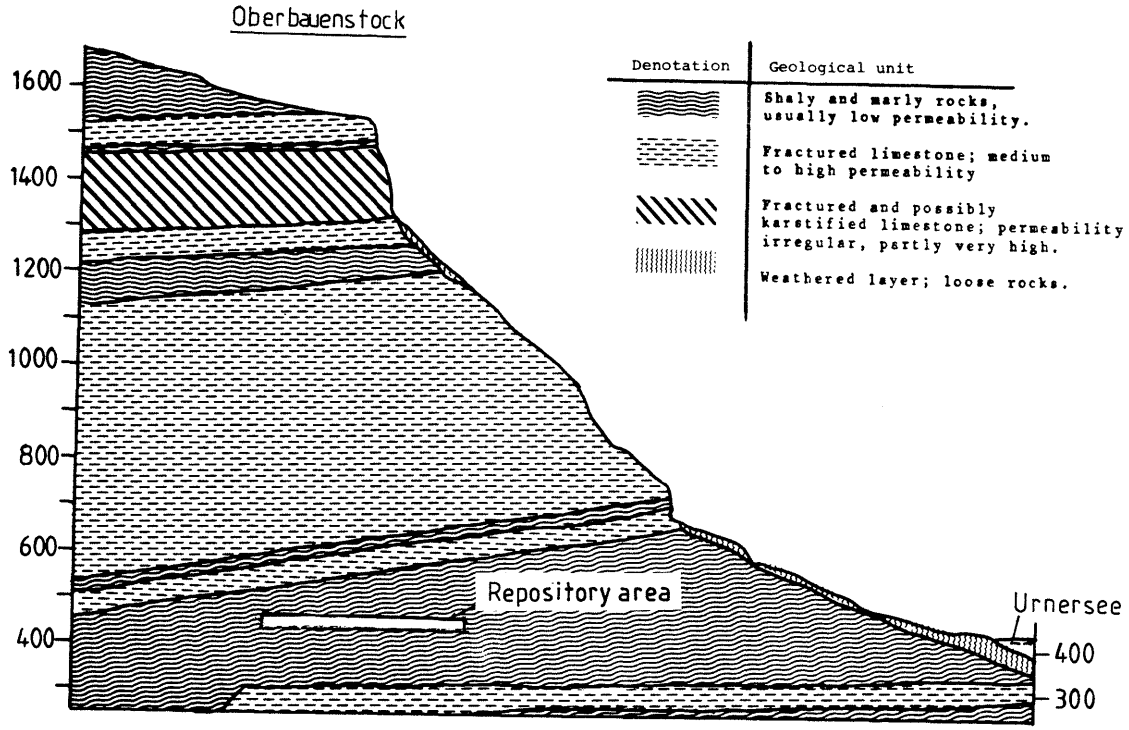

Figure 1-1 Cross-section of the repository area showing the different layers of rock material

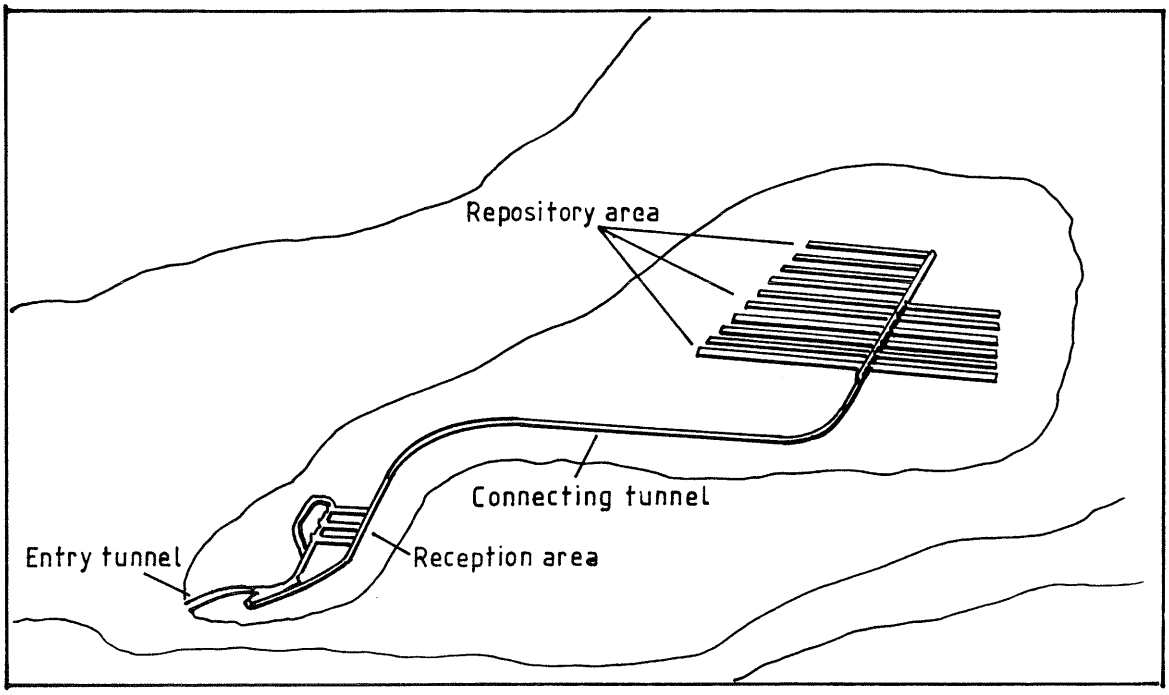

Figure 1-2. Perspective view of the repository

The design of the tunnel with its lining and piles of containers is shown in Figure 1-3. The containers are made of reinforced concrete and contain approximately 40 drums. See also /NGB 85-06/.

Some technical data on the repository are summarized in Table 1-1.

Table 1-1 Some technical data on the repository

Container size	Type I	Type II
length	4.78 m	4.78 m
width	2.18 m	2.18 m
height	2.08 m	1.63 m
Total waste volume	approx.	200,000 m^3
Cross-sectional area of the tunnels		160-180 m^2
Dimensions inside the repository liner	maximum width	11.9 m
	maximum height	12.8 m
Total length of the repository		4,660 m

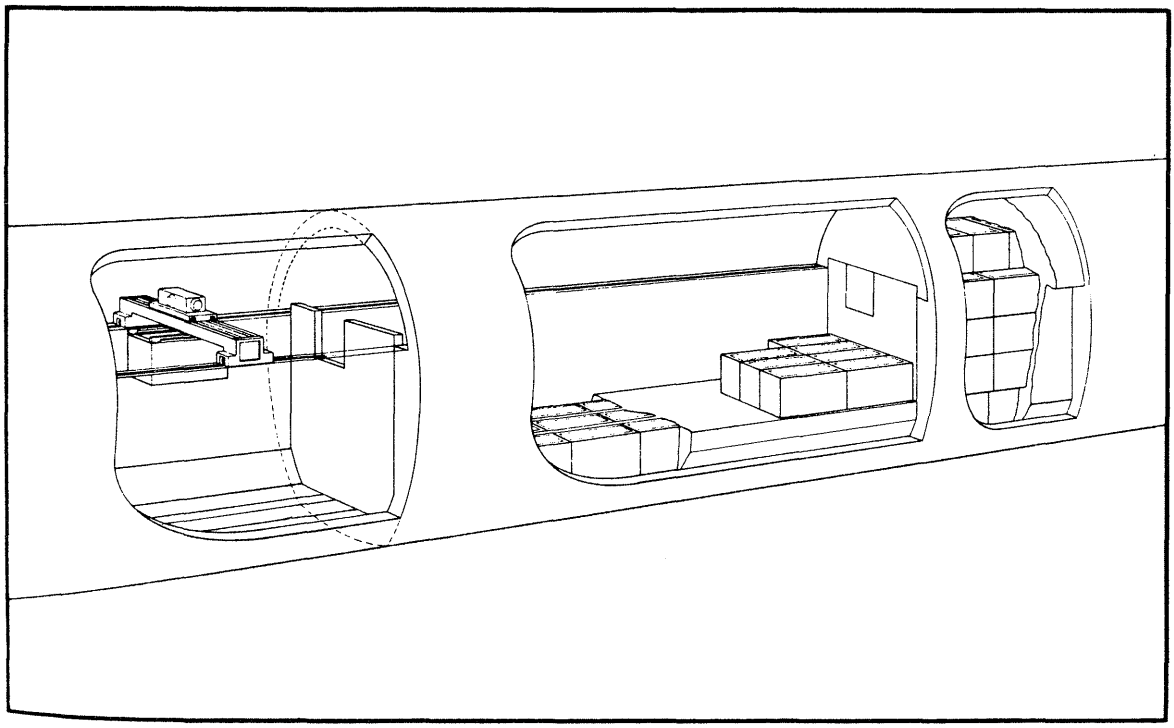

Figure 1-3. The tunnel with piles of containers

1.3 Description of the waste

Most of the waste is contained in 200 litre steel drums. The waste is mixed with concrete and cast into the drums. In some cases, the concrete is replaced by bitumen or polystyrene plastic. The reinforced concrete containers used as overpack for the drums are also used directly for bulky waste from the decommissioning of power plants, with a backfill of concrete.

For information on waste quantities, dimensions, chemical composition and activity content, reference is made to Chapter 2.

1.4 Groundwater chemistry

The analyses from the Oberbauen Stock area are presented in Table 1-2. The presence of H_2S and the $KMnO_4$ consumption indicate that reducing conditions prevail.

Within the repository, the water chemistry is determined by the following circumstances:

- The presence of large quantities of concrete will lead to a pH of 13 in the beginning, which will gradually decrease to 10-11.

- The presence of oxygen-consuming compounds such as corroding metals and cellulose and the absence of oxygen in the surrounding groundwater will lead to anaerobic or reducing conditions.

Table 1-2 Groundwater analyses from the Oberbauen Stock area

	Los Huttegg access tunnel 70	Los Huttegg access tunnel 70 Tm 190 average value	Los Huttegg parallel tunnel 73 Tm 275	Los Huttegg ventilation tunnel 72 Tm 370	Seeröhre 125.873.80 Central Huttegg 16 G 29 Seezentrale Sud, drilling	Seeröhre km 126.262 tunnel 77 Tm 388.5 pilot drilling	Seeröhre km 126.262 tunnel 77 Tm 388.5 excavation front
Date	8.10.71	14.12.71			10.12.73	23.10.73	19.10.73
Temperature(^{o}C)							
pH-value	8.93	9.3	8.7	9.1	7.6	8.25	8.5
electricalconductivity at 20^{o}C (μScm^{-1})	1120		3350	6100	46000	3580	3100
Degree of hardness(French H^{o}):							
Carbonate			3.2	7.4	24.3	2.8	
No carbonate			0	0	359.1	0	
Total	0.75	0.7	3.2	7.4	383.4	2.8	2.2
Concentration(mg/l):							
Sulphate SO_4	trace	5	382	225	101	47	1.8
Chloride Cl	7.6	36	145	1660	20100	174	203
Nitrate NO_3		0					
Nitrite NO_2	0.02	0.02					
Ammonium NH_4	1.0	5.0			15		
Sulphide S		21	92	0		84	85
H_2S		pos.					
$KMnO_4$-consumption (mg/l):	72.5	112					
Alkalinity (mval/l)							
Phenolphthalein p		2.0	1.1	6.8			1.2
Methylorange m		13.2	28.0	36.8		38.0	33.1
Control of:							
Iron tot. Fe^{2+}							
Sodium Na		pos.				strong pos.	strong pos
Potassium		trace				trace	trace
Oxygen							
Calculated (mg/l):							
Sodium bicarbonate $NaHCO_3$		743	2110	1820		3145	2542
Sodium carbonate Na_2CO_3		212	117	720			127
Calcium carbonate Ca_2CO_3		7					22
Sodium sulphate Na_2SO_4			563	333		69	27

2. NUCLIDE CONTENT AND WASTE CHARACTERISTICS

2.1 General

A very extensive waste inventory has been developed /NGB 85-02/ and is used as the basis for this report. However, only those characteristics and contents of direct interest for nuclide release are used here.

The waste categories are described giving quantities, containers, matrix materials used and chemical composition.

The inventory comprises 87 nuclides, many of which are of no significance to the safety analysis. Of the 87 nuclides, a short list of 38 was prepared. The selection was made with the aid of a simplified program for calculating the discharge to the biosphere.

2.2 Waste materials

The waste foreseen for the type B repository can be divided into four main groups with reference to origin:

OPERATIONAL WASTE
REPROCESSING WASTE
DECOMMISSIONING WASTE
MIF-WASTE (RESEARCH, MEDICINE AND INDUSTRY)

A condensed description of the waste from a chemical and physical point of view is given in Table 2-1. In this Table, the waste has been further divided into sub-categories. The figures given in the Table are average values derived from about 200 different waste types.

Steel, ion-exchange resins and salt concentrates constitute the largest amounts of waste materials in the repository. The steel is mainly from decommissioning of power stations but comes also from reprocessing of spent reactor fuel. Ion-exchange resins originate almost exclusively from cleaning of reactor water during operation of power stations. Salt concentrates originate from decontamination during decommissioning work and precipitates from reprocessing of fuel. The activated concrete is mainly from decommissioning of the bioshield around the reactor tank.

Table 2-1 General physical and chemical description of the waste

Waste category	Waste container			Quantity	Conditioning material kg/cont.	Specification of waste (kg/waste container)								
	Type	Void m^3	Inner volume m^3			Steel	Zn/Al	Salt conc.	Ion exch. resins	Ashes	Cellu-lose	Con-crete	Plastic	Other solids
OPERATIONAL														
Ion exch. resins	steel drum	0-0.01	0.16-0.20	161 931	concrete 210-280				60-80					
	"-	0	0.05	4 217	plastic 20				40					
	"-	0-0.01	0.20	22	bitumen 70-100				20-30					
Concentrates and sludges	steel drum	0	0.20	2 610	concrete 380			20						
	"-	0	0.20	2 748	bitumen 120			90-100						
Solids	steel drum	0-0.01	0.20	36 725	concrete 150-320	10-200							0-20	0-100
Ashes	steel drum	0.005	0.15	2 640	concrete 200					70				
REPROCESSING														
Ion exch. resins	concrete container	0.02	0.4	786	concrete 550				90					
Concentrates and sludges	steel drum	0.03	0.2	19 650	bitumen 160			100						
Solids	concrete container	0	0.2-0.4	52 662	concrete 0-700	400-600	10-15				100	10-15		
DECOMMISIONING														
Activated steel	concrete container	0	14.6	2 921	concrete 26 000-35 000	1000-20000	0-500							
Activated concrete	concrete container	0	14.6	527	concrete 17 000-19 000	0-1700						4 000-23 000		
Concentrates	concrete container	0	14.6	583	concrete 15 000			15 000						
Solids	concrete container	0	14.6	442	concrete 13 000-23 000	0-4500				0-1800			4 000-10 000	3 800-7 000
MIF-WASTE	steel drum	0.005	0.20	35 000	concrete 200									100

Detailed information regarding the physical and chemical form of the waste is required because of the different mechanisms for the release of the nuclides from the solid phase into the porewater. This subject is treated in more detail in Section 4.2.

2.3 Matrix materials

Concrete is the predominant matrix material used for immobilisation of low- and intermediate-level radioactive waste. Besides concrete, bitumen and polystyrene are also used for immobilisation of some waste.

Concrete is characterized by its mineral constituents, giving a high pH, and its porous structure with narrow tortuous pores. The high pH is an important parameter when estimating the chemical behaviour of, for example, the actinide elements. The porous structure, on the other hand, is of prime interest when estimating the release rate of radionuclides by diffusion.

The long-term properties of bitumen and polystyren as immobilization materials are for this study, assumed to be comparable to those of concrete and, since the quantities are small, all waste has been treated as being immobilized in concrete.

2.4 Selected nuclides

For the calculations presented in this report, a selection of the most important and hazardous nuclides was made. The selection comprises nuclides which can be expected to reach the biosphere and result in exposure to man.

Typical for the selected nuclides are long half-lives (several thousands of years), a low tendency to be sorbed (low K_d-values) and high toxicity.

The nuclide selection was performed using a mathematical model. Equations 2-1 to 2-5 describe the maximum possible release of nuclides to the biosphere, assuming a constant supply of the nuclides in the repository. The model, which is described in /1/, accounts for radioactive decay of the nuclide, the chemical retention factor, flow rate of water, dispersion and travel distance and has also been complemented with a toxicity index. The toxicity index was derived from ICRP recommendations /2/ for dose conversion factors.

$$TOX = N_o \cdot F \cdot 1/10 \qquad \text{(mrem)} \qquad (2\text{-}1)$$

where:

TOX = toxicity index for the nuclide (number of 10 mrem doses)

N_o = activity of the nuclide (C_i)

F = dose conversion factor ($mrem/C_i$)

$$\frac{C}{C_o} = \exp\left(L\left(\frac{Pe}{2L}\right) - \left(\left(\frac{Pe}{2L}\right)^2 + \frac{\Psi}{D_L}\right)^{1/2}\right) \qquad (2\text{-}2)$$

and

$$\Psi = \lambda + \frac{\lambda D_e R}{b} \qquad (2\text{-}3)$$

$$\lambda = \frac{\ln 2}{T_{1/2}} \qquad (2\text{-}4)$$

where:

C = concentration of the nuclide when released into the biosphere (kg/m^3)

C_o = concentration of the nuclide in the repository (kg/m^3)

L = travel distance,100m (m)

P_e = uL/D_L Peclet number ,1-100

u = flow velocity, implicit in Pe (m/a)

D_L = dispersion coefficient ,1-100 (m^2/a)

D_e = effective diffusivity in host rock, $1 \cdot 10^{-5}$-$1 \cdot 10^{-3}$ (m^2/a)

R = $K_d \cdot \varepsilon_{rock}$, Retention factor

K_d = distributioncoefficient ,nuclide specific (m^3/kg)

ε_{rock} = rock porosity ,0.03 (m^3/m^3)

b = half fracture width $5 \cdot 10^{-4}$-$5 \cdot 10^{-3}$ (m)

λ = decay constant ,nuclide specific (yr^{-1})

$t_{1/2}$ = half-life of the nuclide (a)

To compare the nuclides, the selection index SI has been calculated:

$$SI = C/C_o \cdot TOX \qquad (2\text{-}5)$$

Several combinations of parameter values have been calculated and all nuclides having a selection index greater than $1 \cdot 10^{-30}$ (which is extremely low) have been selected. The selected nuclides are presented in Table 2-2.

Table 2-2 Initial activity (Ci) of selected nuclides of importance for discharge into the biosphere

Nuclide	Half-life	DECOMMISSIONING WASTE	REPROCESSING WASTE	OPERATIONAL WASTE	MIF-WASTE	Total
C-14	$5.7 \cdot 10^{3}$	$4.5 \cdot 10^{3}$	9.4	$6.1 \cdot 10^{2}$	$2.5 \cdot 10^{2}$	$5.4 \cdot 10^{3}$
Cl-36	$3.0 \cdot 10^{5}$	$9.3 \cdot 10^{-4}$	$2.0 \cdot 10^{-1}$	$1.1 \cdot 10^{-1}$	0	$3.1 \cdot 10^{-1}$
Ni-59	$7.5 \cdot 10^{4}$	$4.5 \cdot 10^{4}$	$6.1 \cdot 10^{1}$	$4.7 \cdot 10^{2}$	$2.6 \cdot 10^{-1}$	$4.6 \cdot 10^{4}$
Ni-63	$1.0 \cdot 10^{2}$	$5.9 \cdot 10^{6}$	$8.0 \cdot 10^{3}$	$4.9 \cdot 10^{4}$	$3.5 \cdot 10^{1}$	$6.0 \cdot 10^{6}$
Se-79	$6.5 \cdot 10^{4}$	0	$4.0 \cdot 10^{-1}$	0	0	$4.0 \cdot 10^{-1}$
Sr-90	$2.9 \cdot 10^{1}$	10.0	$6.3 \cdot 10^{4}$	$1.0 \cdot 10^{2}$	$2.6 \cdot 10^{3}$	$6.6 \cdot 10^{4}$
Zr-93	$1.5 \cdot 10^{6}$	0	$3.2 \cdot 10^{2}$	$4.5 \cdot 10^{2}$	0	$7.7 \cdot 10^{2}$
Tc-99	$2.1 \cdot 10^{5}$	5.5	8.5	8.0	$3.1 \cdot 10^{-1}$	$2.1 \cdot 10^{1}$
Pd-107	$6.5 \cdot 10^{6}$	$3.4 \cdot 10^{-21}$	1.5	$1.9 \cdot 10^{-5}$	0	1.5
Sn-126	$1.0 \cdot 10^{5}$	0	$1.1 \cdot 10^{1}$	$9.4 \cdot 10^{-3}$	0	$1.1 \cdot 10^{1}$
I-129	$1.6 \cdot 10^{7}$	0	$1.0 \cdot 10^{-1}$	$5.6 \cdot 10^{-3}$	$7.7 \cdot 10^{-4}$	$1.1 \cdot 10^{-1}$
Cs-135	$2.3 \cdot 10^{6}$	0	1.2	$5.6 \cdot 10^{-2}$	$1.7 \cdot 10^{-2}$	1.3
Cs-137	$3.0 \cdot 10^{1}$	$10.0 \cdot 10^{1}$	$3.2 \cdot 10^{5}$	$1.9 \cdot 10^{4}$	$4.3 \cdot 10^{3}$	$3.5 \cdot 10^{5}$
Ra-226	$1.6 \cdot 10^{3}$	0	$1.6 \cdot 10^{-6}$	$2.1 \cdot 10^{-14}$	$6.6 \cdot 10^{1}$	$6.6 \cdot 10^{1}$
Ra-228	5.8	0	$2.7 \cdot 10^{-10}$	$6.2 \cdot 10^{-16}$	0	$2.7 \cdot 10^{-10}$
Th-228	1.9	0	$8.0 \cdot 10^{-2}$	$2.8 \cdot 10^{-7}$	0	$8.0 \cdot 10^{-2}$
Th-229	$7.3 \cdot 10^{3}$	0	$1.5 \cdot 10^{-6}$	$2.6 \cdot 10^{-10}$	0	$1.5 \cdot 10^{-6}$
Th-230	$7.7 \cdot 10^{4}$	0	$1.1 \cdot 10^{-3}$	$2.1 \cdot 10^{-9}$	0	$1.1 \cdot 10^{-3}$
Th-232	$1.4 \cdot 10^{10}$	0	$1.1 \cdot 10^{-9}$	$2.1 \cdot 10^{-15}$	0	$1.1 \cdot 10^{-9}$
Pa-231	$3.3 \cdot 10^{4}$	0	$2.7 \cdot 10^{-4}$	$1.1 \cdot 10^{-10}$	0	$2.7 \cdot 10^{-4}$
U-232	$7.2 \cdot 10^{1}$	0	$1.1 \cdot 10^{-1}$	$6.2 \cdot 10^{-7}$	0	$1.1 \cdot 10^{-1}$
U-233	$1.6 \cdot 10^{5}$	0	$3.0 \cdot 10^{-4}$	$1.8 \cdot 10^{-8}$	0	$3.0 \cdot 10^{-4}$
U-234	$2.4 \cdot 10^{5}$	0	$2.0 \cdot 10^{1}$	$2.0 \cdot 10^{-6}$	0	$2.0 \cdot 10^{1}$
U-235	$7.0 \cdot 10^{8}$	0	$3.4 \cdot 10^{-1}$	$4.4 \cdot 10^{-7}$	$2.6 \cdot 10^{-5}$	$3.4 \cdot 10^{-1}$
U-236	$2.3 \cdot 10^{7}$	0	4.3	$1.5 \cdot 10^{-5}$	0	4.3
U-238	$4.5 \cdot 10^{9}$	0	5.1	$1.9 \cdot 10^{-5}$	$3.9 \cdot 10^{-4}$	5.1
Np-237	$2.1 \cdot 10^{6}$	$6.0 \cdot 10^{-4}$	3.4	$2.3 \cdot 10^{-4}$	$8.9 \cdot 10^{-4}$	3.4
Pu-238	$8.8 \cdot 10^{1}$	1.4	$3.7 \cdot 10^{4}$	1.3	$6.0 \cdot 10^{1}$	$3.7 \cdot 10^{4}$
Pu-239	$2.4 \cdot 10^{4}$	$6.0 \cdot 10^{-1}$	$4.7 \cdot 10^{3}$	$3.6 \cdot 10^{-2}$	$1.3 \cdot 10^{1}$	$4.7 \cdot 10^{3}$
Pu-240	$6.5 \cdot 10^{3}$	$8.0 \cdot 10^{-1}$	$5.7 \cdot 10^{3}$	$1.4 \cdot 10^{-1}$	6.2	$5.7 \cdot 10^{3}$
Pu-241	$1.4 \cdot 10^{1}$	$1.4 \cdot 10^{2}$	$2.0 \cdot 10^{6}$	$1.4 \cdot 10^{2}$	$3.2 \cdot 10^{2}$	$2.0 \cdot 10^{6}$
Pu-242	$3.8 \cdot 10^{5}$	$2.6 \cdot 10^{-3}$	$3.0 \cdot 10^{1}$	$5.7 \cdot 10^{-5}$	$2.1 \cdot 10^{-3}$	$3.0 \cdot 10^{1}$
Am-241	$4.3 \cdot 10^{2}$	1.4	$1.1 \cdot 10^{4}$	1.3	$4.9 \cdot 10^{2}$	$1.1 \cdot 10^{4}$
Am-242	$1.5 \cdot 10^{2}$	0	$8.9 \cdot 10^{1}$	$6.7 \cdot 10^{-4}$	0	$8.9 \cdot 10^{1}$
Am-243	$7.4 \cdot 10^{3}$	$1.1 \cdot 10^{-2}$	$1.9 \cdot 10^{2}$	$8.8 \cdot 10^{-2}$	$2.4 \cdot 10^{-2}$	$1.9 \cdot 10^{2}$
Cm-244	$1.8 \cdot 10^{1}$	6.0	$1.6 \cdot 10^{4}$	3.2	1.9	$1.6 \cdot 10^{4}$
Cm-245	$8.5 \cdot 10^{3}$	0	1.3	0	0	1.3
Cm-246	$4.7 \cdot 10^{3}$	0	$2.4 \cdot 10^{-1}$	0	0	$2.4 \cdot 10^{-1}$

3 MATERIAL PROPERTIES

3.1 General

The diffusion-controlled release of nuclides from the repository into the surrounding host rock is influenced by:

- The diffusion resistance, e.g. diffusivity of the near-field barriers
- The sorption of some nuclide species on the solid surfaces in fissures and pores
- The solubility limits for some nuclides

All these effects are related to materials and compounds present in the repository, and their properties.

The initial barrier diffusivities are based on measurements on a concrete of corresponding quality. It is also assumed that the concrete undergoes degradation until its diffusivity is finally fairly close to that of compacted sand.

Sorption has a significant retarding effect on the release of some nuclides. This has been utilized in the calculations for the nuclides which are proved to be sorbed. The distribution coefficients used are, however, in most cases conservatively selected.

In general, all nuclides are assumed to be dissolved in the porewater from the beginning. For a few nuclides, their content in the waste is higher than that which can be dissolved in the available porewater. For these nuclides, a solubility limitation can be taken into account in the calculations.

The possible influence of complexing agents on the mobility of some nuclides has been studied.

3.2 Degradation of barrier materials, selection of diffusivities

The release of radionuclides from the repository depends on the material properties of the concrete barriers. One of the critical parameters is the diffusion coefficient. The diffusion coefficient depends on the porous structure of the concrete and varies for different concretes. Due to chemical interactions with the groundwater, the porous structure of the concrete will gradually change.

The properties of a porous material are often represented in terms of a formation factor:

$$G_F = \varepsilon_p \frac{\delta_d}{\tau^2} = \varepsilon_p G \qquad (3\text{-}1)$$

where:

G_F = formation factor

G = geometric factor

ε_p = porosity of the porous material (m^3/m^3)

δ_d = constrictivity

τ^2 = tortuosity

The physical interpretation of the geometric factor is the difference between diffusion rate in real pores with narrow totuous paths and the diffusion rate in straight cylindrical tubes of the same average diameter as the real pores. The geometric factor can also be expressed in terms of constrictivity and tortuosity. The constrictivity of the pores is a measure of the amount of narrow passages in the pore system of the porous medium. The tortuosity of the pores is a measure of the increased diffusion path length caused by twisting pores.

The porosity affects diffusion by limiting the cross-sectional area available for diffusion.

The transport capacity of the porous material is then given by:

$$D_p = D_w \cdot G \qquad (3\text{-}2)$$

where

D_p = diffusivity in a pore (m^2/s)

D_w = diffusivity in bulk water (m^2/s)

From this, the apparent diffusivity, D_a, can be defined:

$$D_a = \frac{D_p}{R} = \frac{D_e}{\varepsilon_p R} \qquad (3\text{-}3)$$

where

D_a = apparent diffusivity (m^2/s)

R = chemical retention factor (-)

D_e = effective diffusivity (m^2/s)

The apparent diffusivity describes the build-up of the concentration profile in the porous material, while the effective diffusivity describes the local transport rate in the porous material.

Three different types of chemical interaction with groundwater can be distinguished /3/, /4/, /5/:

- Leaching by groundwater
- Ion-exchange reactions
- Formation of new, expanding solid phases.

The leaching by groundwater will proceed in three phases:

- the sodium and potassium hydroxides are leached
- the content of free calcium hydroxide is dissolved
- the major constitutents of the concrete, i.e. the calcium aluminates and calcium silicates, are attacked by the water.

When approximately 20% of the analytical content of calcium oxide has been leached, the concrete can be regarded as completely deteriorated /3/. The leaching of calcium by groundwater has been found to be the most likely mechanism for concrete degradation in the repository studied /NTB 86-15/.

The ion-exchange reactions which can take place are mainly exchange of calcium for magnesium and ammonium ions and are detrimental for the concrete. In the groundwater of Oberbauen, however, the content of magnesium and ammonium ions is low and the influence of ion-exchange reactions was judged to be less important than the effect of leaching.

Among the reactions that lead to the formation of expanding solid phases, the reaction between tricalcium aluminate and sulphate to form ettringite must be mentioned. The formation of ettringite can destroy the concrete by internal cracking within a short time. Use of sulphate-resistant concrete can probably avoid this effect, or at least reduce it.

To account for the chemical degradation of concrete by groundwater, the diffusion coefficients have been increased with time. In the calculations the previously defined geometric factor, G, has been used to represent the expected changes in the pore structure as the interaction with groundwater proceeds. In high quality concrete, a value of 10^{-3} has been assumed for the geometric factor. As a result of leaching, the pH value of the porewater will drop from an initial 13.0-13.5 to 12.0-12.8 during the first phase of leaching as described above. It is reasonable to expect that structural changes, such as recrystallisations and mineralizations, will follow on this reduction in pH. Hence, a new value of 10^{-2} was assumed for the geometric factor after the pH has dropped /NGB 85-07/.

During the second and third phases of leaching, dissolution of solid constituents will change the pore structure and the pH will drop to about 10.0 -10.5. To account for these changes, the geometric factor was set at 10^{-1}, which corresponds to a fully degraded concrete.

In the safety analysis /NGB 85-07, NGB 85-08/, the changes were modelled as occurring stepwise at 500 years and 10,000 years respectively. These times have been selected according to estimations of the duration of the different phases of leaching. In the present report, calculations have also been made using continuously varying values for the geometric factor.

In Figure 3-1 below, the pore diffusivities, D_p, corresponding to the selected values for the geometric factors, assuming stepwise degradation, are presented.

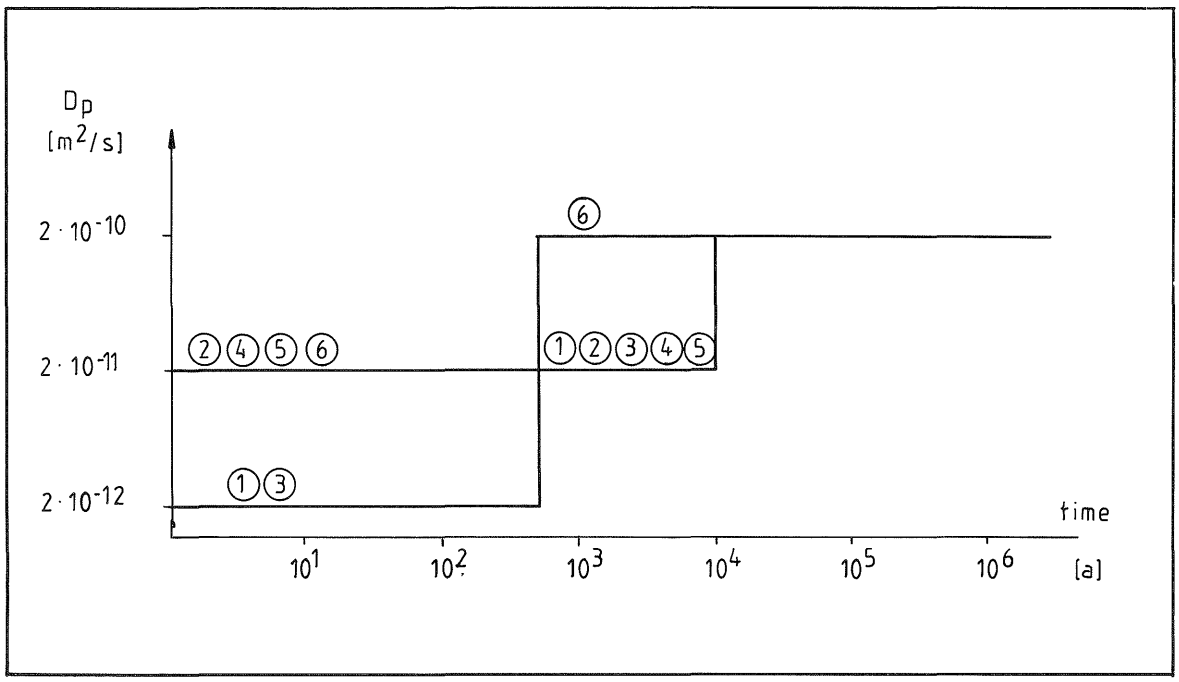

1. Matrix
2. Repository backfill
3. Container wall
4. Container backfill
5. Lining (inner)
6. Lining (outer)

Figure 3-1 Data used. Pore diffusivities used for the base case (N1). Values have been calculated from selected values of the geometric factor G.

3.3 K_d-values in barrier materials

The concrete in the repository is a porous medium with water-filled pores. The chemical condition in the pores is determined by the cement phase i.e. high pH, high ionic strength, high concentrations of Na^+ and K^+, low concentrations of Ca^{2+}, CO_3^{2-}, SO_4^{2-} etc. /NTB 85-21/.

The sorption of a solute, in this case the radionuclides, on a water-exposed solid phase is related to the following processes:

- Electrostatic interaction
- Physical adsorption
- Chemisorption
- Precipitation
- Substitution processes

The total sum of all the contributions from the various sorption processes is expressed as a distribution coefficients (K_d-value).

The distribution coefficient, K_d, is defined as the ratio between the concentration in the solid phase and the concentration in the solution. It is empirically determined and has no specific thermodynamic significance.

Allard /NTB 85-21/ reports ranges of radionuclide sorption data for some important nuclides in low-and intermediate-level waste in concrete/water systems. These K_d-values are given in the literature and are summarized and presented as ranges shown in Figure 3-2.

From these ranges, recommended values were derived (Table 3.1).

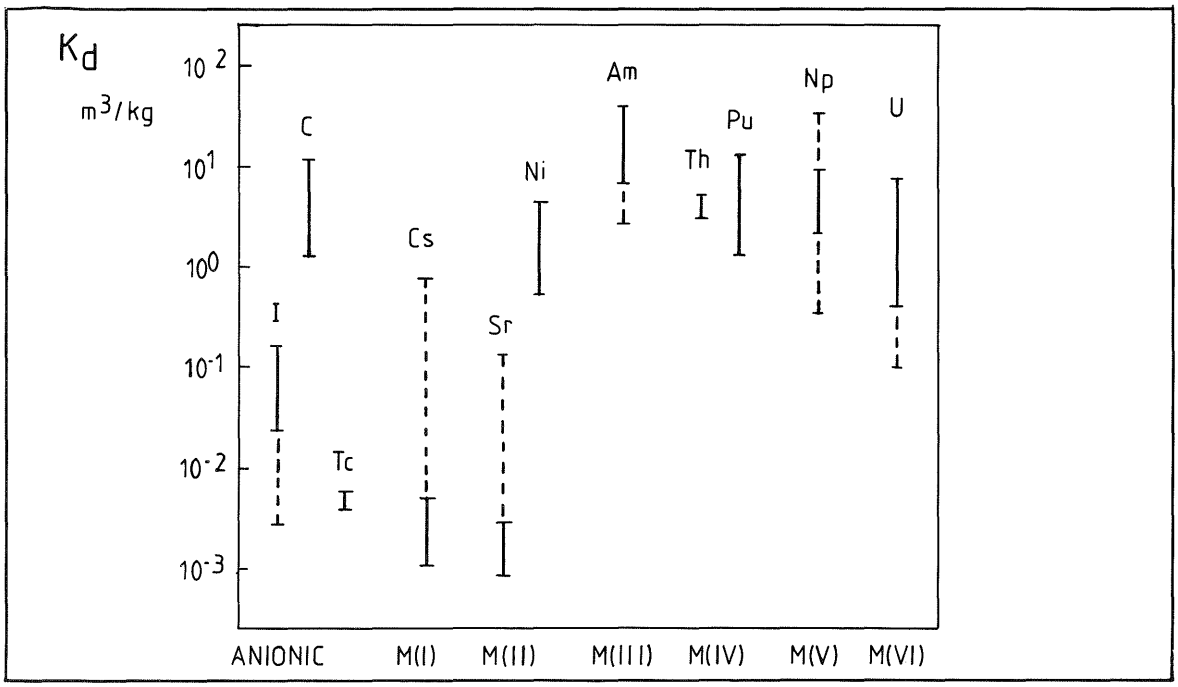

Figure 3-2 Ranges of distribution coefficients (K_d) in concrete systems /NTB 85-21/

Table 3-1 Recommended distribution coefficients (K_d) for transport calculations in a concrete repository system /NTB 85-21/

Element	K_d, m^3/kg	Comment
C	5	Experimental value
Ni	1	Experimental value
Sr	0.002	Experimental value
Zr	1	Tetravalent; 20% of the Th(IV)-value assumed
Tc	0.001	Experimental value
Pd	0.2	Divalent; 20% of the Ni-value assumed
Sn	0.2	Divalent; 20% of the Ni-value assumed
I	0.03	Experimental value
Cs	0.002	Experimental value
Th	5	Experimental value
U	5	Same as for Th assumed
Np	5	Same as for Th assumed
Pu	5	Experimental value
Am	5	Experimental value

The conservatively selected distribution coefficients for the nuclides used in the release calculations are listed in Table 3-2. The principle for selection of these values is that for nuclides with relatively high recommended values for the distribution coefficient, the value 0.1 m^3/kg has been used in the calculations. If a low value has been recommended, or if information is lacking, it has been assumed that there is no sorption and the K_d-value has been set at zero. In the selected values, the effect of complexing agents has been taken into account.

Table 3-2 Data used. Selected K_d-values

The following distribution coefficients have been used for the nuclides in concrete/water in the nuclide release calculations

Nuclide	K_d
C	0.1
Cl*	0
Ni	0
Se*	0
Sr	0
Zr	0.1
Tc	0.1
Pd	0
Sn	0
I	0
Cs	0
Ra*	0.1
Th	0.1
Pa*	0.1
U	0.1
Np	0.1
Pu	0.1
Am	0.1
Cm	0.1

*) Values selected according to conclusions drawn from similar nuclides.

3.4 Solubility limits

3.4.1 Principles

From the list of 38 nuclides (Table 2-2), 11 were selected which were known from earlier release calculations /NGB 85-08/ to contribute significantly to the total release if solubility limitation is not taken into account. These nuclides are:

- The actinides Th, U, Np, Pu and Am
- The fission and activation products Se, Tc, Sn, Ni, Zr and Pd.

For the release calculations in this report, with the exception of those under the heading "Solubility Limitations"(Section 5.6), it is assumed that the total inventory of each nuclide is dissolved in the available porewater. This concentration determines the initial diffusion gradient.

If this concentration exceeds the solubility of the nuclide in question, the calculation gives too high release rates and the solubility-limited concentration should be used instead.

The solubility of the nuclides is determined by the porewater chemistry. The most important features of the porewater are a high pH and a low redox potential, E_h.

3.4.2 Actinides

The solubilities of the most important actinide species in the concrete porewater system have been calculated as a function of pH, Eh and the carbonate concentration.

A probable pH-range for the porewater in fresh concrete would be 12.5-13.5, determined by the high concentrations of NaOH and KOH and dissolution of $Ca(OH)_2$. Later, when the concrete degrades, the pH will probably decrease to about 10. In a closed repository, the corrosion of steel can be assumed to be the redox potential-determining system. This gives, for 25°C, Eh = 0.2 - 0.059 pH (Eh in Volt). This is the normal potential of the redox pair Fe_2O_3/Fe_3O_4.

In the Eh-pH-range of interest i.e.

$-0.6 < Eh < -0.4$ and
$13.5 > pH > 10$

the tetravalent actinide dioxides will be the thermodynamically stable species. Their solubilities are given in Table 3-3. These solubilities are used in the release calculations in Section 5.6.

Table 3-3 Data used. Actinide speciation and concentration in concrete porewater /NTB 85-18/

Element	Solubility limit mole/l	Predominant species in solution
Th	$3 \cdot 10^{-10}$	$Th(OH)_4$
U	$3 \cdot 10^{-7}$	$U(OH)_4$
Np	$1 \cdot 10^{-7}$	$Np(OH)_4$
Pu	$1 \cdot 10^{-7}$	$Pu(OH)_4$
Am	$3 \cdot 10^{-6}$	$Am(OH)_4^-$

3.4.3 Fission and activation products

Due to lack of literature data, the solubility limits for tin (Sn), technetium (Tc), palladium (Pd), selenium (Se), zirconium (Zr), and nickel (Ni) in concrete porewater had to be calculated from hydrolysis and redox data.

If the Eh and the pH are treated as independent variables and the logarithmic function of the concentrations of the substances as parameters, E_h-pH equilibrium diagrams can be established.

These equilibrium diagrams are helpful in determining the thermodynamic possibility of precipitation. They do not give any information about the rate or kinetics of the chemical reaction and are, therefore, only tools and must be used in conjunction with other means of investigation. If these aspects are considered, the equilibrium diagrams can give a fairly good interpretation of, for example, a total solubility of an element.

When establishing these diagrams for the above mentioned nuclides, no complexing reactions other than the formation of hydrolysis products have, so far, been considered.

The equilibrium diagrams for these nuclides in water systems are shown in Figures 3-3 - 3-8. The substances considered and the reaction formulae used when establishing these diagrams are described in Appendix 1.

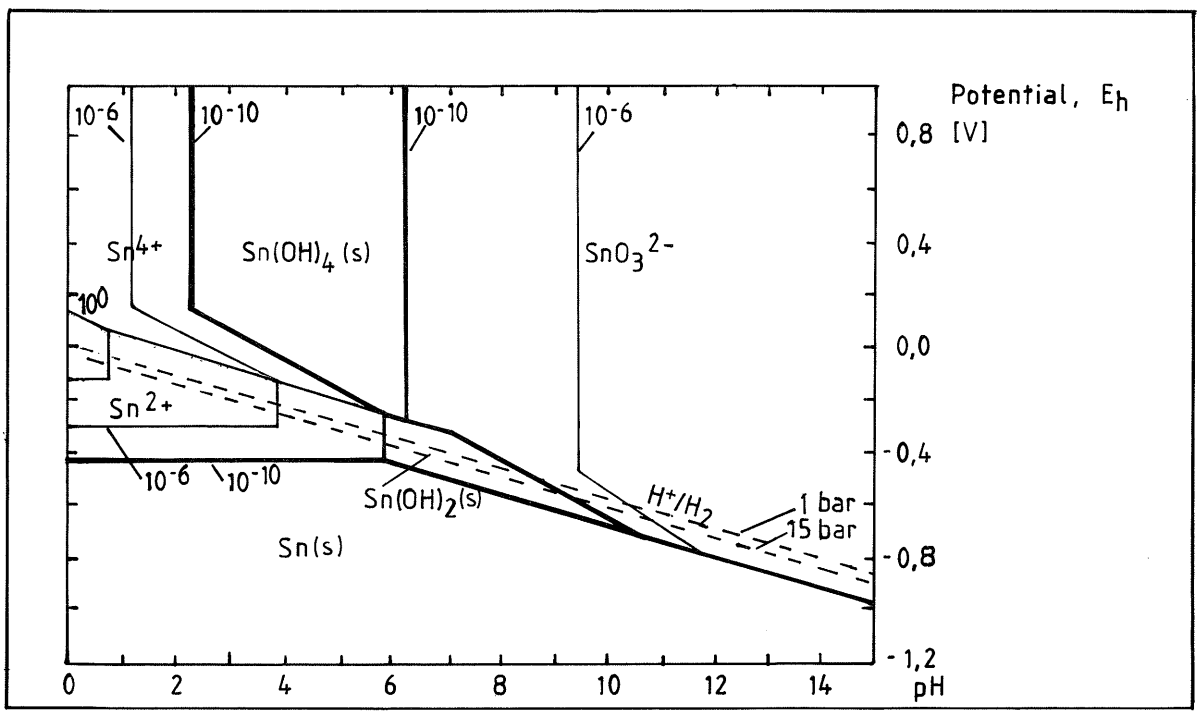

Figure 3-3 Equilibrium diagram for Sn

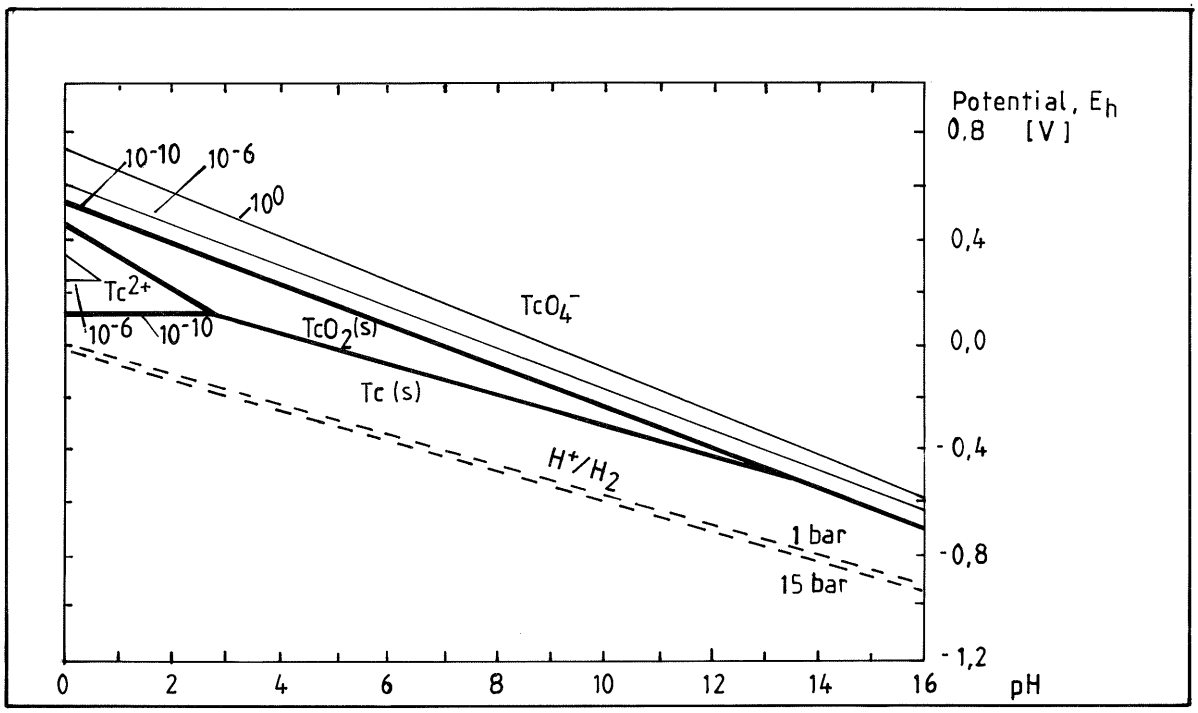

Figure 3-4 Equilibrium diagram for Tc

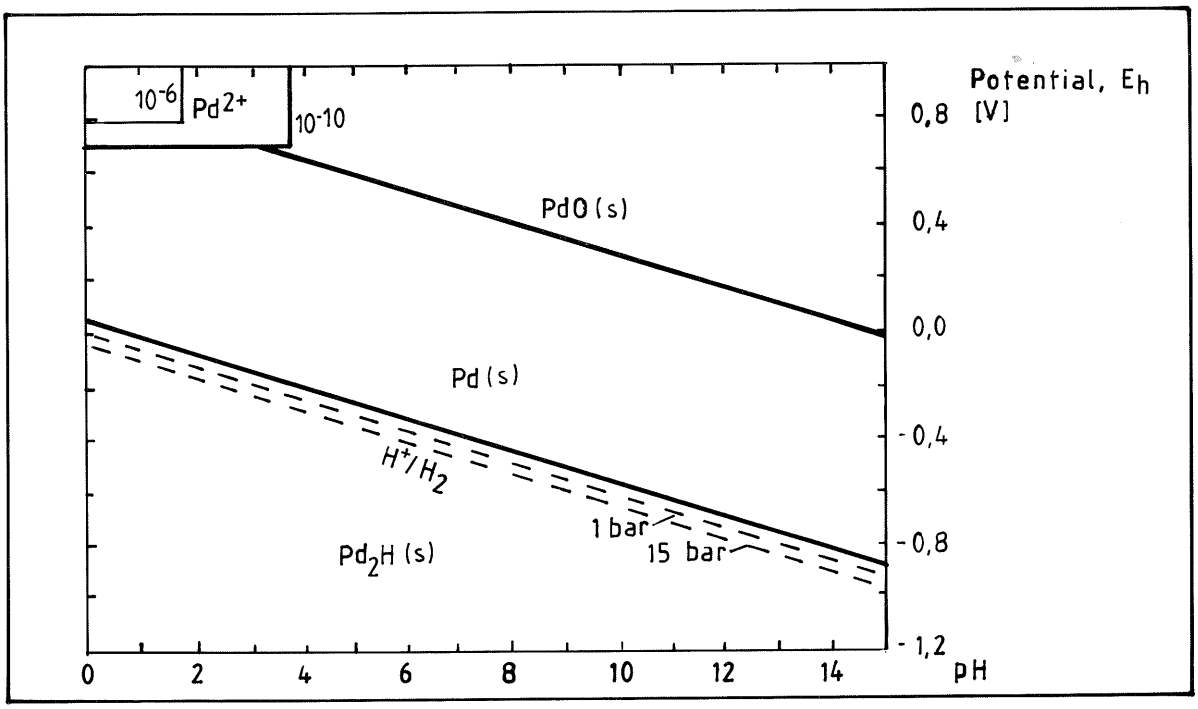

Figure 3-5 Equilibrium diagram for Pd

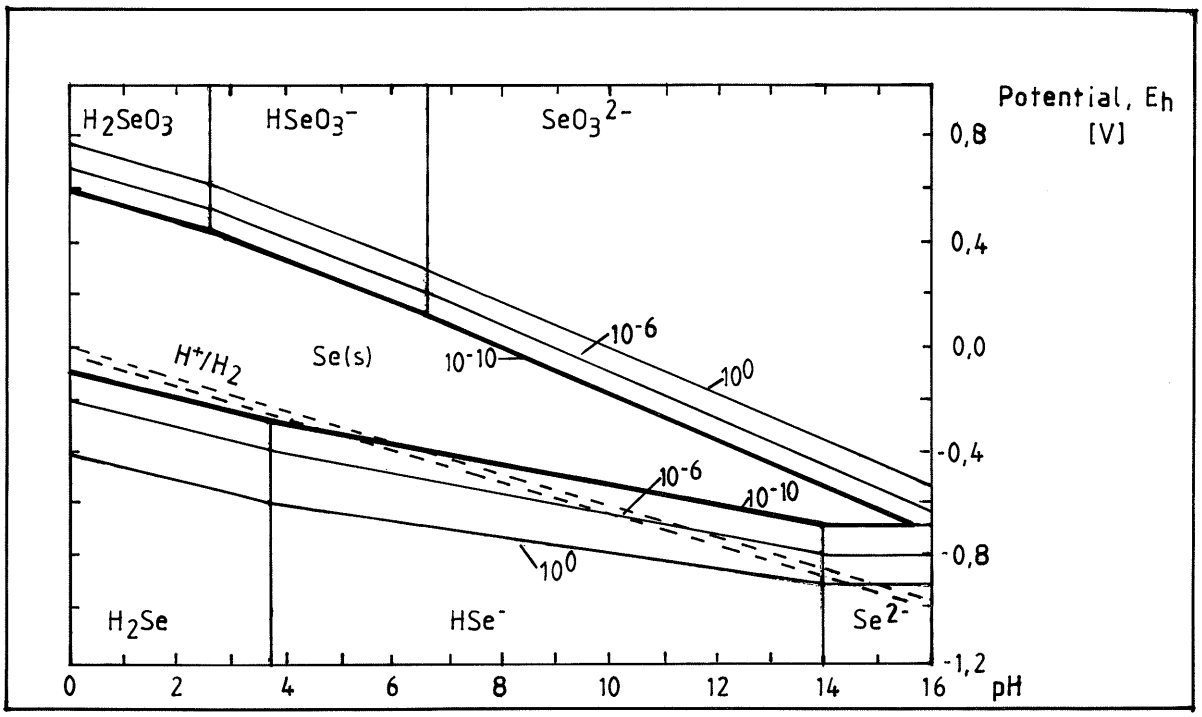

Figure 3-6 Equilibrium diagram for Se

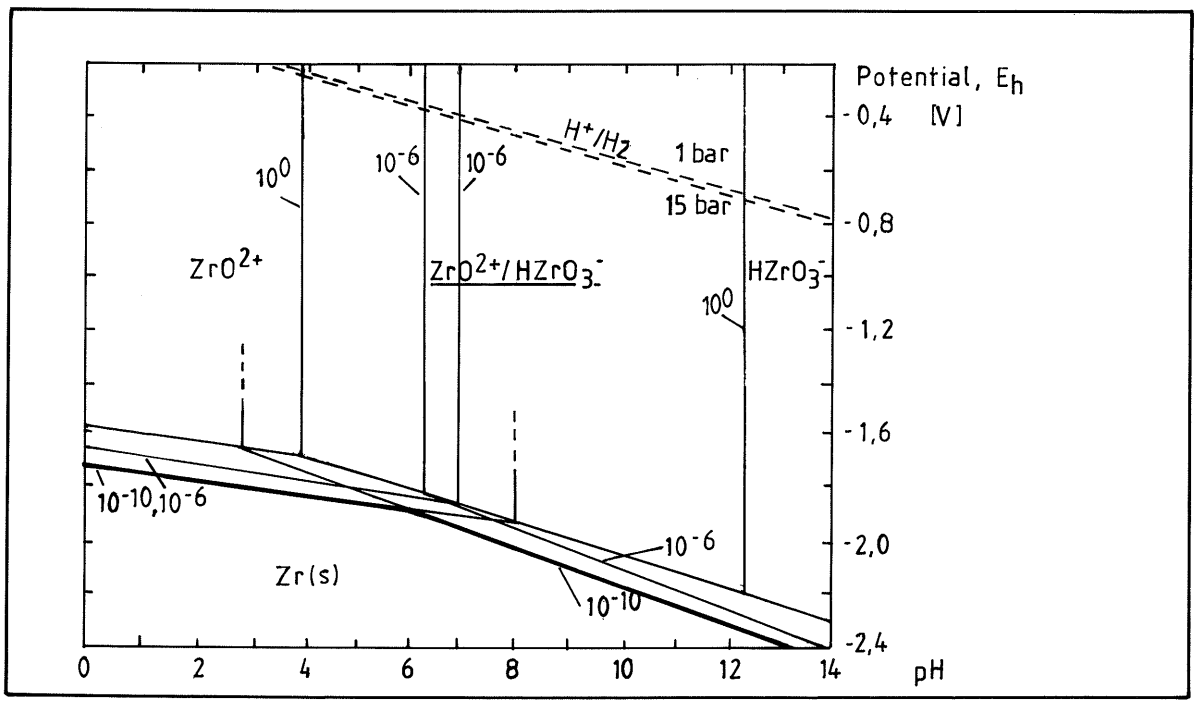

Figure 3-7 Equilibrium diagram for Zr

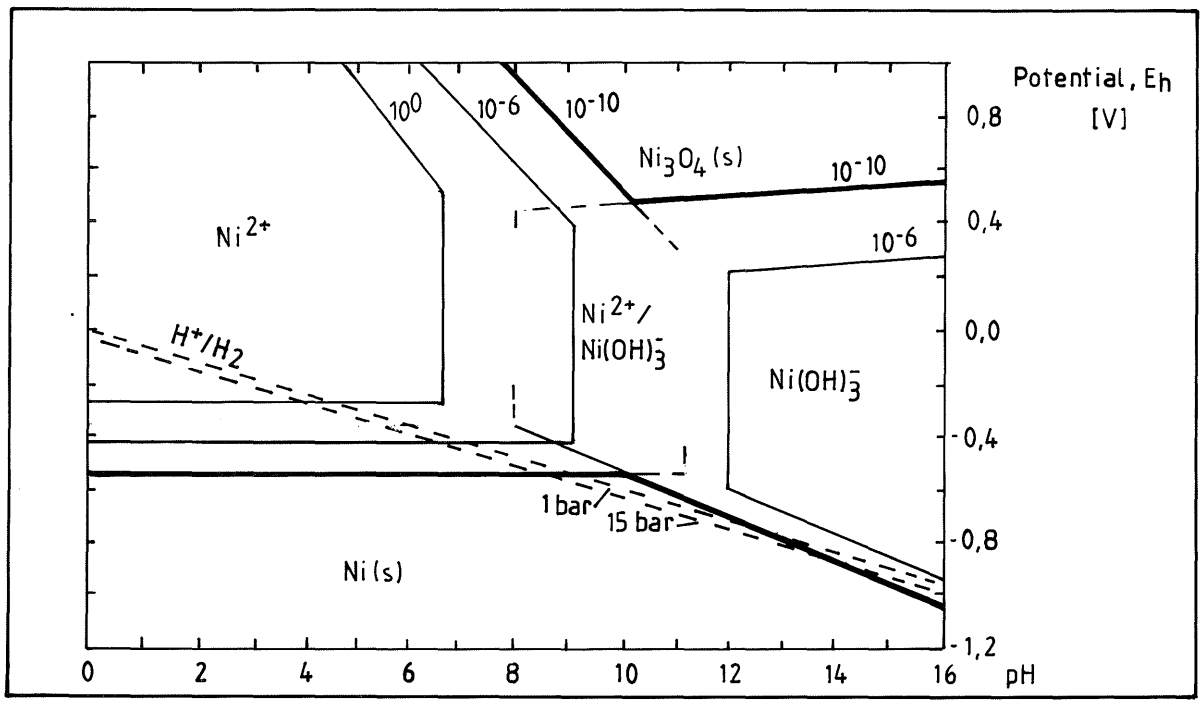

Figure 3-8 Equilibrium diagram for Ni

The dashed lines express the reduction equilibrium of water according to the reaction $H_2=2H^+ +2e^-$ at hydrogen pressures of 1 atm and 15 atm. The continuous lines marked with 10^0, 10^{-6} and 10^{-10} represent the concentrations (activities) in mole/l of dissolved compounds in equilibrium with a solid substance. The lines between two solid substances express the equilibrium condition between the solid substances in question. The solubility limits for the actual nuclides could either be estimated from the diagram in Figures 3-3 - 3-8 or calculated using the reaction formulae and equations described in Appendix 1.

The solubility limits calculated for these nuclides in concrete porewater (pH = 10.5 - 13) and under highly reducing conditions (Eh = -0.4 - -0.6) are shown in Table 3-4.

Table 3-4 Estimated solubility limits for some of the nuclides from Figures 3-3 - 3-8.

Nuclide	Solubility limit mole/l	pH
Sn	10^{-6}	10.5
Sn	none	>13
Tc	$<10^{-10}$	10.5-13
Pd	$<10^{-10}$	10.5-13
Se	10^{-6}	10.5
Se	$<10^{-3}$	13
Zr	10^{-2}	10.5
Zr	none	>12.25
Ni	$<10^{-10}$	10.5-13

The solubility could, however, also be affected by precipitation with ions or species not considered here, i.e. species or ions in the solution which form insoluble compounds with the nuclides. Such substances could either occure naturally in the concrete-groundwater system (e.g. S^{2-}, SO_4^{2-}, CO_3^{2-} etc.) or could have been introduced to the system with the waste (e.g. Se^{2-}, Fe^{2+} etc.).

In Table 3-5, the selected data on the solubility limits for the nuclides in question are shown:

Table 3-5 Data used. Speciation and concentration in concrete porewater for fission and activation products

Nuclide	Solubility limit mole/l	Predominant species in solution
Sn	no limit	SnO_3^{2-}
Tc	10^{-10}	TcO_4^-
Pd	10^{-10}	Pd^{2+}
Se	10^{-3}	HSe^-
Zr	no limit	$HZrO_3^-$
Ni	10^{-10}	$Ni(OH)_3^-$

3.5 Complex formation

The operational waste (BA) and the reprocessing waste (WA) will contain agents with complexing properties or agents that can be converted into compounds with complexing properties. These so-called complexing agents can affect the solubilities of the radionuclides in the waste.

Table 3-6 gives a summary of compounds with complexing properties which could be present in intermediate- and low-level waste from reprocessing operations.

Table 3-6 Organic compounds with complexing properties in intermediate- and low-level waste /NTB 85-19/

Compound	Waste source
TBP (tri-butyl-phosphate)	TBP-waste, Crud
DBP (di-butyl-phosphate)	TBP-waste, Crud
MBP (mono-butyl-phosphate)	TBP-waste, Crud
Organic nitro compounds[1)]	TBP-waste, Crud
Organic nitrates[1)]	TBP-waste, Crud
Organic carbonyl compounds[1)]	TBP-waste, Crud
Do-bads[2)]	TBP-waste, Crud
Oxalic acid (oxalate)	Technol. waste, WWT-waste[3)] (Technol. waste)
Citric acid (citrate)	WWT-waste (Technol. waste)
Tartaric acid (tartrate)	WWT-waste (Technol. waste)
EDTA (ethylene-di-amine-tetra-acetic acid)	WWT-waste (Technol. waste)
DTPA (di-ethylene-tri-amine-penta-acetic acid)	WWT-waste (Technol. waste)
NTA (nitrilo-tri-acetic acid)	WWT-waste (Technol. waste)
Soap	WWT-waste
Alkyl sulphonates	WWT-waste
Amines (tert., sec., prim.)	WWT-waste, Spent ion-exch.[4)]
Anal. separations reagents (HTTA, HDEHP, etc.)	TBP-waste(?)
Subst. phenyl compounds	Spent Ion-exchange resins

1) Information on specified compounds not available

2) Degradation products made up from phosphorus-containing derivates of TBP. They have strong complexing properties

3) WWT-waste, Waste-Water-Treatment-waste

4) Degradation products

The potential formation of radionuclide complexes with organic complexing agents from the waste should be compared with complexes formed with natural ligands in the environment (e.g. OH^-, CO_3^{2-}, SO_4^{2-} and humic and fulvic acids etc). Generally, the complex strength decreases in the following order /NTB 85-19/:

DTPA
EDTA
NTA
humic acid
tri-carboxylic acids
OH^-
CO_3^{2-}
di-carboxylic acids
SO_4^{2-}
monocarboxylic acids

To investigate the influence of complexing agents on the solubilities of the radionuclides earlier mentioned, the presence of DTPA and EDTA was assumed. The reasons are:

- DTPA and EDTA are representative of the strongest possible agents in the waste
- The data available for other strong complexing agents are insufficient.

The following conditions have been assumed in the calculations:

- pH is 12.5 in the aqueous phase. This corresponds to a minimum pH in an intact concrete environment.
- The electrochemical potential is low (Eh -0,5V) i.e. the conditions are reducing. The radionuclides are present as oxides in low oxidation forms.

Table 3-7 Selected formation constants for complexes with DTPA or EDTA and selected radionuclides Data from /NTB 85-18/ and /6/.

Nuclide	$\log K_1$	
Sn^{2+}	18.3	
Pd^{2+}	24.6	
Zr^{4+}	28.4	
Tc^{4+}	28.4	(same as for Zr assumed)
Ni^{2+}	18.7	
Th^{4+}	28.8	
U^{4+}	28.8	
Np^{4+}	29.8	
Pu^{4+}	25.6	
Am^{3+}	22.3	

The concentrations of EDTA or DTPA required to generate radionuclide 1,1-complexes with EDTA or DTPA and thus increase the solubilities of the radionuclides are shown in Table 3-8:

Table 3-8 Concentrations of EDTA or DTPA required to cause increased solubilities of radionuclides that are solubility-limited according to Table 3-5

Nuclide	Required concentration of complexing agent, mole/l
Tc	>1
Pd	>1
Se	>1
Zr	>1
Ni	$>10^{-11}$
Th	>1
U	>1
Np	>1
Pu	>1
Am	$>10^{-11}$

This means that the presence of strong complexing agents such as DTPA and EDTA in the waste with reducing conditions might not affect the solubility of the actinides (except for americium) as it is not realistic to believe that the concentrations of EDTA and DTPA will exceed 1 mole/l.

4. PHENOMENOLOGY AND NEAR-FIELD MODEL DESCRIPTION

4.1 General

The near-field model calculates the release of radionuclides from the waste matrix into the surrounding host rock (far-field).

Basic assumptions for the calculations are:

- The radionuclides are available and evenly distributed in the pores of the waste matrix
- The transport mechanism is diffusion.

An overview of the information flow and the calculation models used is shown in Figure 4-1.

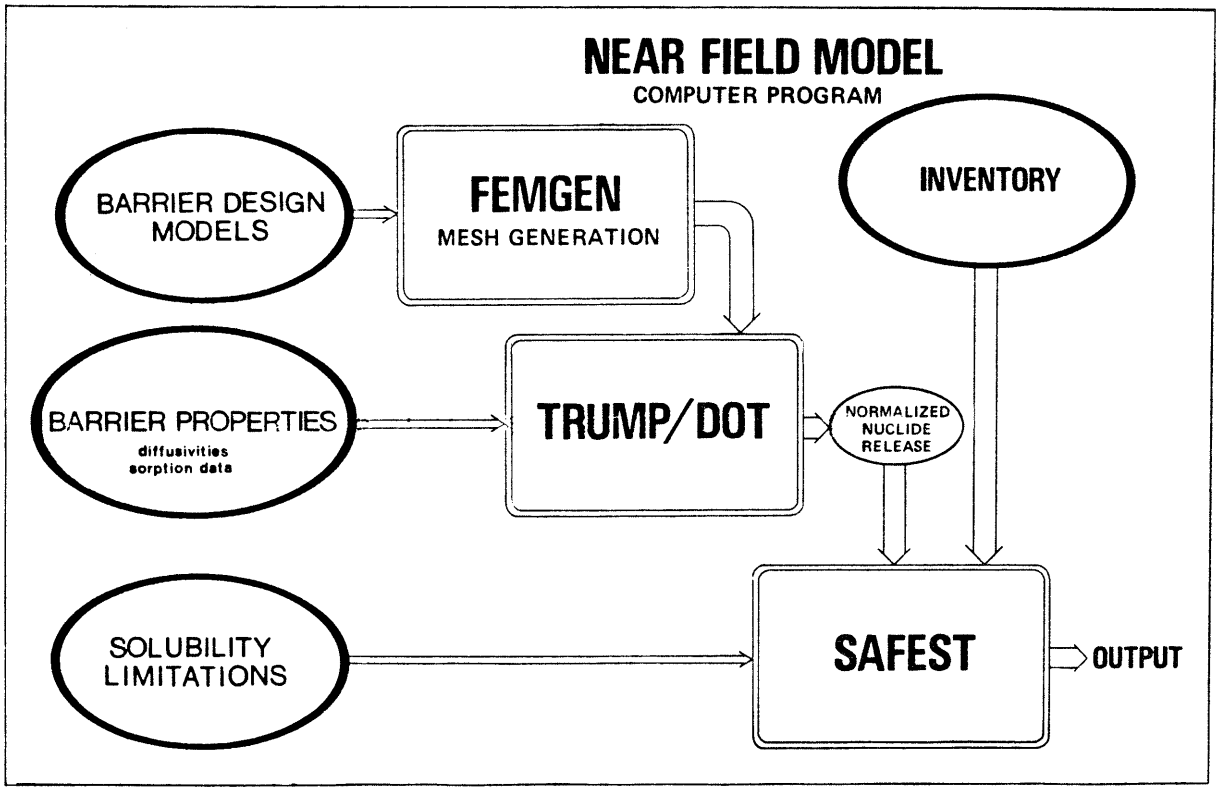

Figure 4-1 Information flow and calculation programs used. FEMGEN, TRUMP, DOT and SAFEST are computer programs and the rest constitute input and output

For the diffusion calculations either the numerical code TRUMP or DOT is used, depending on the requirements of the cases.

Input data needed are:

- Material properties of the engineered barriers in the repository, most importantly the diffusivities.
- Simplified configurations describing the barriers as realistically, but still feasibly, as possible.
- The sorption of some nuclides on the solid surfaces inside the barriers (K_d-values).

The diffusion resistance of the barriers is assumed to decrease with time due to the degradation of the concrete.

A simplified geometric design of the repository is made and transformed into a computerized net with the aid of FEMGEN.

With the inputs the TRUMP/DOT calculations give, as output, normalized release curves, one for each K_d-value used. (For the definition of normalized output, see page 60).

These curves are used as input to a progam(SAFEST) developed for the following purpose. With the aid of the waste inventory data and the nuclide decay chains, the code transforms the normalized curves into actual release rates for each nuclide.

The calculations are made for a base case with best estimates as input data. In addition, a sensitivity analysis is made by varying the diffusivities and the simplified configuration used.

In these calculations, all nuclides were assumed to have unlimited solubility. This conservative assumption has been tested by investigating the solubilities of some nuclides in the concrete pore-water. The near-field model has also been changed to make it possible to handle solubility limitation.

4.2 General formulae

The hydraulic properties of concrete are such that convective transport of water and dissolved radionuclides is not initially probable. When the concrete is degraded, convective transport might be more likely. This is not treated here but results of convective transport calculations are given in /NGB 85-08/.

As the nuclide release is assumed to be caused by diffusion through the porous barrier materials, the transport rate of nuclides can be calculated from a transport coefficient (the diffusivity) and a driving force (the concentration gradient). In general, dissolved molecules or ions are transported from a region of higher concentration into a region of lower concentration; see Figure 4-2. Under steady-state conditions, the rate of transport is determined by:

$$j_i = - D_{w_i} \frac{\varepsilon_p \delta_d}{\tau^2} \nabla C_{p_i} \qquad (4\text{-}1)$$

or

$$j_i = - D_{e_i} \nabla C_{p_i} \qquad (4\text{-}2)$$

also known as Fick's First Law of diffusion where:

j_i = rate of transport of species i through a unit area

D_w = diffusivity in pure, bulk water of species

ε_p = porosity of the porous medium

δ_d = constrictivity of the pores, which is a measure of the amount of narrow passages in the pore system of the porous medium

τ^2 = tortuosity of the pores, which is a measure of the increased path length of diffusion caused by winding pores

∇C_{p_i} = concentration gradient in the porewater with respect to species i

D_e = effective diffusivity

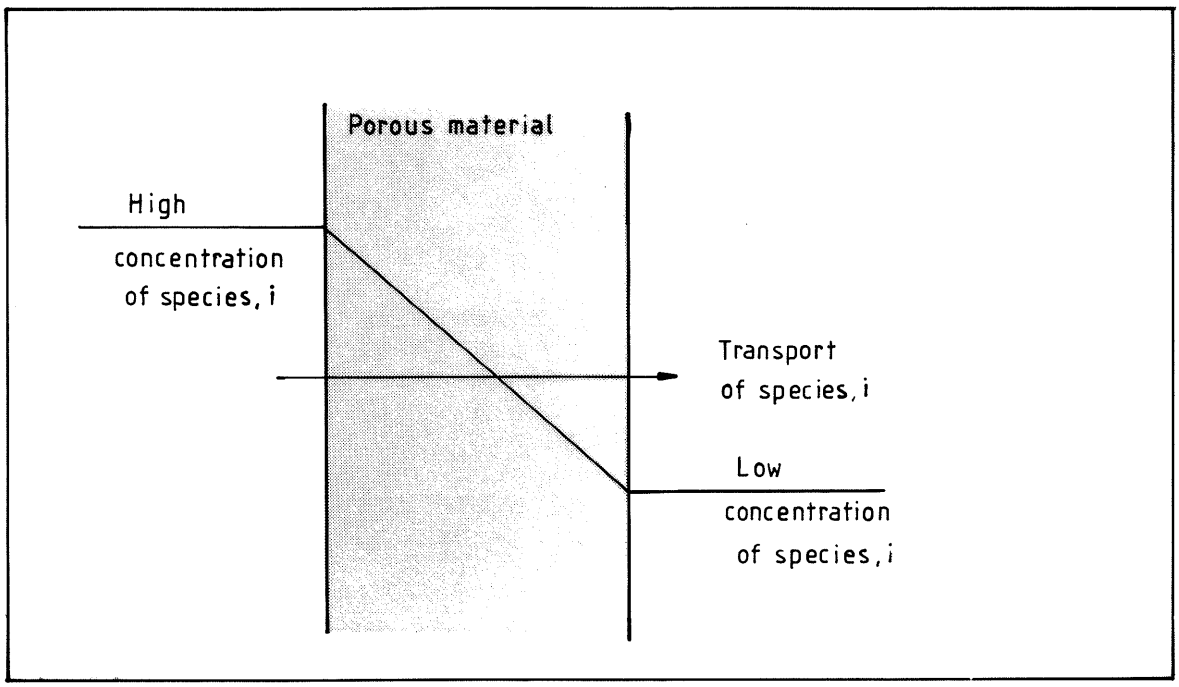

Figure 4-2 Steady-state concentration profile for the diffusion of species i through a porous material

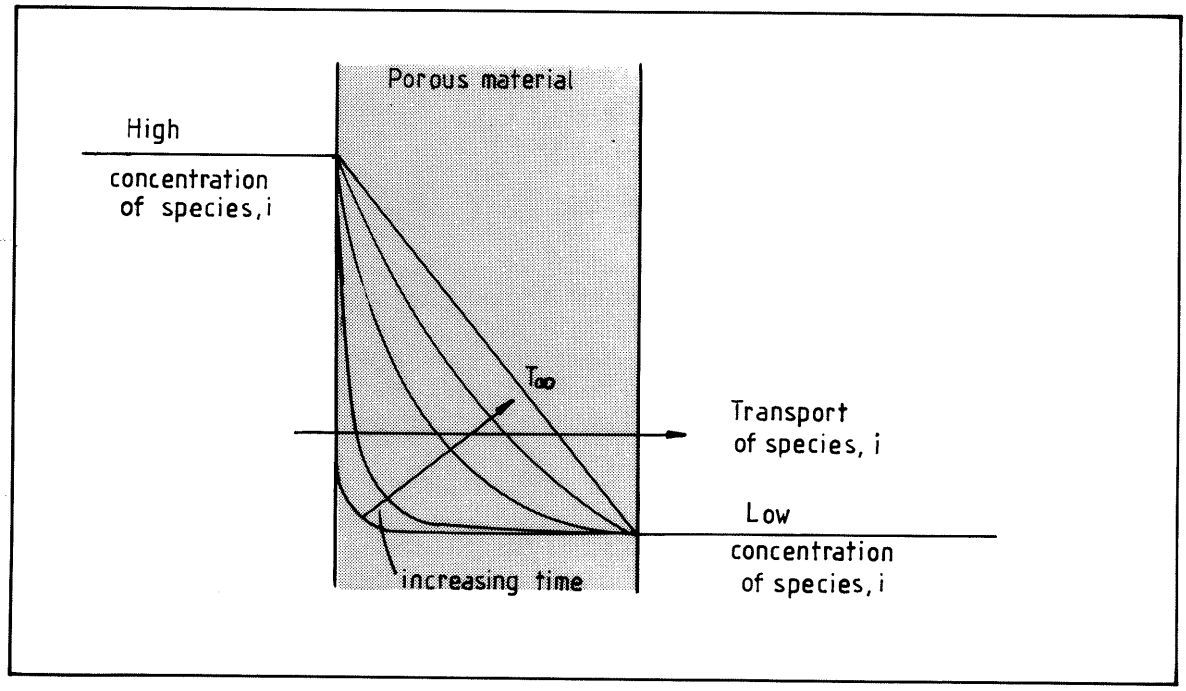

Figure 4-3 Transient diffusion of species i through a porous material, showing the development of the concentration profile with time. The steady-state concentration profile is indicated by T^∞

However, for a porous material like concrete, the rate of diffusion is very low and there is a considerable time lag before steady-state conditions are established. Thus, we also need to consider the transient phase of diffusion. During this phase, the build-up of the concentration profile in the material is described by Eq. 4-3, while radioactive decay is dealt with by the SAFEST code at the end of the calculation.

$$\varepsilon_p R_i \frac{\partial C_{p_i}}{\partial t} = \nabla(D_{e_i} \nabla C_{p_i}) \qquad (4\text{-}3)$$

also known as Fick's Second Law of diffusion where:

ε_p = porosity of the porous material (m^3/m^3)

R_i = chemical retention factor for species i in the porous material (-)

C_{p_i} = concentration of species i in the porewater ($mole/m^3$)

t = time (s)

∇ = nabla operator

D_{e_i} = effective diffusivity (m^2/s)

The chemical retention, R_i, is a capacity factor for the porous material and is defined by:

$$R_i = 1 + \frac{(1 - \varepsilon_p)}{\varepsilon_p} K_{d_i} \rho_s \qquad (4\text{-}4)$$

where:

ε_p = porosity of the porous material (m^3/m^3)

K_{d_i} = distribution coefficient for species i between solution and solid phase (m^3/kg)

ρ_s = crystal density of the solid phase (kg/m^3)

The distribution coefficient, K_d, is defined as the ratio between the concentration in the solid phase and the concentration in the solution.

The distribution coefficient depends on many parameters such as pH, E_h, temperature and solute concentrations. The value used in the calculations does give a measure of the overall sorption behaviour of a species on a solid phase but does not consider effects such as concentration dependence. Fast reversible sorption is also assumed.

The distribution coefficient is the usual way of determining experimental data for the sorption capacity in a solute/solid system.

The chemical retention factor can be interpreted as the ratio between the travel time through a porous material for a sorbing species and that for an average water molecule.

4.3 Initial and boundary conditions

To solve the Equations (4-2) and (4-3), the diffusivity and the chemical retention factor which depends upon the chemistry of water, the porous material and the diffusing species must be known. In addition, it is necessary to specify how the species are distributed within the porous material and also to describe the water flow at the boundary. Such specifications are made with initial and boundary conditions and represent principal information about the system studied.

4.3.1 Dissolved radionuclides

In the case of disposal of radioactive waste in an underground repository, the initial condition is usually given as the initial concentration of the radionuclides in the different barrier materials. As a basis for the calculations, the assumption is that all radioactive materials are contained within the waste matrix and that all radionuclides are dissolved in the porewater of the waste matrix; see Figure 4-4.

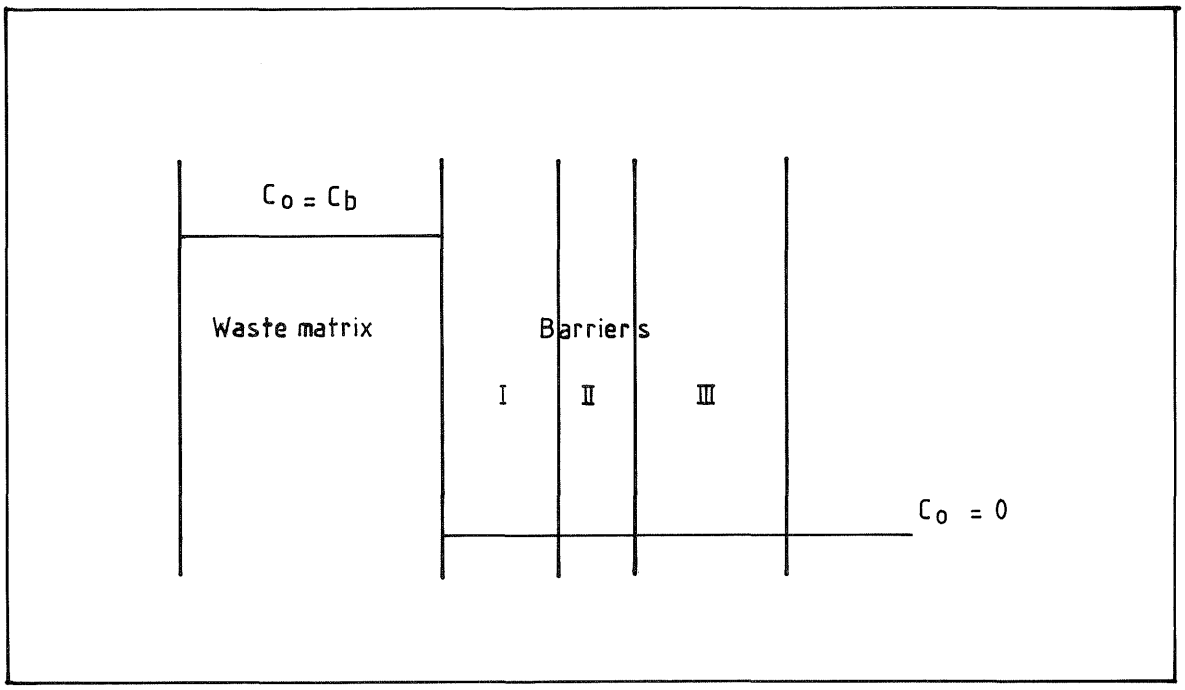

Figure 4-4 Initital conditions in the barrier system. The initial concentration is C_b in the waste matrix bulk. In all other barriers, the initial concentration is zero.

The concentration of radioactive material is often given as the bulk concentration i.e. the content of radionuclides per volume of solidified waste. For the calculations, however, the concentration in the porewater is needed. The relationship between the bulk concentration and the porewater concentration is given by:

$$C_{p_i} = \frac{C_{b_i}}{\varepsilon_p R_i} \qquad (4\text{-}5)$$

$$R_i = 1 + \frac{1 - \varepsilon_p}{\varepsilon_p} K_{d_i} \rho_s \qquad (4\text{-}6)$$

where:

C_{p_i} = porewater concentration of species i (mole/m^3)

C_{b_i} = bulk concentration of species i (mole/m^3)

R_i = chemical retention factor, as defined in Section 4.1 (-)

ε_p = porosity of the porous material (m^3/m^3)

K_{d_i} = distribution coefficient for species i between solid material and solution

ρ_s = crystalline density of solid material (kg/m^3)

Up to this point, the processes that influence the radionuclide transport have been diffusion and equilibrium sorption in the solid material. In the next sections, however, some additional effects which can reduce the transport rate of radionuclides are treated.

4.3.2 Solubility-limited nuclides

The maximum possible concentration of a chemical element in a solution is determined by the solubility of its most stable solid phase. The solubility can be evaluated from the solubility product.

$$mM + nN = M_mN_n \text{ (solid)} \qquad (R4\text{-}1)$$

For this reaction, the equilibrium constant is given by:

$$K_{eq} = \frac{(a_M)^m \cdot (a_N)^n}{a_{M_mN_n}} \qquad (4\text{-}7)$$

where:

M,N = reacting species

m,n = stoichiometric coefficients

K = equilibrium constant

a_i = chemical activity of species i

By definition, the activity of a solid phase is unity. Thus, we may write;

$$K = (a_M)^m \cdot (a_N)^n \qquad (4\text{-}8)$$

also know as the solubility product.

If the actual content of a nuclide in the waste matrix is higher than the amount that is soluble in the porewater according to the solubility product, the nuclide is solubility-limited.

The effect on the diffusion process is that only the soluble fraction of the nuclide content is mobile, while the solid fraction is immobile. In order to dissolve more of the solid phase of the nuclide, the dissolved species must first be transported away by diffusion and, thereby, reduce the solute concentration in contact with the solid phase. This has the effect that the solid material will be dissolved within a thin zone until all material is dissolved. As long as some of the solid phase remains within the zone, the concentration of the dissolved species is constant and equals the solubility limit of the nuclide. As more and more of the solid phase is dissolved, the zone where dissolution takes place will slowly move from the outmost parts of the matrix material towards the inner parts. This type of problem is known as a moving boundary problem and is illustrated in Figure 4-5.

The additional difficulties in this type of calculation are; firstly, the need to identify the fraction of the nuclide which exists as a solid phase and, secondly, the need to know the distribution of the elements between different isotopes, since it has been assumed that the dissolution is congruent and proportional to the amounts of isotopes.

The solution of the problem is simplified if the amount of material in the solid phase is large compared to the rate of dissolution, i.e. if the zone moves very slowly. This assumption has been used in the calculations and the problem can be solved as a diffusion problem with prescribed concentration at the surface of the matrix. The solubility limit of the element in the actual chemical environment is then given as a boundary condition.

To evaluate the effect of a limited solubility on the rate of nuclide transport, the competing effect of sorption must also be considered. The sorption is assumed to be proportional to the porewater concentration and has the consequence that the nuclide is redistributed from a solid state into a sorbed form. The amount of material affected is determined by the distribution coefficient, K_d, and the solubility limit. This has been accounted for in the calculations.

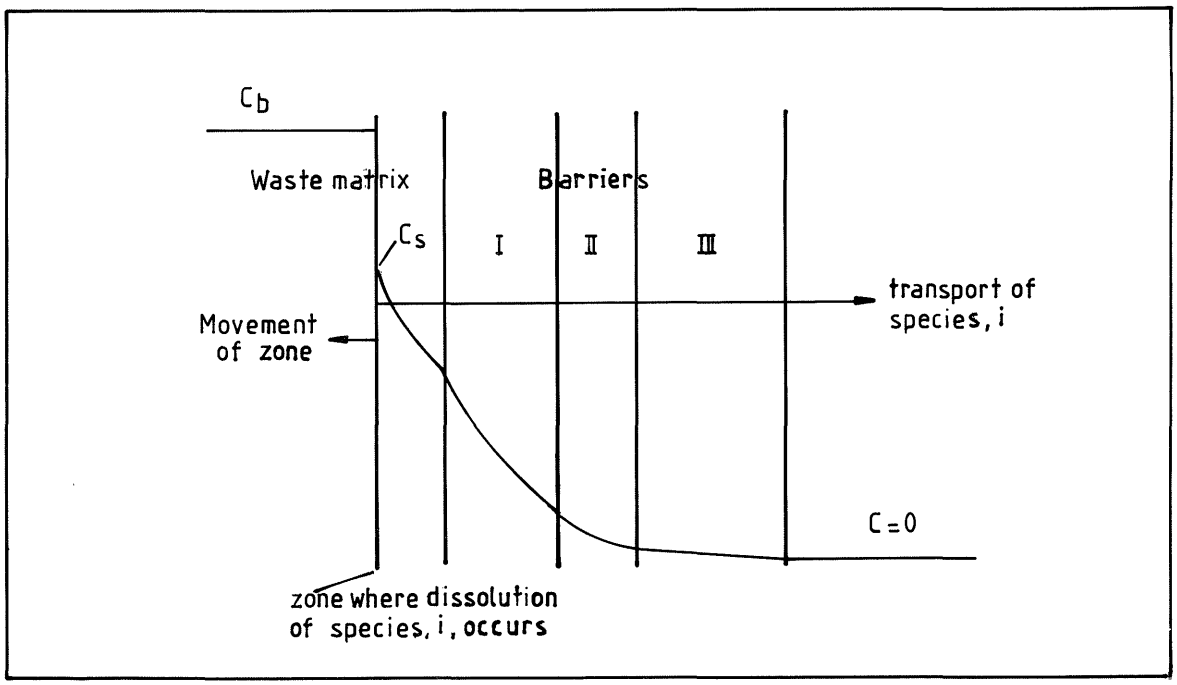

Figure 4-5 Schematic representation of a moving boundary problem relevant for solubility-limited nuclides

4.3.3 Activated steel, discharge from steel matrix

The release of radionuclides, especially nickel, from activated steel requires separate discussion. The radioactivity in these steels is induced by the neutron flux inside the nuclear power reactors and is, therefore, formed inside the steel itself. Consequently, such radionuclides have a very limited mobility since they are embedded in the steel matrix. Thus, we can conclude that the discharge of these nuclides will be affected by the rate at which the steel corrodes.

In addition, corrosion will limit the nuclide release rate only if the corrosion rate is low and the diffusion rate is high, so that the concentration of the radionuclide in the porewater in contact with the activated steel is lower than the solubility limit. The solubility limit of nickel is, however, low, so that the assumed corrosion rate in the repository environment /NTB 85-33/ will not limit the nuclide release any further.

In the calculations for the base case, the parameter variation and the design variations, it was assumed that the total content of activated nickel was available for transport.

Treatment of solubility limitations also included nickel. However, only the radioactive isotopes of nickel were taken into account and not the inactive nickel.

4.3.4 Interface with the geosphere

Inside the repository and within the barriers themselves, the water phase is assumed to be stagnant and does not contribute to the transport of nuclides, i.e. there is no advective transport of nuclides within the repository. Outside the barrier system, on the other hand, the groundwater flows past the repository and, at some distance from the repository, the predominant transport mechanism will be advective transport by groundwater.

When the water flows along the outer surface of the repository, a stagnant film of water will be formed close to the surface. This thin layer of stagnant water will offer resistance to the nuclide release from the repository. The nuclides released from the repository must first diffuse into the flowing groundwater before they are finally removed from the repository /7/.

Figure 4-6 shows the concentration profiles at the surface of the repository.

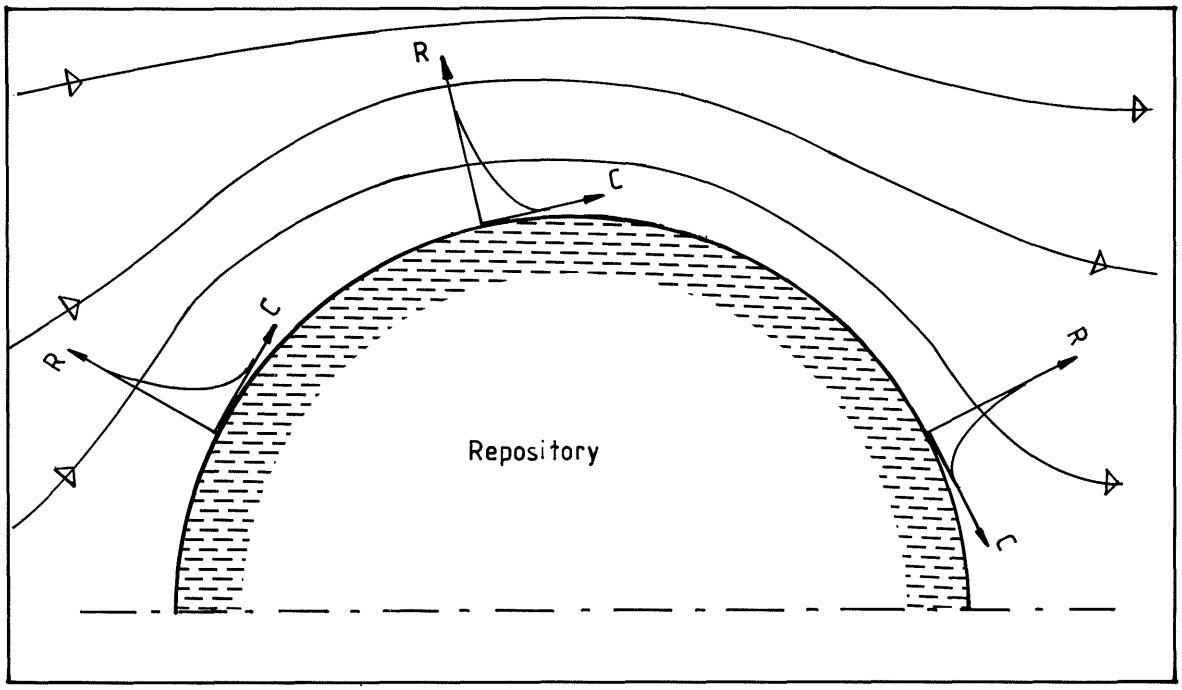

Figure 4-6 Schematic representation of the diffusive transport of nuclides through the stagnant layer of water at the surface of the repository and into the flowing groundwater

In the calculations, it has been assumed that the rate of nuclide release from the repository is proportional to the concentration of the nuclide at the surface of the repository. Thus:

$$j = K_V \, \varepsilon \, C_{S_i} \qquad (4\text{-}9)$$

where:

j = nuclide release rate per unit area

K_V = mass transfer coefficient describing the transport from the repository into the groundwater

ε = rock porosity

C_S = concentration of species i at the surface of repository

The mass transfer coefficient, K_v, can be evaluated from a mass balance over the layer of stagnant water. The derivation of the expression for K_v is given in /7/ and a similar theoretical treatment can be found in /8/. Thus:

$$K_v = \sqrt{\frac{4D_w \nu}{\pi^2 r}} \qquad (4\text{-}10)$$

where:

D_w= diffusivity in pure bulk water

ν = velocity of the groundwater in the rock pores

r = radius of the repository

By combination of Equations (4-1) and (4-9), we obtain the boundary condition for Equation (4-3), also called a convective boundary condition:

$$\nabla C_{p_i}\big|_{x=r} = - \frac{K_v \varepsilon}{D_e} C_{s_i} \qquad (4\text{-}11)$$

where:

∇C_p= concentration gradient in porewater of species i at x = r, i.e. at the surface of the repository

K_v= mass transfer coefficient as defined above

ε= rock porosity

D_e= effective diffusivity in the porous barrier material

C_s= concentration of species i at the surface of the repository

This phenomenon is shown in Figure 4-7.

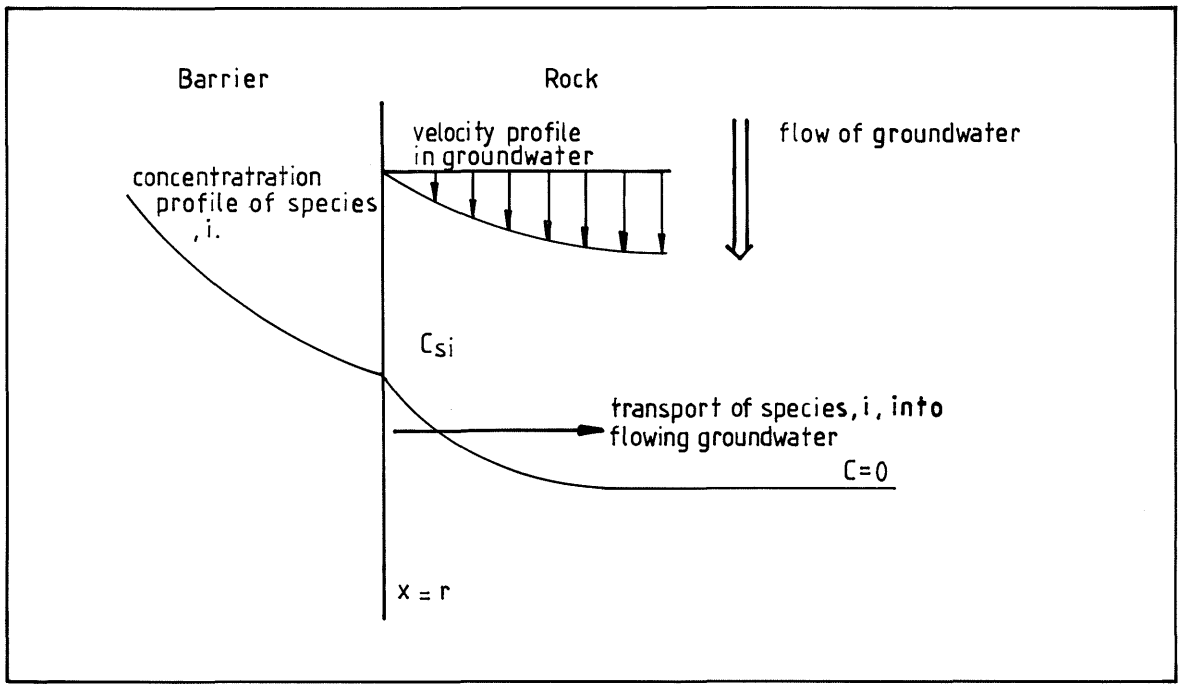

Figure 4-7 Schematic representation of the groundwater velocity profile and the resulting concentration profile of species i, when a convective boundary condition is used in the calculations

4.4 Modelling of the barrier system

The barrier system in the repository consists of several layers. The waste matrix is stored either directly in concrete containers or in steel and concrete drums inside the concrete containers. The space between the drums in the containers is backfilled with concrete. The concrete containers are piled in the repository cavern, which is surrounded by a concrete lining. The space between the container piles and the cavern lining is also filled with concrete.

The cross-section of the repository is shown in Figure 4-8 and the amount of barrier materials and the dimensions are summarized in Table 4-1.

The principal path for nuclide transport through the engineered barriers in the repository is shown in Figure 4-9. It should be noted that the steel drums have been assumed to be damaged or corroded shortly after disposal in the repository and, therefore, no account has been taken of the possible resistance to nuclide transport.

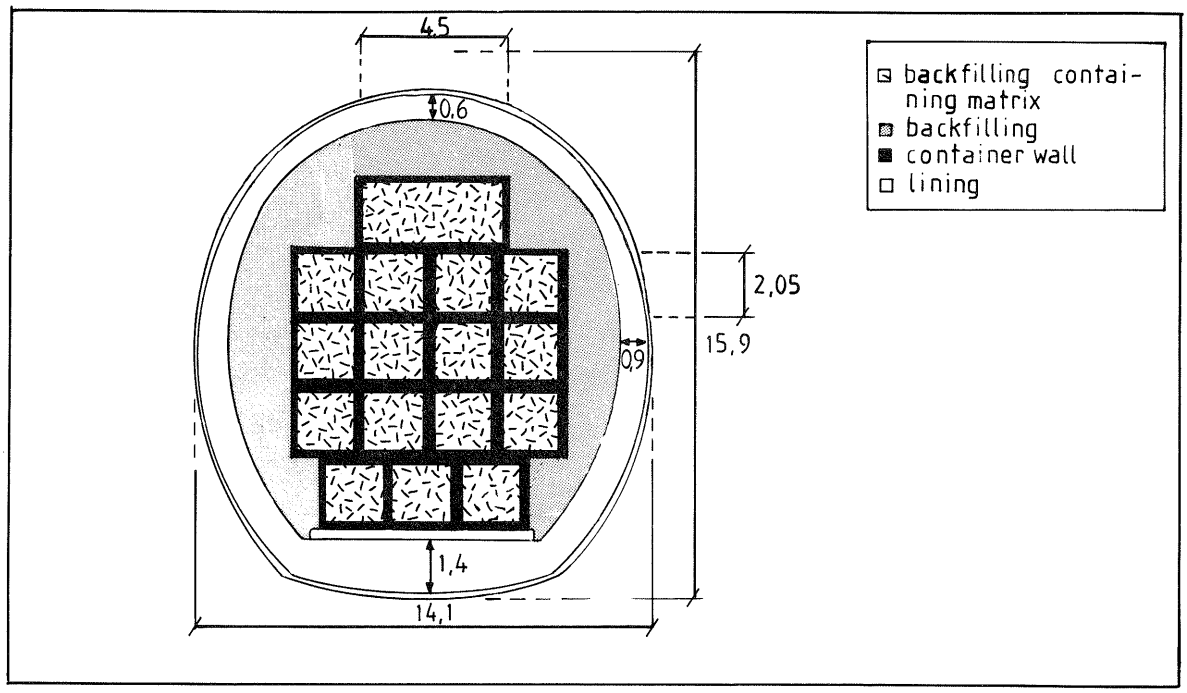

Figure 4-8 Cross-section of the repository showing the storage pattern of concrete containers

Table 4-1 Geometric data on the repository

Parameter	Waste matrix*	Backfill*	Concrete container wall	Repository backfill	Repository lining	Whole repository
Total volume ($\cdot 10^3$ m^3)	127	13	72	296	200	820
Volume per m repository (m^3/m)	5-35	0-30	15	64	43	176
Total surface area ($\cdot 10^3$ m^2)	466-1,630	-	800	-	250	250
Surface area per m repository (m^2/m)	100-350	-	170	-	53	53
Horizontal cross-sectional area ($\cdot 10^3$ m^2)	-	-	-	-	-	66
Barrier thickness ($\cdot 10^{-2}$ m)	60**	5-30	10	0-250	80-120	-
Total repository length ($\cdot 10$ m)	-	-	-	-	-	466

* For decommissioning waste, the backfill is treated as waste matrix
** Diameter

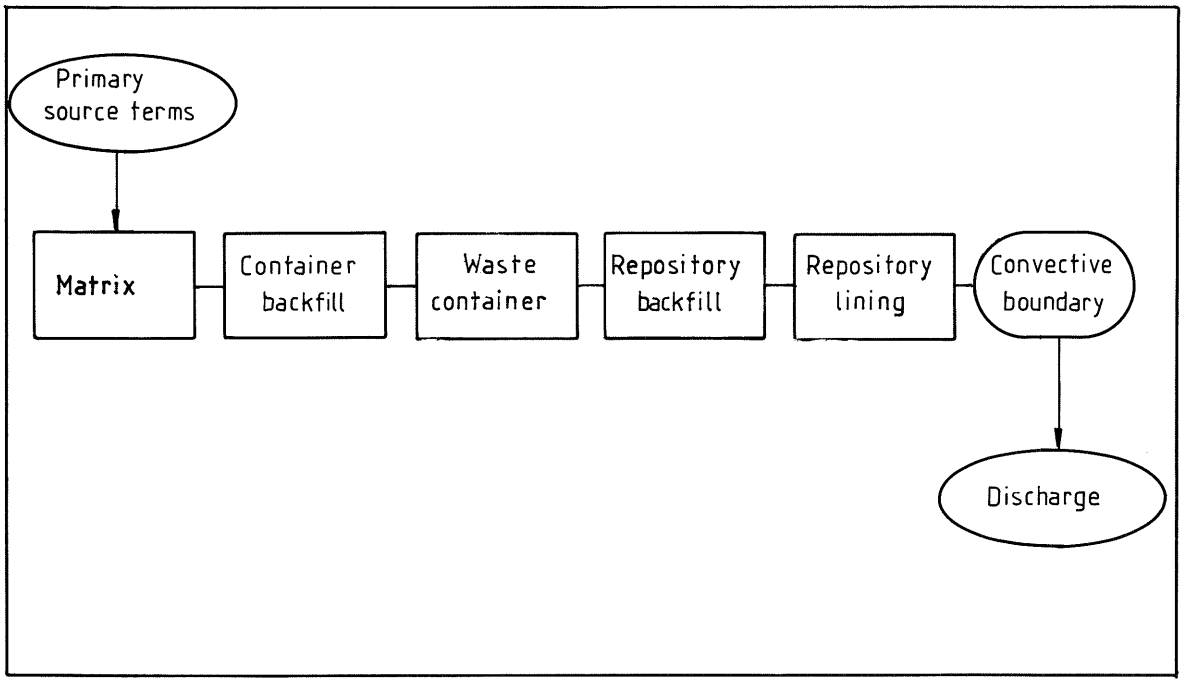

Figure 4-9 The path for nuclide transport through the engineered barriers

In the calculations, the representation of the engineered barriers has to be simplified. However, the model of the repository must be in good agreement with reality with respect to some important dimensions:

- The nuclide inventory
- The waste matrix volume
- The surface of the barriers through which the nuclides diffuse
- The thickness of the barriers, i.e. the diffusion length.

To obtain a view of the significance of the modelled geometry for nuclide release, three alternative geometry simplifications(denoted NET1, NET2 and NET3), have been developed and used in the calculations. NET1 was used in the near-field calculations in /NGB 85-08/, denoted base case (N1) and parameter variation (N2). NET2 and NET3 have been used for verification of the results presented in /NGB 85-08/. The aim has also been to develop a simplified model which gives results similar to those obtained with NET1 and can be used to study more complicated phenomena such as continuously degrading

barrier materials.

Description of geometric simplifications, NET1

The barriers are modelled as concentric cylindrical shells with different thicknesses. The repository lining is 0.9 m thick, which is an average value for the real lining design. The repository backfill is 0.5 m thick. The container walls are represented as a 0.1 m thick barrier interrupted every metre by a vertical section, corresponding to the vertical container walls perpendicular to the repository tunnel axis, Figures 4-10 a-b. The volume of the waste matrix is 32.5 m^3/metre of repository, which was estimated with the assumption that each concrete container is filled with 42 steel drums.The waste matrix is modelled as two concentric barriers surrounded by 0.05 m container backfill.

As can be seen in Table 4-2, the thickness of some barriers is underestimated. As a result, an empty space had to be modelled in the centre of the repository. The boundary between the empty space and the waste matrix has been modelled as being insulated, i.e. no material transport occurs. The average travel distance from the waste matrix to the rock wall is shorter than it would be in a real repository, which is conservative. The diameter of the axisymmetrical model repository is 14.8 m, which is an average value for the real elliptical repository.

The total length of the three model repositories presented in this section is 3,809 m, to be compared with 4,660 m for the real repository. The deviation depends on the fact that the storage of waste is less dense in some sections, e.g. decommissioning waste, which has not been accounted for.

Table 4-2 Geometric data, NET1

Parameter	Waste matrix*	Backfill*	Concrete container wall	Repository backfill	Repository lining	Whole repository
Total volume ($\cdot 10^3$ m)	124	29	40	81	150	654**
Volume per m repository ($\cdot 10^{-1}$ m^3/m)	325	77	106	213	393	1720**
Total surface area ($\cdot 10^3$ m^2)	564	-	442	-	175	175
Surface area per m repository (m^2/m)	148	-	116	-	46	46
Horizontal cross-sectional area ($\cdot 10^3$ m^2)	-	-	-	-	-	56
Barrier thickness ($\cdot 10^{-2}$ m)	60	5	10	50	90	-
Total repository length ($\cdot 10^1$ m)	-	-	-	-	-	381

* including drums
** including the empty space ($230 \cdot 10^3$ m^3)

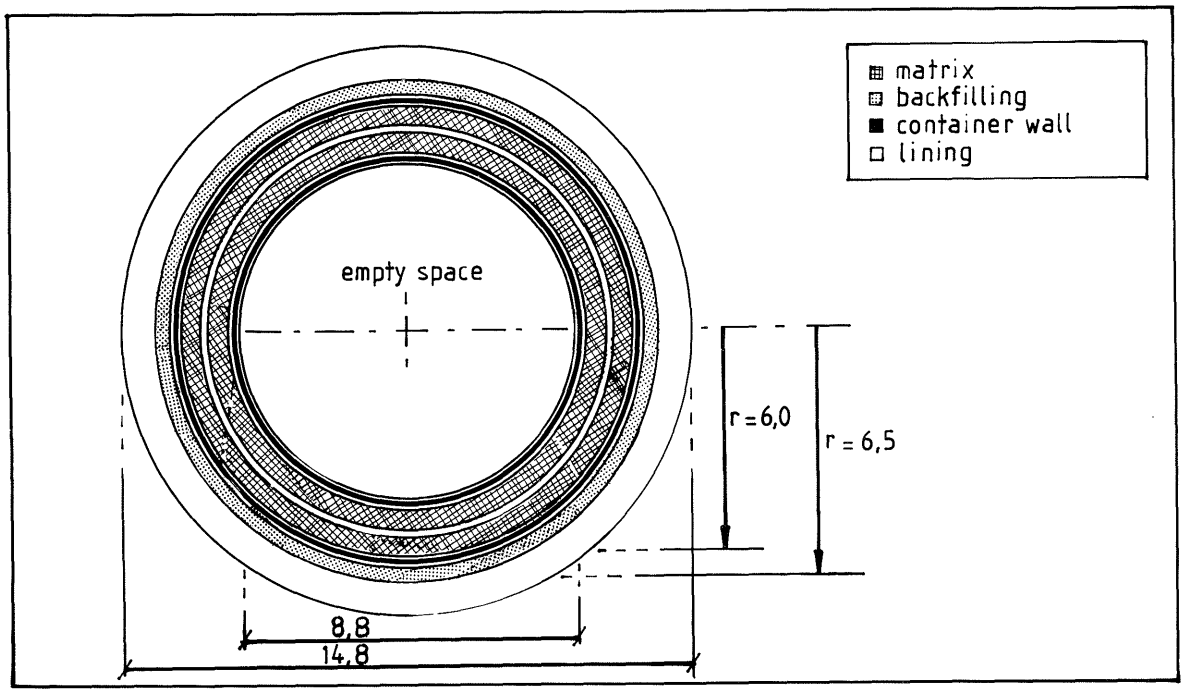

Figure 4-10a Cross-section, geometric simplification, NET1

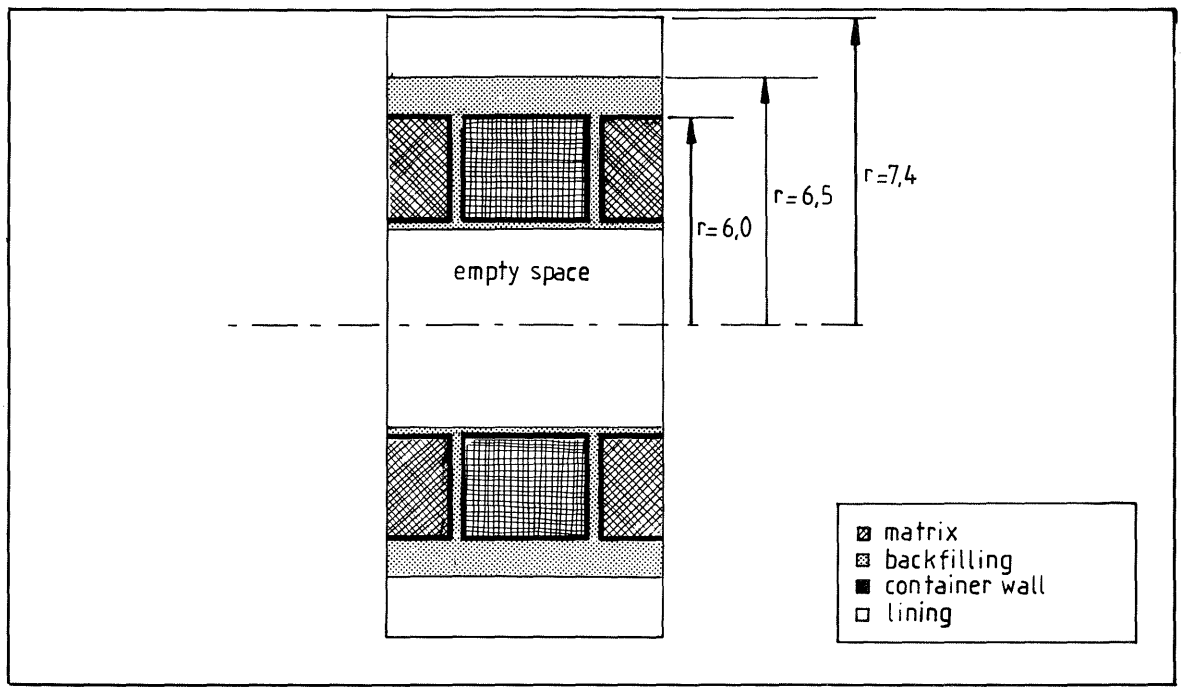

Figure 4-10b Longitudinal section, geometric simplification, NET1

Description of geometric simplification, NET2

The cross-section of this geometric simplification agrees more closely with that of the real repository.

The dimensions of the technical barriers are the same as in the real repository, except for the walls of the storage containers in the centre of the pile. These container walls have been disregarded. No drums are modelled inside the containers and the backfill is a 0.1 m thick layer inside the container wall. The matrix volume is overestimated, but this is compensated for in the calculations by proportionally reduced nuclide concentrations. It can be regarded as a mixture of waste matrix and container backfill.

The driving force for diffusion is underrated because of the lower concentrations, but the break-through time for the nuclides in the container backfill becomes shorter as the amount of uncontaminated material is less than in the real container pile. The dimensions of this model design are presented in Table 4-3 and the cross-section in Figure 4-11.

Table 4-3 Geometric data, NET2

Parameter	Waste matrix	Container backfill*	Container wall	Repository backfill	Repository lining	Whole repository
Total volume ($\cdot 10^3$ m^3)	274	-	15	229	152	670
Volume per m repository (m^3/m)	72	-	4	64	43	183
Total surface area ($\cdot 10^3$ m^3)	73	-	141	-	202	202
Surface area per m repository (m^2/m)	33	-	37	-	53	53
Barrier thickness ($\cdot$ 10^{-1} m)	20-50	-	1	0-25	8-12	-
Horizontal cross-sectional area ($\cdot 10^3$ m^2)	-	-	-	-	-	54
Total repository length ($\cdot 10^1$ m)	-	-	-	-	-	381

* mixed with waste matrix

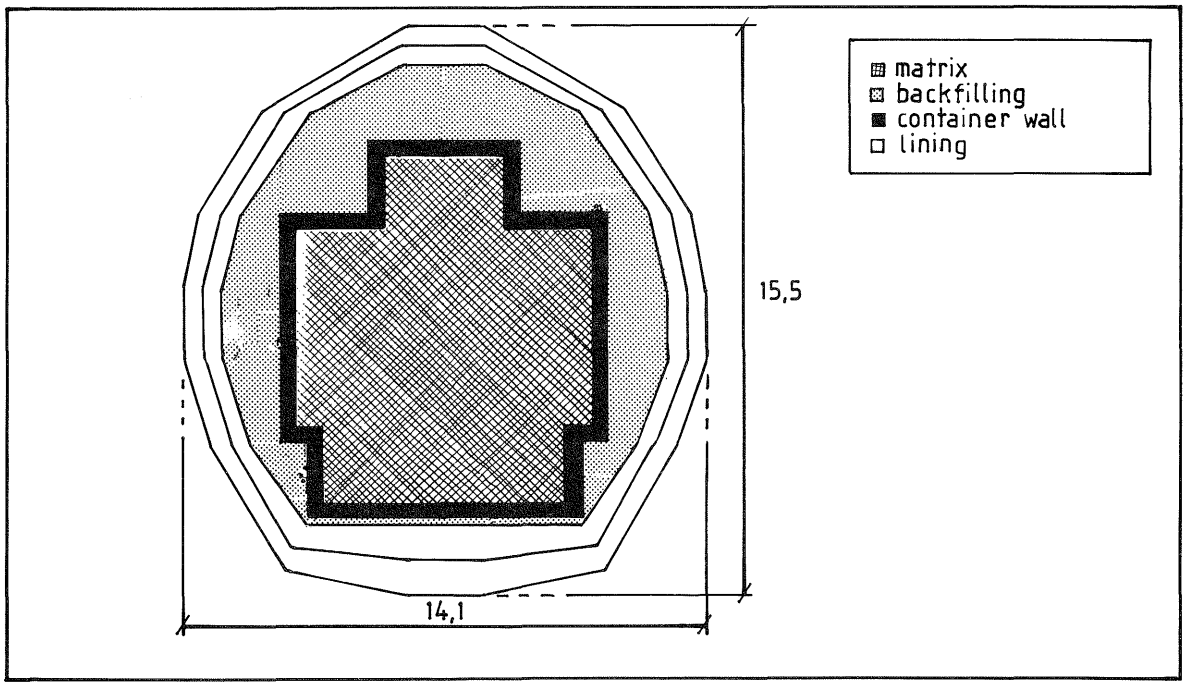

Figure 4-11 Cross-section, geometric simplification, NET2

Description of the geometric simplification, NET3

This model of the repository design is less complicated than the other two models presented. It is one-dimensional and axisymmetric.

The barriers are modelled as cylindrical shells of different thicknesses. The total diameter is 14.1 m, corresponding to the smallest diameter of the real elliptical repository. The repository liner is 0.9 m, the repository backfill 1.0 m, the container wall 0.1 m and the container backfill 0.05 m thick. The vertical container walls in the container pile which were modelled in NET1 have not been considered in this repository model. The thickness of the waste matrix is 1.2 m.

As in model NET1, an empty space with an insulated boundary has been modelled in the centre of the repository, thereby underestimating the average travel distance within the repository. In addition, some of the container walls have been disregarded in the model. Also, the amount of repository backfill is less than in the real repository. The dimensions of the different barriers are shown in Table 4-4 and, in Figure 4-12, a cross-section through the simplified geometry is presented.

Table 4-4 Geometric data, NET3

Parameter	Waste matrix	Container backfill*	Container wall	Repository backfill	Repository lining	Whole repository
Total volume ($\cdot 10^3$ m^3)	123	6	12	135	142	594**
Volume per m repository (m^3/m)	32	2	3	36	37	156**
Total surface area ($\cdot 10^3$ m^3)	120	121	123	147	169	169
Surface area per m repository (m^2/m)	31	32	32	39	44	44
Barrier thickness ($\cdot 10^{-2}$ m)	120	5	10	100	90	-
Horizontal cross-sectional area ($\cdot 10^3$ m^2)	-	-	-	-	-	54
Total repository length ($\cdot 10^1$ m)	-	-	-	-	-	381

* including drums
** including the empty space ($176 \cdot 10^3$ m^3)

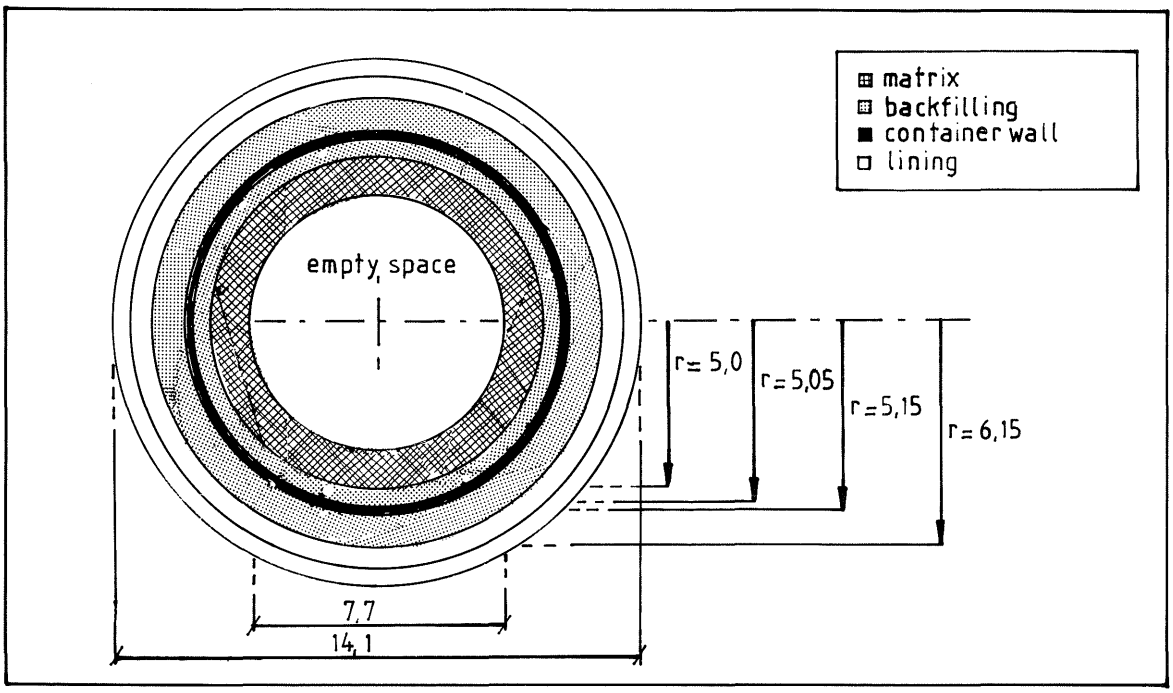

Figure 4-12 Cross-section, geometric simplification, NET3

4.5 Description of the near-field model

The nuclide release from the near-field is determined by many factors, e.g. the transport mechanism, barrier material properties, repository design and location, the waste properties and information about the chemical environment in the repository. The near-field model used for the nuclide release calculations is presented below.

The transport mechanism considered is diffusion of nuclides dissolved in the porewater of the matrix through the barriers. The governing equations for the nuclide release are presented in Section 4.2, where initial and boundary conditions are also discussed.

To solve the differential equations (4-2) and (4-3), two different computer codes have been used; either a finite element method - DOT ('Determination of temperature') /9/ or an integrated finite difference method -TRUMP /10/. Both programs were written for heat transfer problems but are adapted to mass transfer problems by using analogies. The advantage of using TRUMP is that time-dependent material properties can be handled. The disadvantage is the complicated net generation. DOT, on the other hand, can not solve the equations with time-dependent material properties, but, using the computer program FEMGEN /11/, net generation for very complex geometries is possible.

The repository geometry used in the models i.e. the net, is a simplification of the real repository. The information required to characterize the nuclide transport properties of the different barrier materials are porosities, densities, sorption capacities and diffusivities. As mentioned earlier, the release depends also on the convective boundary condition which is governed by the convective water flow around the repository. The convective boundary condition is given by a mass transfer coefficient, K_v. To determine the mass transfer coefficient, the flow rate of water and the porosity of the surrounding rock must be known. The diffusion equations are solved for nuclides(disregarding decay) with specified sorption in the barriers, i.e. the equation must be solved for every permutation of sorption in the different barriers and for every activity source term. Decay is calculated with the SAFEST code.

The calculations are made for normalized concentrations/activities. Thus, the activity in the matrix for non-sorbing, soluble nuclides is given as an initial unity matrix concentration. The spreading of the concentration front-line in the near-field and the resulting rate of release are then calculated.

For sorbing nuclides, the initial concentration of nuclides dissolved in the porewater of the matrix is adjusted according to the sorption capacity of the matrix material. For solubility-limited nuclides on the other hand, the initial concentration in the porewater is given as a time-independent, constant concentration (equal to the solubility limit) at the waste matrix surface. The constant concentration at the matrix surface corresponds to the concentration of a fully saturated solution of the nuclide i.e. the solubility limit.

The results from the calculations described are denoted as normalized nuclide release curves and represent the time-dependent release rate from 1 metre of the repository for an arbitrary nuclide with an initial unity concentration in the waste matrix, disregarding the decay.

If the amount of solid phase is large i.e. if there is a strong influence on release by the limited solubility, a steady-state rate of release is reached after some time. The duration of the steady-state period depends on the waste inventory and is calculated separately for every nuclide in each waste type in the SAFEST computer program /12/ described below.

The total release rate from the near-field is then calculated by adding the contributions from the individual waste types. Input data to the SAFEST computer program are the normalized nuclide release rate curves, information about the nuclide inventory and selected solubility limits.

The information about the nuclide inventory is given for every specified waste category and includes the concentration (Ci/m^3 matrix) of, and the distribution coefficient (m^3/kg) for, the 38 selected nuclides presented in Section 2.4. The information also comprises the repository model length of the categories, estimated as described in Section 4.4, and the toxicity classification which determines the allocation within the repository /NGB 85-02/.

Selected solubility limits of the elements are supplied as input to the program. The porewater concentrations in the waste matrix for possibly solubility-limited elements are examined in all waste categories separately. If the porewater concentration of an element is found to be above the solubility limit, the concentrations of the different isotopes of this element in the porewater are assumed to be distributed in proportion to their contents in the matrix.

The normalized release of a solubility-limited nuclide can reach steady-state. The duration of the steady-state period depends on the amount of solid phase left in the matrix. Thus, the remaining solid phase must be computed at every time step, taking into account the decay of the radionuclides. When the solid phase is totally dissolved, the release rate decreases very quickly, see Figure 4-13.

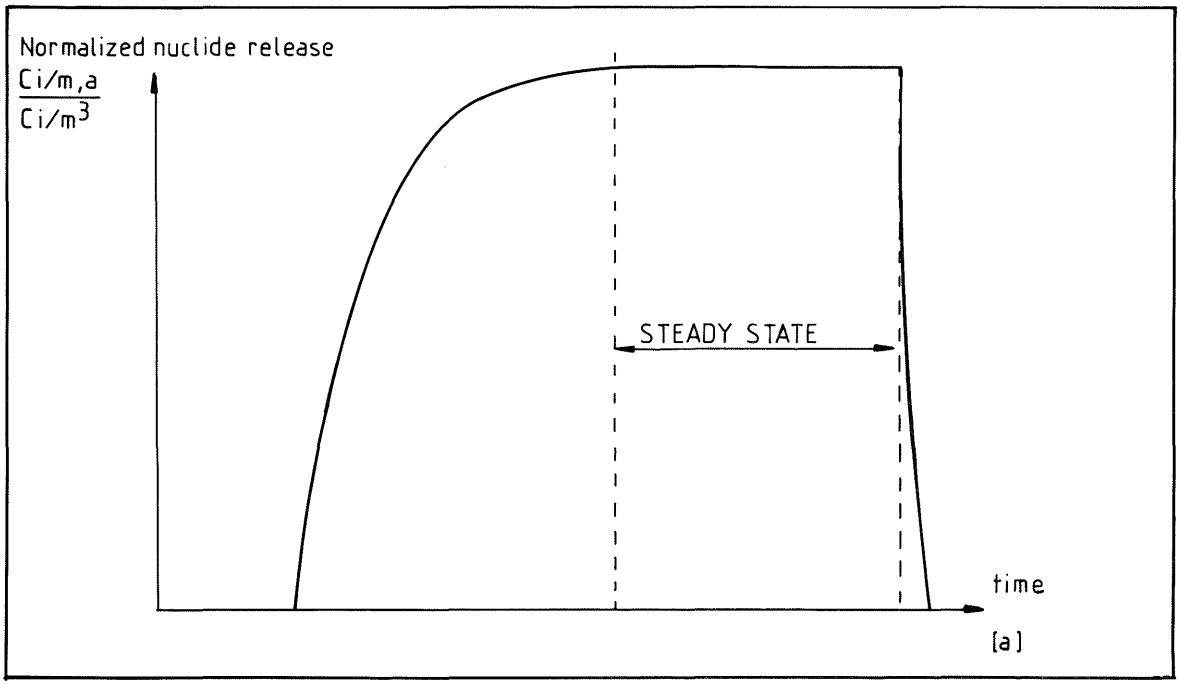

Figure 4-13 Schematic representation of the normalized nuclide release for solubility-limited nuclides

The decay or chain decay of the radionuclides in the different waste categories is computed in the SAFEST program and is superimposed on the normalized release curves. The decay calculations are analytical solutions of a system of linear differential equations describing chain decay where the initial activities of the chain members are given as input /13/.

A condition for calculating the release rate and the chain decay separately instead of in parallel is that all nuclides in one decay chain must have the same chemical retention in the barriers. For the Kd-values used in the present calculations, this is the case.

The four actinide decay chains with mass number 4N to 4N+3 are presented in Figure 4-14. The decay chains are shortened according to:

- radioactive equilibrium, (the daughter nuclide is short-lived in relation to the parent nuclide.)
- short-lived parent nuclide, which decays completely before the start of the release.

The reduced decay chains used in the calculations are shaded in Figure 4-14.

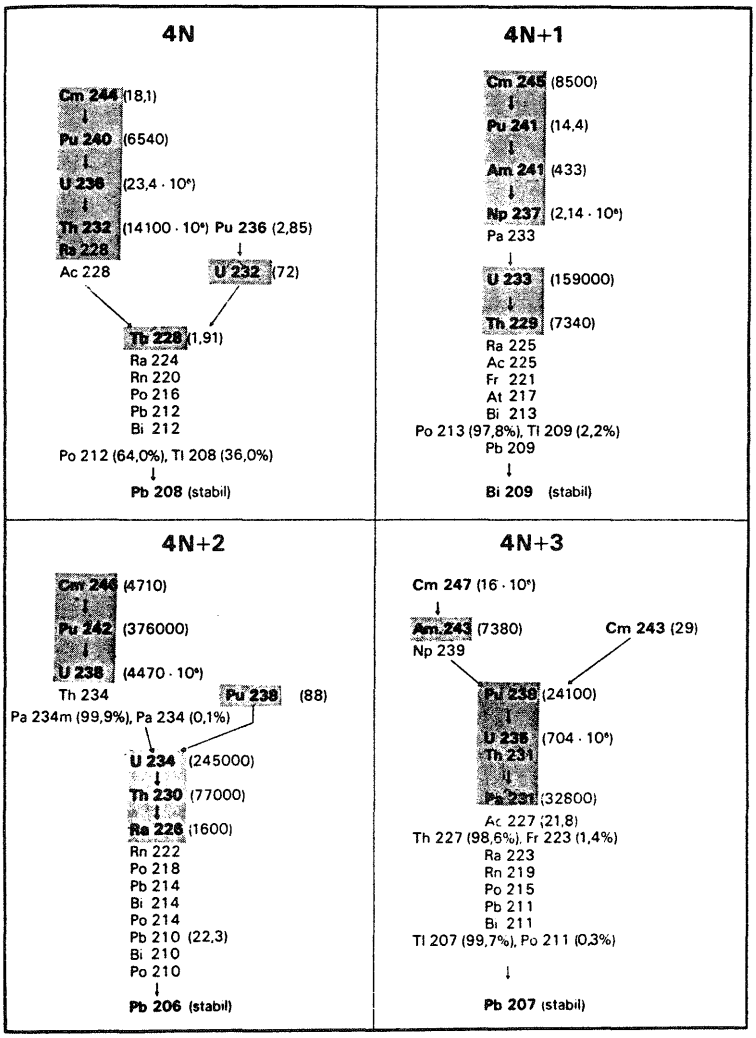

Figure 4-14 The four actinide decay chains with mass numbers 4N to 4N+3. The reduced decay chains are shaded

The SAFEST computer program allows a choice of desired output. The presentation of the release rates of the 38 radionuclides can be selected from a menu comprising:

- category-wise releases from 80 different waste categories
- releases from groups of waste, i.e. reprocessing, operational, decommissioning and medical waste
- releases from the four classes of toxicity into which the waste has been divided
- releases from the whole repository

SAFEST facilitates calculation of the effect of different waste allocation strategies and the output menu can be changed to give information about the release from a specific part of a repository e.g. one of the repository caverns.

5. RESULTS

5.1 General

The results presented in this chapter will show the effects on diffusive nuclide release from the near-field of:

- barrier material properties
- modelling strategy for the barrier design
- solubility limitations

As a reference case, the base case (N1) in /NGB 85-08/ has been selected and is presented in Section 5.2. The influence of barrier material properties is treated in Section 5.3, where the sensitivity to changes in the diffusivities due to early crack formation in the concrete containers and waste matrices is presented. In Section 5.5, the stepwise barrier degradation used in the base case calculations has been replaced by a continuous degradation.

The nuclide releases from two different simplifications of the barrier configuration are presented in Section 5.4 and are compared with the release obtained with the simplification used in the base case calculations. Furthermore, the decrease in nuclide release depending on limits of nuclide solubility in the porewater has been estimated in Section 5.6

The input data which are common to all calculations are given once, in the presentation of the base case.

The results of the calculations are presented as normalized nuclide release rates for both sorbing and non-sorbing nuclides, except for the base case and the parameter variation, for which the presentation comprises the individual nuclide releases.

5.2 Base case (N1)

The release rates for the predominant nuclides are presented for non-sorbing nuclides in Figure 5-2 and for sorbing nuclides in Figure 5-3.

Input data are presented below and divided into two sections; input data common to all calculations and specific base case input data.

Input data common to all calculations:

The nuclide inventory /NGB 85-02/ referred to is discussed in Chapter 2.

Material properties such as retention factors, porosities and densities for the engineered barriers are given in Table 5-1. The convective mass transfer coefficient, K_v, has been calculated to $6.5 \cdot 10^{-9}$ m/s assuming that the mean radius of the repository is 7.4 m, the porosity in the surrounding host rock is 4% and the velocity of the groundwater in the pores is $4 \cdot 10^{-7}$ m/s. This water velocity has been used in order to compare the results with those presented in /NGB 85-08/. A better estimation of the velocity of water can be found in /NTB 85-31/. Selecting a representative value of $1 \cdot 10^{-2}$ $m^3/m^2 \cdot$year for the ground water flux would give a K_v-value of $9.3 \cdot 10^{-10}$ m/s.

Table 5-1 Material properties common to all calculations

Barrier	Retention factor K_d*=0 m^3/kg	Retention factor K_d**=0.1 m^3/kg	Effective porosity m^3/m^3	Material density kg/m^3
Waste matrix	1	1000	0.2	2,300
Container backfill	1	1000	0.2	2,300
Concrete container	1	1000	0.15	2,300
Repository backfill	1	-	0.15	2,200
Repository liner	1	1000	0.15	2,300

* Non-sorbing Cl, Ni, Se, Sr, Pd, Sn, I, Cs
** Sorbing nuclides C, Zr, Tc, Ra, Th, Pa, U, Np, Pu, Am, Cm

Input data specific to the base case:

The diffusivity in the barriers is changed stepwise at 500 years and at 10,000 years; see Figure 5-1. The geometry simplification used is NET1 (see Section 4.4) and has been calculated with the computer code DOT. All nuclides are supposed to be soluble in the pore water, also the nuclides in the activated steel matrix.

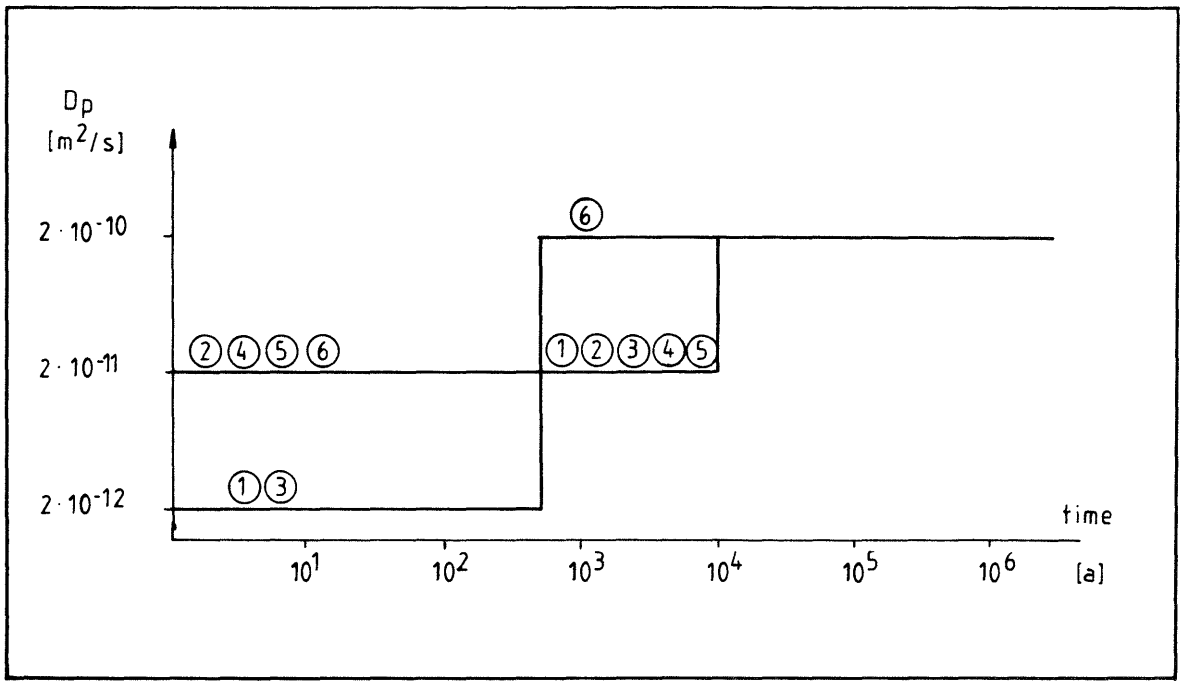

Figure 5-1 The diffusivities used for the base case N1
1) Matrix
2) Repository backfill
3) Container wall
4) Container backfill
5) Lining (inner)
6) Lining (outer)

The stepwise changes in diffusivities cause the sharp peaks in the release rate curves.

The predominant nuclides during different time periods are given below. It should be noticed that some nuclides decay almost completely within the system of barriers, e.g. Pu-241, Pu-238 and Cm-244 (compare Table 2.2).

Time period: 0 - 1000 years

During this period, Ni-63 is the predominant nuclide. The contribution from Ni-59 is also significant and increases towards the end of this period. Cs-137 and Sr-90 contribute markedly during the first hundred years but are of minor importance thereafter.

Time period: 1 000 - 10 000 years

Ni-59 is the predominant nuclide during the whole period.
Sn-126 is the second most important nuclide
Pd-107 and Cs-135 also contribute significantly to the release rate.

Time period: 10 000 - 100 000 years

During the first part of this period, Ni-59 is still the predominant radionuclide. From about the year 20 000 Pu-239 and Zr-93 will have higher release rates than Ni-59. Pu-240, with a maximum release rate at 30 000 years, is also of importance. Many of the other actinides also become more important towards the end of this period.

Time period: 100 000 - 1 000 000 years

Zr-93 reaches a maximum after 150 000 years and is the predominant nuclide during the whole period. Most of the actinides will also reach their maximum release rate. Although Pu-239 reaches a maximum after 50 000 years, the contribution from this nuclide is still significant during the first part of the period. At the end of the period, Th-229 and Np-237 will start to become the most important nuclides besides Zr-93.

Time period: After 1 000 000 years

After 1 million years, Zr-93 still gives the highest release rate. Some of the actinides, such as Np-237 and Th-229, are also significant.

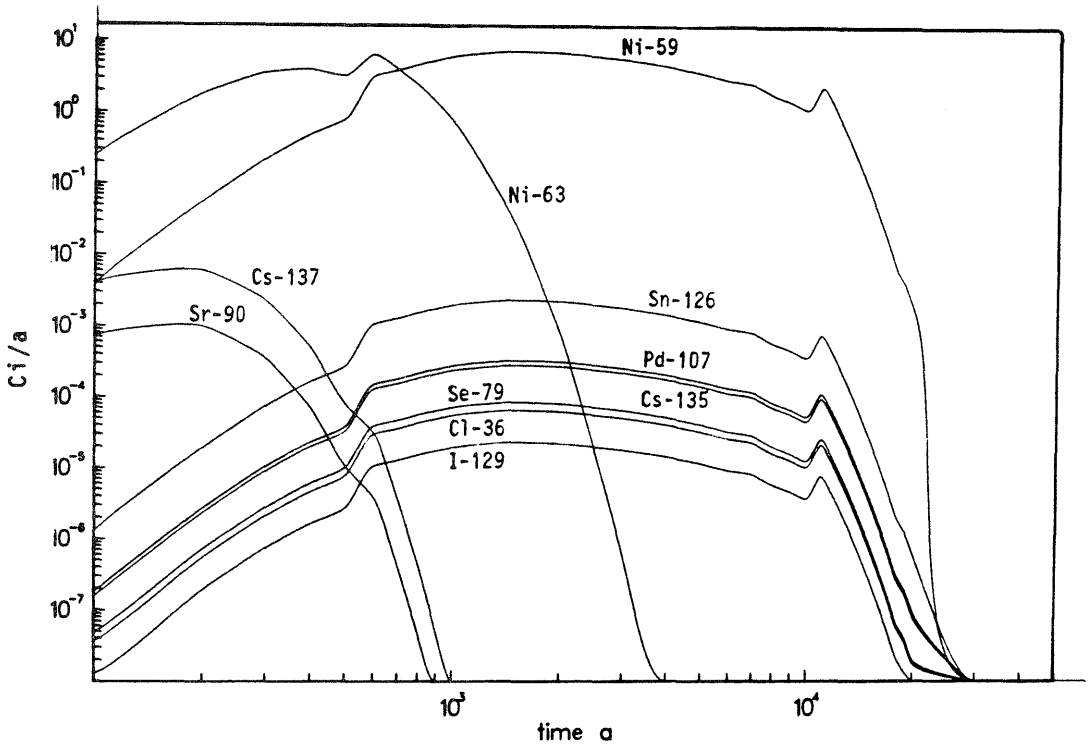

Figure 5-2 Radionuclide release rate (Ci/a) for the base case (N1), non-sorbing nuclides

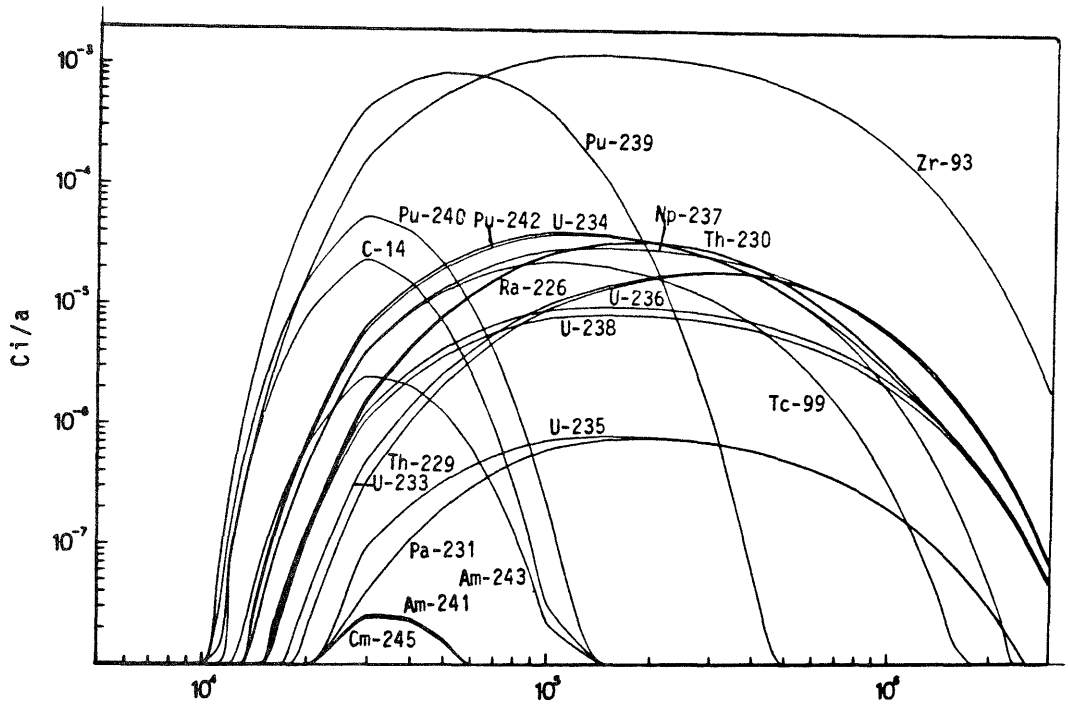

Figure 5-3 Radionuclide release rate (Ci/a) for the base case (N1), sorbing nuclides

5.3 Parameter variation (N2)

In the parameter variation it is assumed that extensive cracking has occurred in the waste matrix and the concrete containers during the first 500 years of storage. The diffusivities for both barriers are estimated to be $2 \cdot 10^{-11}$ m^2/s, compared to $2 \cdot 10^{-12}$ m^2/s for the base case (N1). The material properties are presented in Figure 5-4.

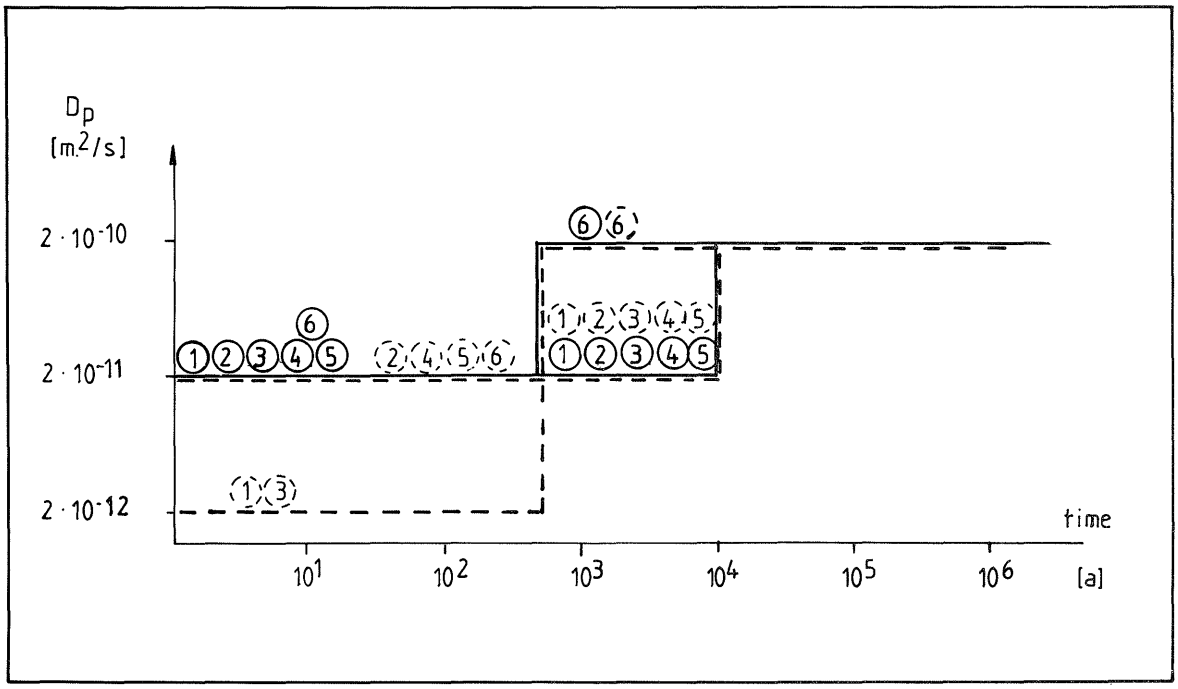

Figure 5-4 Diffusivities used for the parameter variation (N2) as compared with those of the base case (dotted lines)
1) Matrix
2) Repository backfill
3) Container wall
4) Container backfill
5) Lining (inner)
6) Lining (outer)

The effects of the cracked barriers can be seen by comparing Figures 5-5 and 5-6, where the normalized nuclide release rates for the base case (N1) and the parameter variation (N2) are presented respectively.

The normalized release rate is the release rate from one metre of the repository of an arbitrary non-decaying nuclide with a unity matrix concentration. Different release curves are obtained for sorbing and non-sorbing nuclides.

A higher diffusivity in both the waste matrix and container walls during the first 500 years influences only non-sorbing nuclides.

As can be seen in Figure 5-5, the release starts almost 200 years earlier and the maximum rate of release is somewhat higher. The latter conclusion is obscured by the peak on the curve introduced by the stepwise change in the diffusivity after 500 years.

As can be seen in Figure 5-6, the parameter variation has no significant influence on the release of the sorbed nuclides.

To facilitate the comparison, individual nuclide release curves were also calculated and are presented in Figures 5-7 and 5-8 for non-sorbing and sorbing nuclides respectively.

A comparison between Figure 5-7 and the corresponding Figure for the base case, Figure 5-2, confirms the principal conclusions drawn from the normalized release curves. The increase in the release rate is a factor of 2.

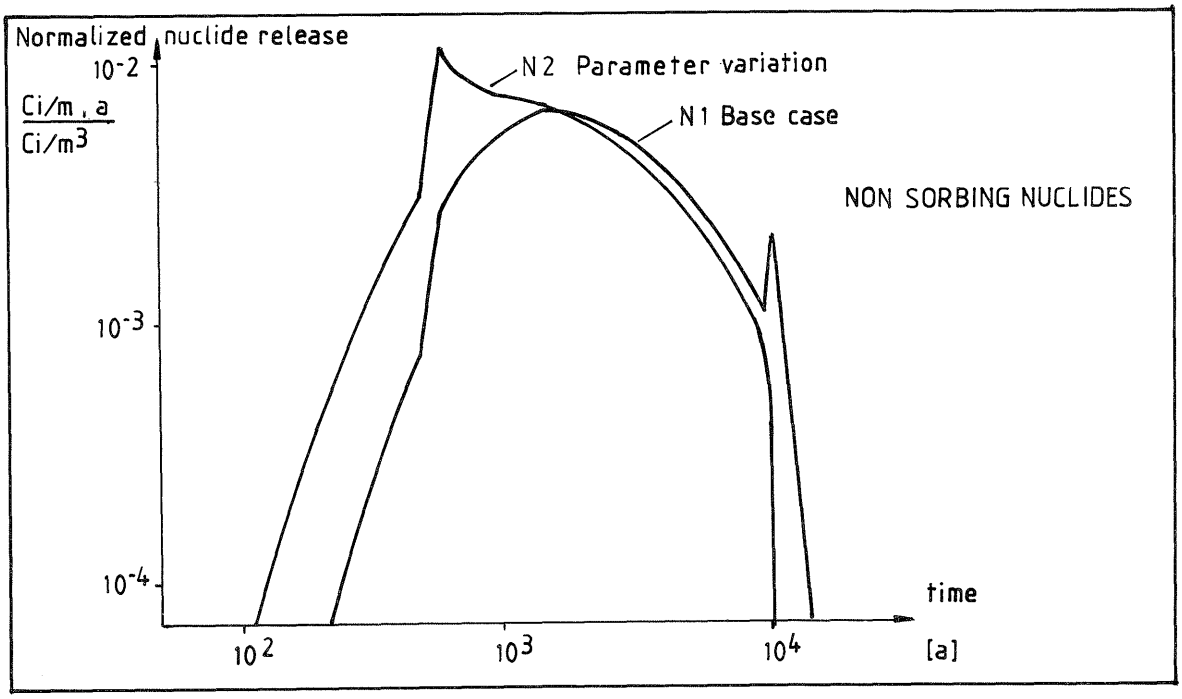

Figure 5-5 Normalized nuclide release rate, assuming no decay, for the base case (N1) and the parameter variation (N2), non-sorbing nuclides (Kd=0.1 m^3/kg)

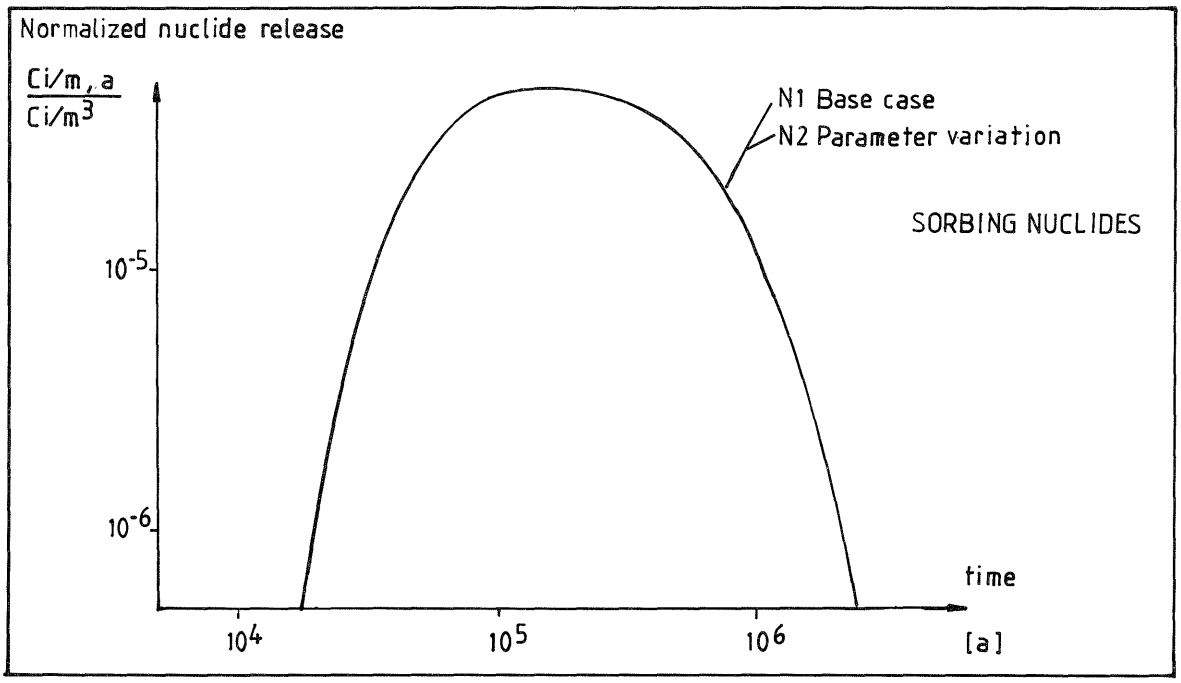

Figure 5-6 Normalized nuclide release rate, assuming no decay, for the base case (N1) and the parameter variation (N2), sorbing nuclides (Kd=0.1 m^3/kg)

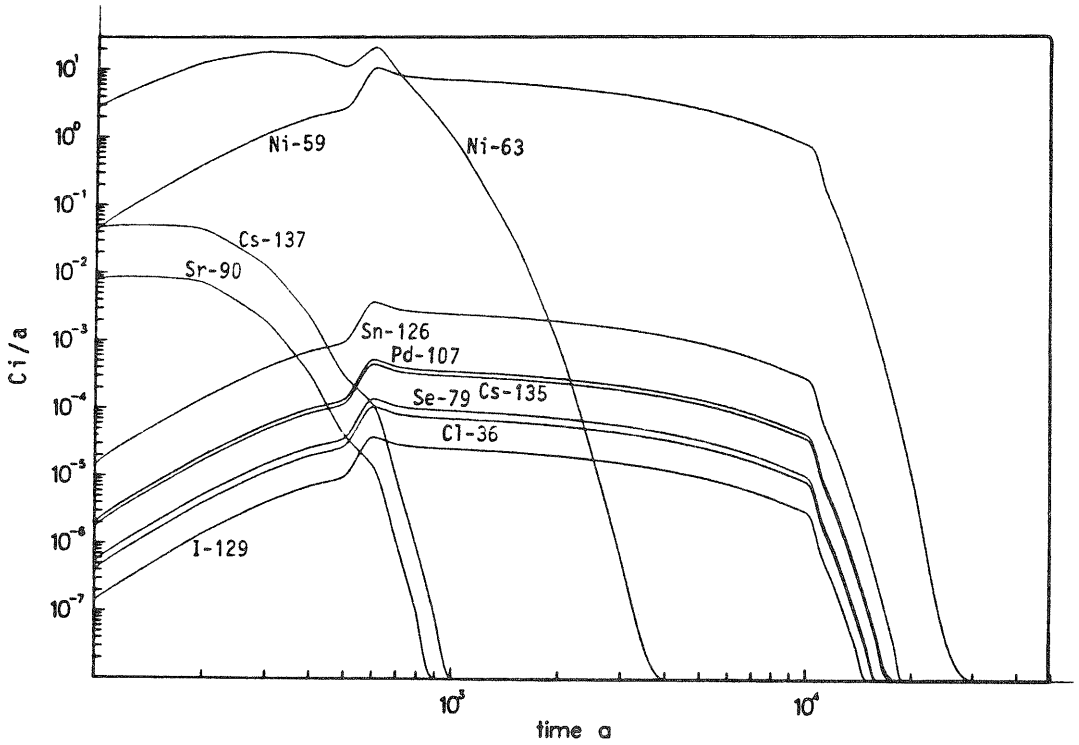

Figure 5-7 Radionuclide release rate for the parameter variation (N2), non-sorbing nuclides (Kd=0 m^3/kg)

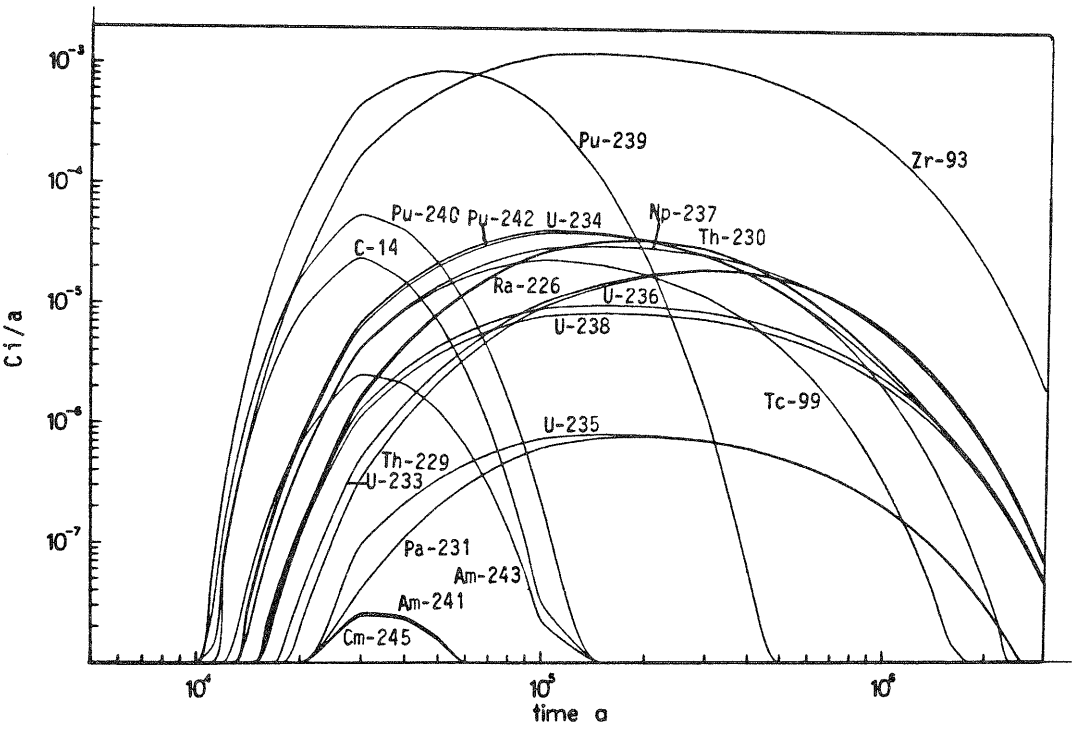

Figure 5-8 Radionuclide release rate for the parameter variation (N2), sorbing nuclides (Kd=0.1 m^3/kg)

5.4 Other simplifications of the barrier geometry

To verify the simplification of the repository geometry used in the base case (N1) calculations, the releases from two other simplifications have been computed. As indicated in Table 5-2, the diffusion equations have been solved with DOT for NET2 and with TRUMP for NET3. A presentation of the barrier dimensions for the nets is found in Section 4.4.

Table 5-2 Case presentation

Case	Model net*	Computer code**
N1	NET1	DOT
NR1	NET2	DOT
NR2	NET3	TRUMP

* see Section 4.4
** see Section 4.5

The same barrier material properties have been used in all three calculations, i.e. the values used for the base case (N1)μ see Section 5.2.

The total release from the repository can be checked with a mass balance. The release curves integrated over the time during which nuclides are released should equal the initial inventory for a non-decaying nuclide. In Table 5-3, a comparison is made between the calculated integrals of release and the initial inventories for the different calculated cases. It can be concluded that the agreement is good.

Table 5-3 Mass balance check for the normalized release rates from the repository. The initial activity in the repository is given for comparison. All figures are given for a one metre section of the repository caverns

Case content	Cumulative release according to mass balance (Ci)		Initial in the repository (Ci)
	non-sorbing (Kd=0. m^3/kg)	sorbing (Kd=0.1 m^3/kg)	
N1	34.9	37.4	32.5
NR1	29.3	33.4	32.4
NR2	32.2	32.3	32.2

The results are presented as normalized nuclide release rates for both non-sorbing and sorbing nuclides; Figures 5-9 and 5-10. The stepwise diffusivity changes at 500 and 10,000 years are responsible for the peaks that can be seen in the curves.

The results for the different simplifications of the repository geometry differ by less than a factor of 3. This shows that the effects of the simplifications made in the different models are acceptable. The results obtained for the more detailed geometry (NR2) show that the release rates can be expected to be somewhat lower that those presented in the base case calculations for Project Gewähr /NGB 85-08/.

The observed differences in the peak heights after 10^4 years depend on the different remaining contents of nuclides in the repository at the time of diffusivity changes.

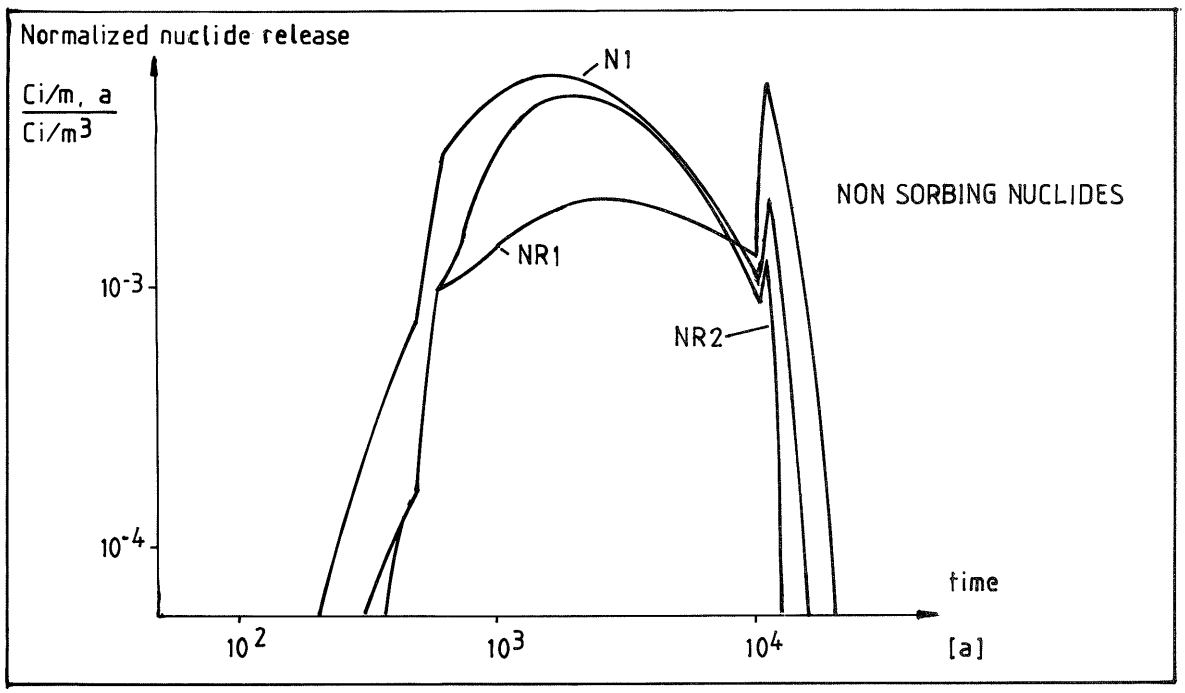

Figure 5-9 Normalized nuclide release from different simplifications of the geometry, non-sorbing nuclides (Kd=0. m^3/kg)

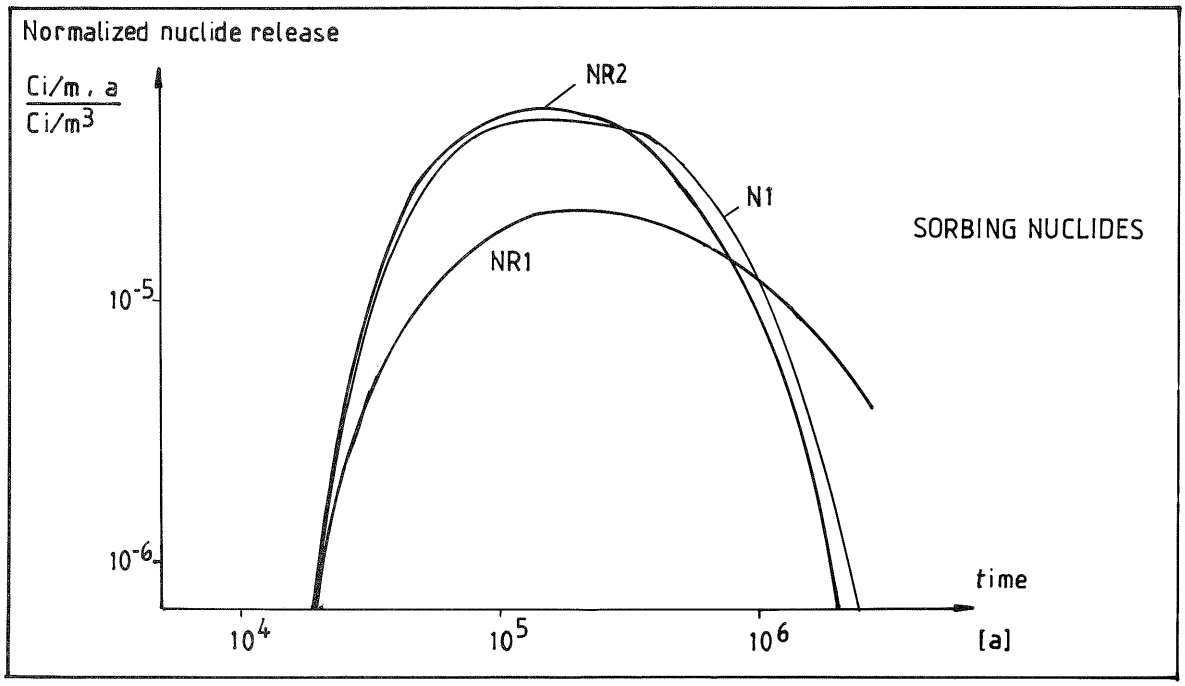

Figure 5-10 Normalized nuclide release from the different simplifications of the geometry, sorbing nuclides (Kd=0.1 m^3/kg)

5.5 Continuously degrading barriers (NR3)

To improve the representation of barrier degradation, the nuclide release rates have been calculated using continuously degrading barriers, i.e. continuous changes in the barrier diffusivities. These calculations have been carried out with NET3 which is in good agreement with the base case geometry. For these calculations, it was necessary to use the computer code TRUMP which can handle time-dependent material properties. Except for the differences due to continuous instead of stepwise changes in the diffusivities (Figure 5-11), all other input data are the same as those used in the base case calculations.

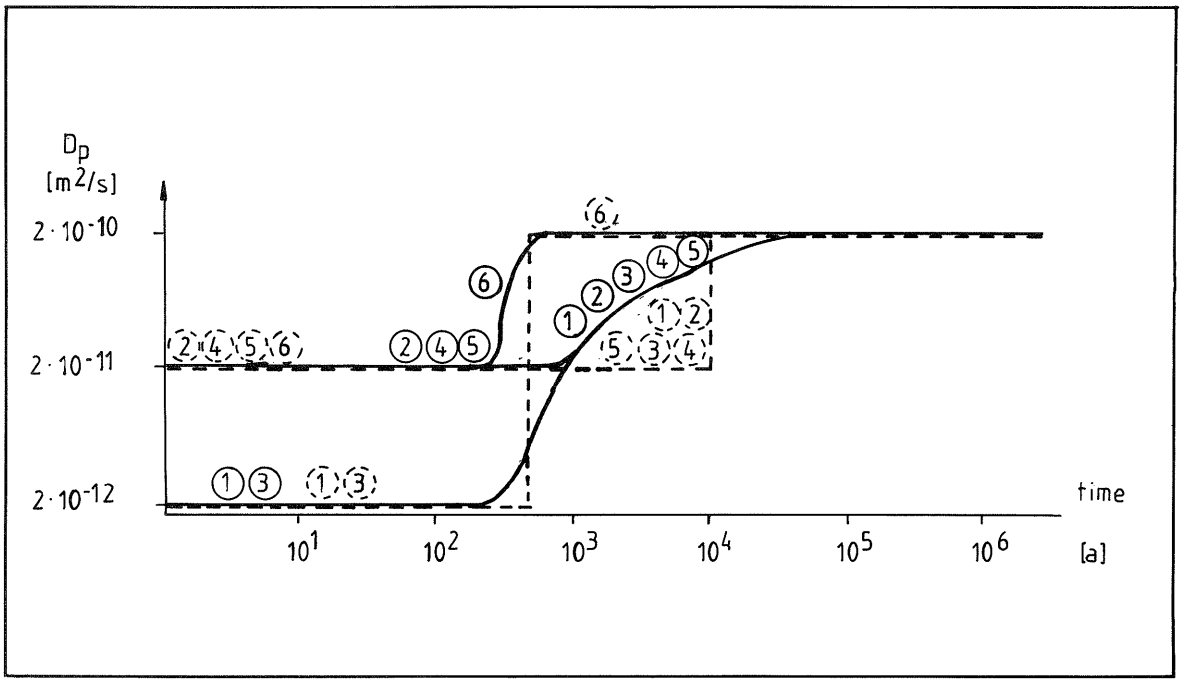

Figure 5-11 The continuously changing diffusivities used as compared with the base case diffusivities
1) Matrix
2) Repository backfill
3) Container wall
4) Container backfill
5) Lining (inner)
6) Lining (outer)

The diffusivity change in the outer half of the lining begins at 250 years and increases linearly from $2 \cdot 10^{-11}$ to $2 \cdot 10^{-10}$ m^2/s at 750 years.

The diffusivity in the inner half of the lining and in the container and repository backfill is a constant $2 \cdot 10^{-11}$ m^2/s during the first 750 years and then increases linearly during the time period 750 -15,000 years to $2 \cdot 10^{-10}$ m^2/s.

The degradation of the waste matrix and the container walls begins after 250 years and the diffusivity increases linearly from $2 \cdot 10^{-12}$ to $2 \cdot 10^{-11}$ m^2/s at 750 years. Thereafter the degradation rate decreases and the diffusivity changes from $2 \cdot 10^{-11}$ to $2 \cdot 10^{-10}$ m^2/s during the following 14,000 years.

The continuous degradation of the barriers begins earlier than the stepwise, after 250 years rather than after 500 years. This can be seen in the normalized nuclide release rate curves, Figures 5-12 and 5-13. The release rate is higher at an early stage for both non-sorbing and sorbing nuclides. The maximum release rate for continuously degrading barriers (NR3) is two times higher than the maximum release rate for stepwise degradation (NR2) in the case of non-sorbing nuclides. For sorbing nuclides, no difference in the maximum value of the release rate can be detected.

The conclusion is that NR3 is slightly more conservative but deviates from NR2 within acceptable limits.

In Section 5.4, it was concluded that NR2 was in good agreement with the base case. Consequently the agreement between the base case and NR3 is also acceptable and the combination NR3 (NET3, TRUMP, continuously changing diffusivities) can be used for future base case calculations.

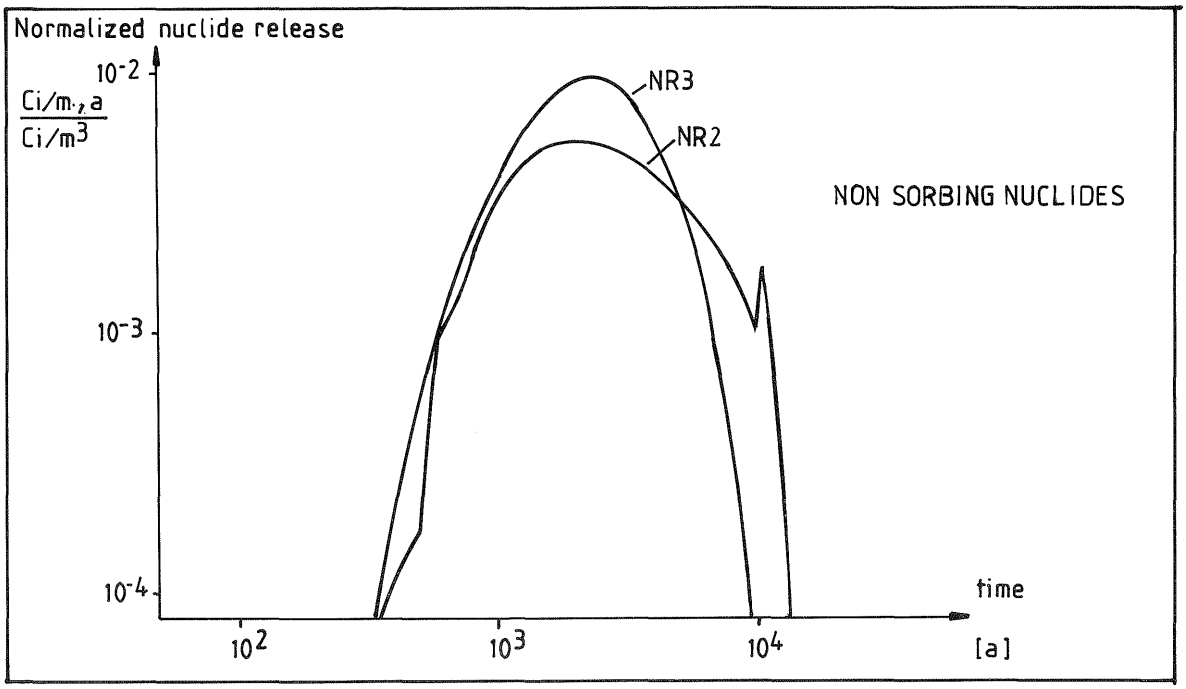

Figure 5-12 Normalized nuclide release, stepwise (NR2) and continuously degrading barriers (NR3), non-sorbing nuclides (Kd=0. m^3/kg)

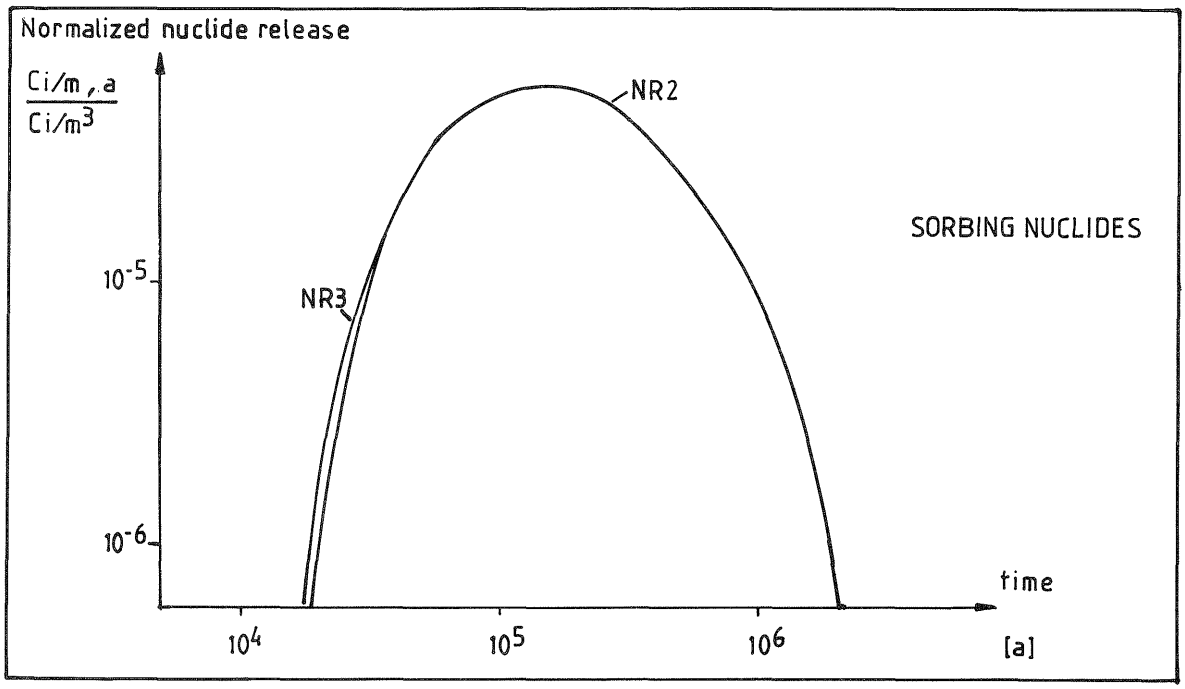

Figure 5-13 Normalized nuclide release, stepwise (NR2) and continuously (NR3) degrading barriers (NR3), sorbing nuclides (Kd=0.1 m^3/kg)

5.6 Solubility limitations (NR4)

Solubility limitations can markedly lower the release of some nuclides from the repository, e.g. Ni, Se, U. The effect depends, however, on the degree of uncertainty in the predicted solubility limits. The calculation of solubility limits for the nuclides in the repository is discussed in Chapter 3 and the selected data are presented in Tables 3-3 and 3-5. For the following calculations, the repository geometry NET3 has been used (see Section 4.4). As described in Section 4.3, the concentration at the waste matrix boundary is kept constant during dissolution of the solid phase as long as there is solid phase present and the effects of a moving boundary are disregarded. With this approach, the normalized release rate curves reach steady-state after 17,000 years for nonsorbing nuclides (Figure 5-14) and after 100,000 years for sorbing nuclides (Figure 5-15).

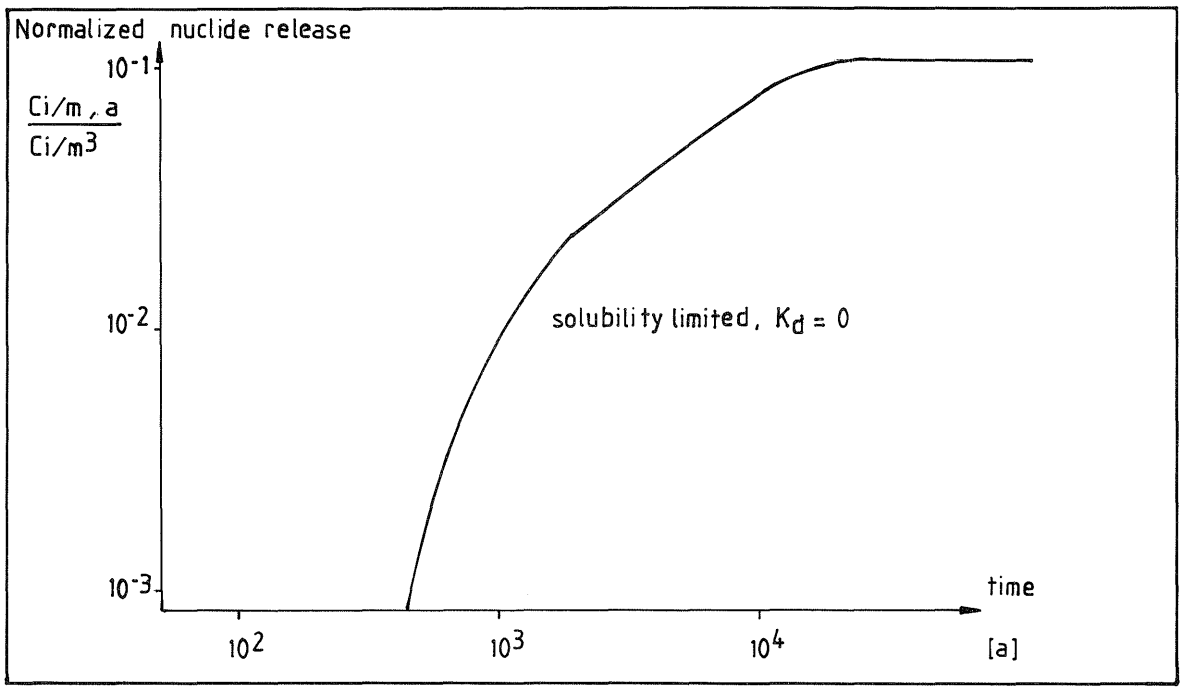

Figure 5-14 Normalized nuclide release, solubility-limited, non-sorbing nuclides

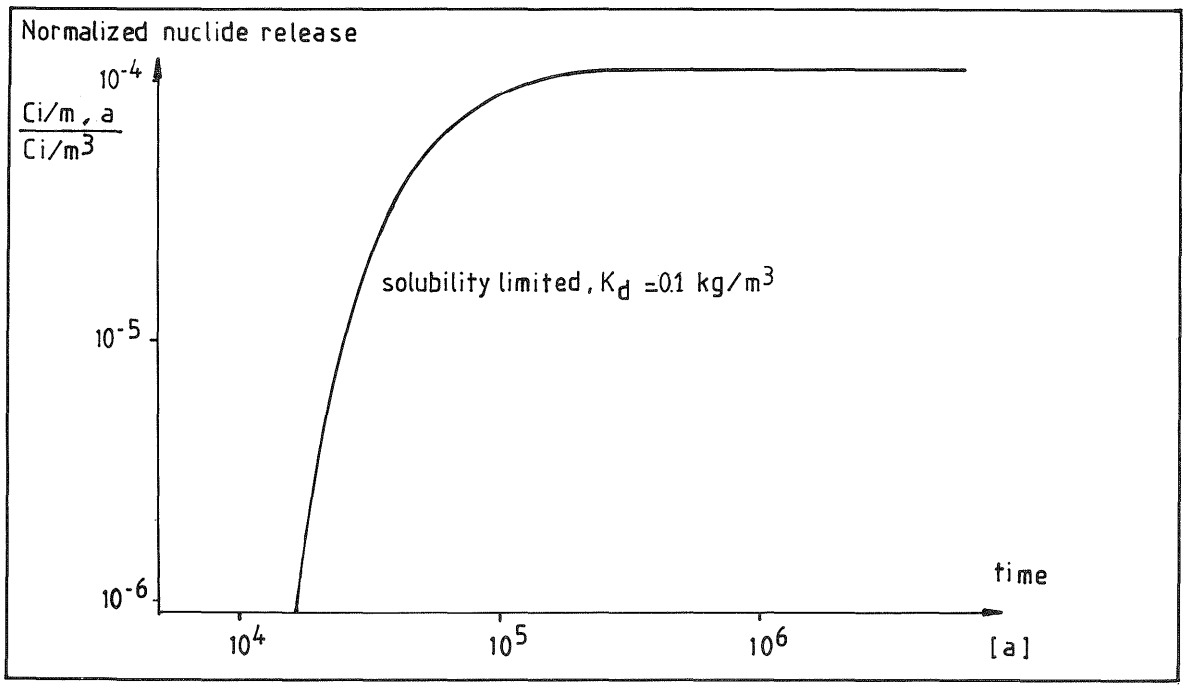

Figure 5-15 Normalized nuclide release rates, solubility-limited, sorbing nuclides

The significance of the solubility limitations for the nuclide release rate is shown in Figures 5-16 and 5 - 17a-b where the release rates from calculations with and without solubility limitations are compared. From these Figures, it is obvious that the calculated solubility limits have an effect on the release of nickel, palladium, uranium, neptunium, thorium and technetium.

When more than one isotope of an element is present in the waste, the solubility of the radioactive isotopes is determined by equation 5-1. Accordingly the solubility will determine the algebraic sum of the concentration of the isotopes. It has been assumed that the concentrations of the different isotopes are proportional to their relative content in the waste.

$$C_{s_i} = \frac{C_i}{\sum_i C_i} C_{s_e} \qquad (5\text{-}1)$$

where

C_{si} = actual solubility of isotope i
C_i = total concentration of isotope i
C_{se} = total solubility of the element

The relative content of the long-lived isotopes will increase with time due to the decay of the short-lived nuclides. Thus, the release of long-lived isotopes will increase with time. This effect can be seen in e.g. Figure 5-17 a-b for the uranium isotopes. The calculated maximum release rate of uranium isotopes is decreased more than thirty times when solubility limitations are considered, even though uranium has a limited solubility only in some of the waste categories. Plutonium initially has a limited solubility in a few waste categories but the effect is small and does not affect the total release rate.

The maximum release rates of thorium isotopes are decreased about five times. This is about the same as for technetium. The decrease for nickel is more than 10^3 times and for selenium about 50 times. It should be noticed that the maximum release rate is directly influenced by a limited solubility, whereas the total integrated release is affected indirectly via the decay since the nuclides are contained in the barriers for an extended time period.

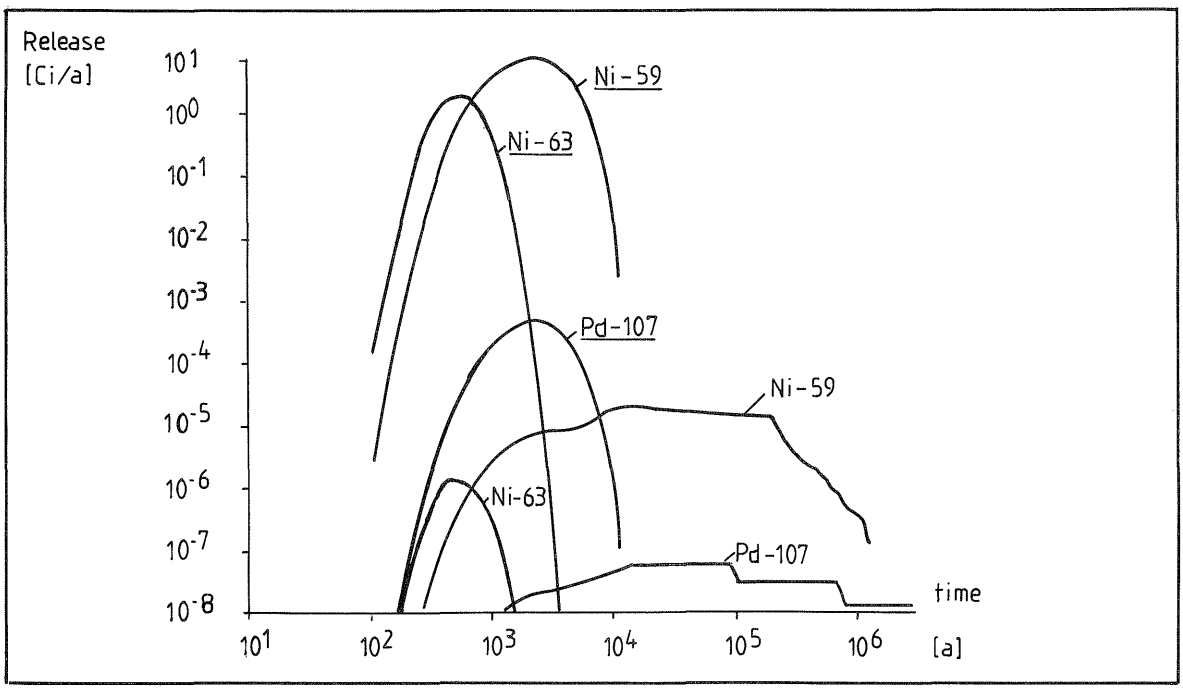

Figure 5-16 Comparison between nuclide release rates for nuclides assumed to be either solubility-limited or soluble, non-sorbing nuclides (Ni and Pd) (Kd=0. m^3/kg)

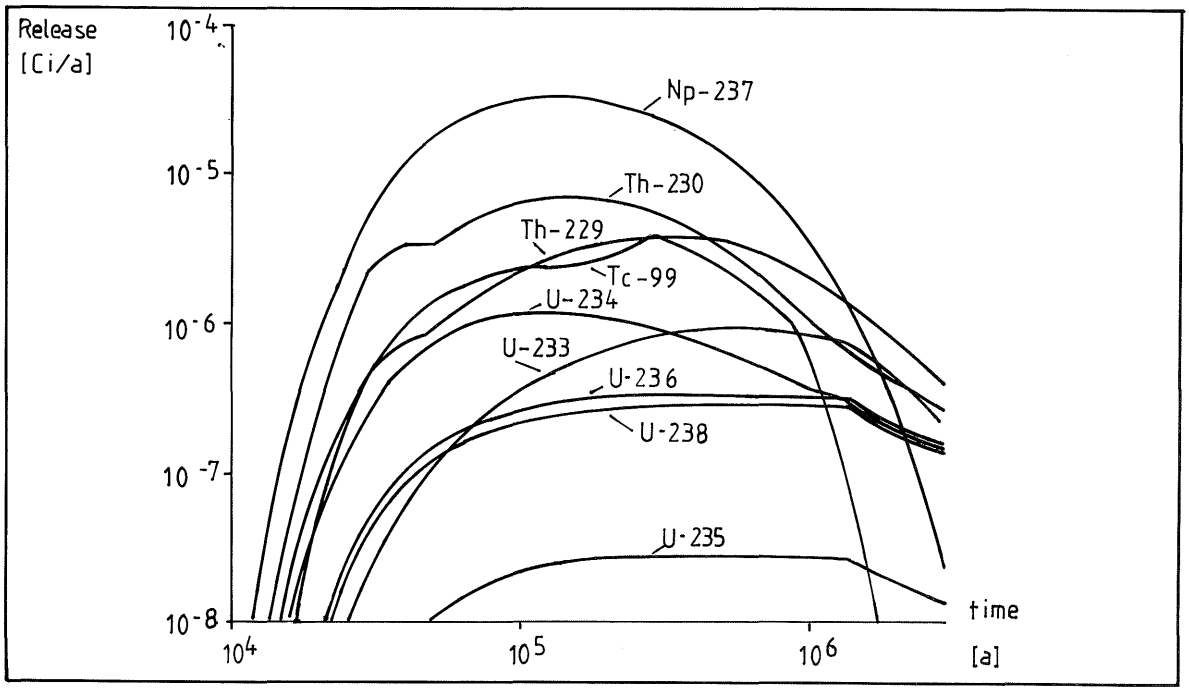

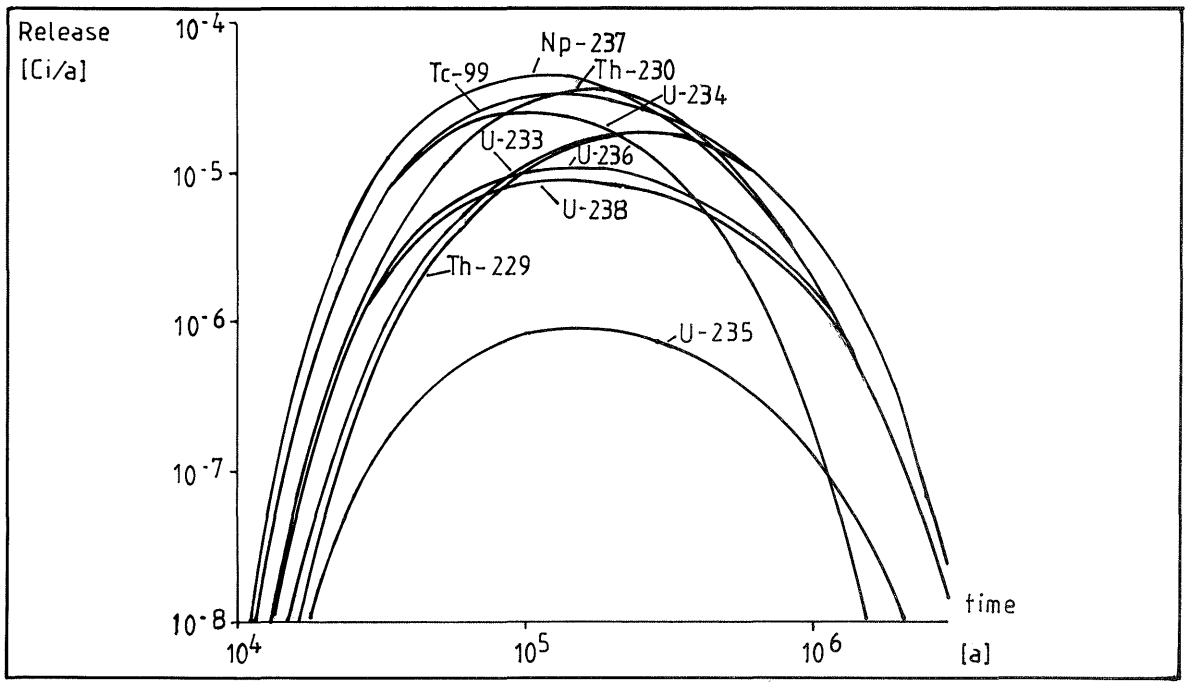

Figure 5-17a-b Comparison between nuclide release rates for nuclides assumed to be either solubility-limited (a), or soluble (b), sorbing nuclides (U, Np, Th, Tc) (Kd=0.1 m^3/kg)

5.7 Combination of the effects. Total release from the repository

The total nuclide release rates presented in Figures 5-18 and 5-19 are based on calculations including some effects which were disregarded in /NGB 85-08/. These effects are continuously degrading barriers and solubility limits.

The input data are summarized in Table 5.4.

Table 5-4 Summary of input data for the case presented in Figures 5-18 and 5-19

Repository model	NET3, Figure 4-11, Table 4-4
Material properties	Table 5-3, common input data
Solubility limitations	Table 3-5

It can be concluded that the release of some of the critical radionuclides will be considerably reduced when solubility limitations are considered. The effect is clearly visible for Ni, Pd, Tc, U and Th. The maximum release rate of nickel is decreased 100,000 times, palladium is decreased 5000 times, uranium 30 times and technetium and thorium are reduced about five times.

The continuous degradation of the barriers has no significant effect on the nuclide release rates, except that the sharp peaks on the curves occurring in the base case are eliminated.

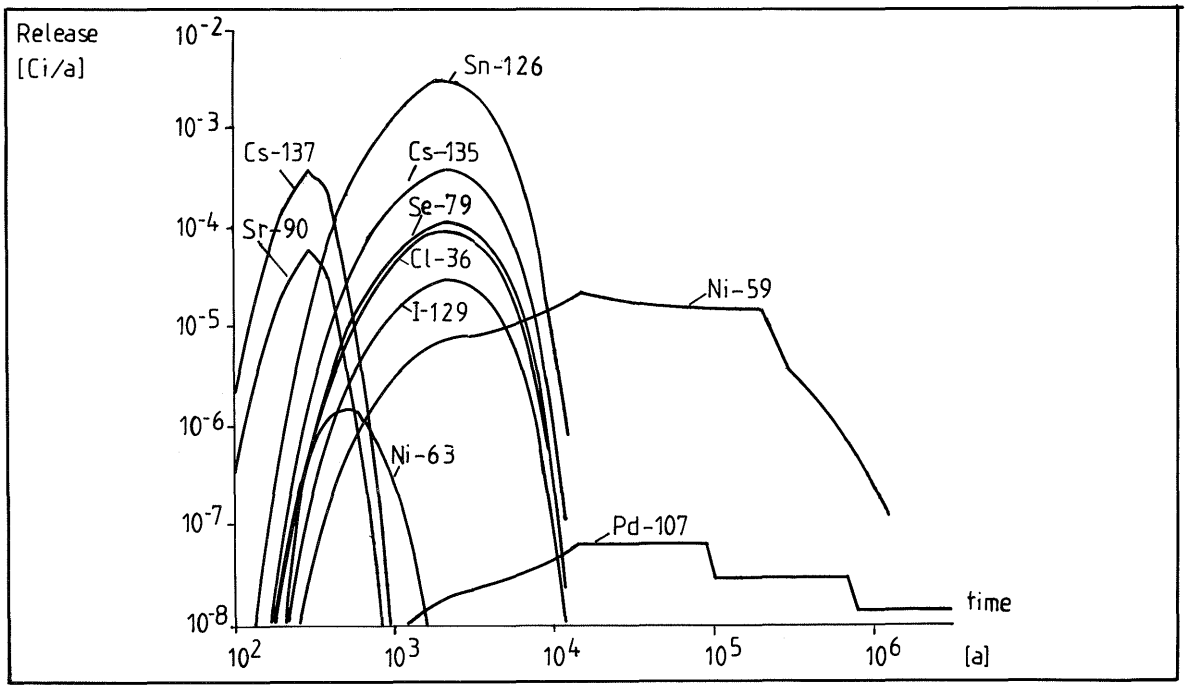

Figure 5-18 Total radionuclide release rates (Ci/a), non-sorbing nuclides (Kd=0. m^3/kg)

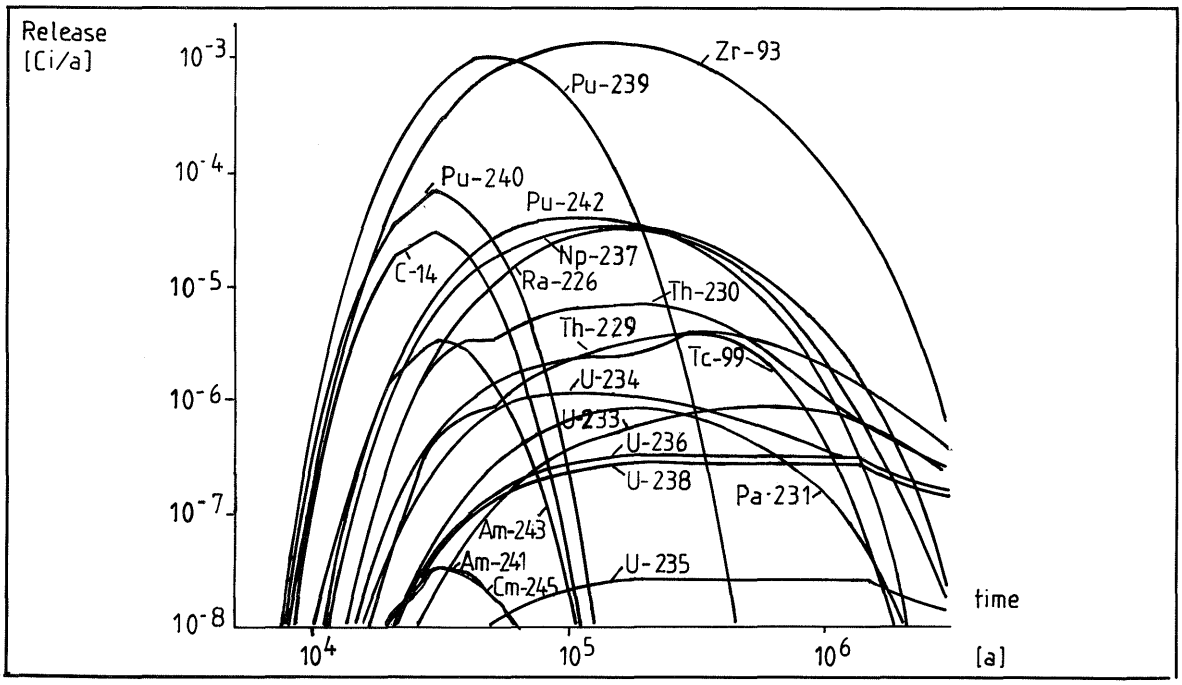

Figure 5-19 Total radionuclide release rates (Ci/a), sorbing nuclides (Kd=0.1 m^3/kg)

6. CONCLUSIONS

The basic purpose of this report is to present the release rates from the near-field of the repository for all radionuclides which may be significant for the safety analysis. These release curves serve as source terms for the far-field calculations.

The calculations are performed for a base case defined by a simplified barrier configuration in the repository for the selected model site at Oberbauen Stock. An important item is also the division of the waste into several categories which can be handled with a specially designed computer program.

6.1 The base case release

There are noticeable differences in release rates between non-sorbed and sorbed nuclides. The sorption on solid surfaces within the barriers will result in a considerable delay of release and, thereby, the effect of radioactive decay within the barriers is more pronounced. The actinides and some of the fission and activation products belong to the sorbing radionuclides.

The earliest release of non-sorbed nuclides will be delayed by the near-field barriers for less than 100 years, but the release rate will be limited and will not exceed 10^{-2} Ci/a. The only exception is the release of nickel which is currently predicted to be higher but which will be discussed separately below.

None of the sorbed nuclides will be released (limit $<10^{-8}$ Ci/a) before 10,000 years and will not reach a rate higher than 10^{-3} Ci/a at any time.

When judging these release rates it must be kept in mind that the release is further delayed and dispersed in the geosphere and biosphere. There is also a considerable difference in radiotoxicity between the nuclides.

6.2 Aspects on uncertainties and sensitivities

The uncertainties in the results can be related to the following components of the calculations:

- Assumptions of the conceptual model
- Mathematical formulation of the conceptual model
- Parameter uncertainties
- Simplifications, e.g. of the configuration, discretization

An overriding source of uncertainty is the influence of parameter changes with time as well as of changes in the phenomenology with time.

The fundamental phenomenological assumption made is that the release is diffusion-controlled. Two aspects are worth mentioning:

- The water flow in the surrounding rock is limited. Around the repository, a decompressed zone is believed to exist with a higher permeability than the host rock. The permeabilities of the repository lining and the barriers inside the repository are low. Consequently, it can be proved that the advective flow of water inside the repository will be negligible until major degradation of the barriers occurs. The effects of advective flow were not described in this report but can be found in /NGB 85-08/.
- Substantial quantities of gas are generated inside the repository. Whether or not the flow of gases can cause transport of nuclides dissolved in water from inside the repository to the host rock is still not clearly known. This effect is not treated in this report but the consequences of a gas displacement scenario are described in /NGB 85-08/.

Another phenomenological assumption is that the total content of radionuclides in the waste is completely dissolved in the porewater and available for diffusive transport.

This is obviously an overconservative assumption for some cases. One example is nuclides inside activated steel, another is nuclides with low solubilities.

Modelling essentially consists of two parts:

- Simplification of the repository geometry enabling a computerized description of the real barriers in the repository (discretization).

- Diffusion transport models including solubility limits, sorption and decay.

The risk of introducing major errors in these areas is small. A cross-comparison between three geometry simplifications and two computer codes was made with small deviations between the results obtained.

The major uncertainty of the input data is their unknown time- and concentration-dependence. The data of the greatest importance are the properties of the barrier materials, mainly concrete.

Due to the chemical interaction with groundwater, but also due to processes within the waste, the concrete will degrade. A first estimate of such a degradation was made and applied to the diffusivities of the barriers. The diffusivities were assumed to increase from values typical for newly made concrete to values close to those of sand.

The consequences for the release rates of an early formation of cracks in the matrix and the container walls were tested by a parameter variation and were found to be limited.

Even more important than the diffusivities are the K_d-values describing the sorption of the nuclides. For most of the nuclides, no sorption was assumed, which is the most conservative approach. For almost all the sorbed nuclides, the K_d-values used were lower than those reported from experiments in a concrete-controlled environment. No parameter variations have been made for the K_d-values but it is known that the release rates are very sensitive to this parameter.

6.3 Improvements

Several areas exist where improvements are possible to reduce the calculated release rates. Also, the uncertainties in prediction of some processes can be improved.

It has been demonstrated in this report that several nuclides should not be treated as completely dissolved in the porewater. Their solubilities are too low.

When solubility limits are applied to the calculations, the release rates of some nuclides are reduced by several orders of magnitude. Nickel was mentioned above as a predominant nuclide. By the introduction of solubility limits, it becomes unimportant. A more detailed study of the chemical situation in the waste would give more reliable information on the actual nuclide solubilities.

A second area where improvements are required is the long-term interaction between the groundwater and the concrete barriers. The results of such a study will have a bearing on important long-term properties of the concrete such as diffusivities, K_d-values and permeabilities.

A third area of interest is a deeper understanding of the consequences of gas formation within the repository.

REFERENCES

/1/ Bengtsson, A., Magnusson, M., Neretnieks, I., Rasmuson, A. (1983): Model calculations of the migration of radionuclides from a repository for spent nuclear fuel. KBS Technical Report TR 83-48.

/2/ International Commission on Radiological Protection (1979): Limits for intake of radionuclides by workers, ICRP Publ. 30, Ann. ICRP 3 (4).

/3/ Biczok, I. (1968): Beton korrosion - Beton schutz. Bauverlag GMBH, Wiesbaden-Berlin.

/4/ Bergström, S.G., Fagerlund, G., Romben, L. (1977): Bedömning av egenskaper och funktion hos betong i samband med slutlig förvaring av kärnbränsleavfall i berg. Cement- och Betonginstitutet, KBS Technical Report TR-12.

/5/ Snellman, M., Uotila, H. (1984): Chemical conditions in the repository for low- and intermediate-level reactor waste. Report YJT-84-11. Nuclear Waste Commission of Finnish Power Companies.

/6/ Högfeldt, E.: Stability Constants of Metal-Ion Complexes. (Part A). (Chemical Data Series: No. 21) 1, Pergamon Press, 1982. Perrin, D.D., Stability Constants of Metal-Ion Complexes. (Part B). (Chemical Data Series: No. 22), Pergamon Press, 1979. Sillen, L-G., Stability Constants of Metal-Ion Complexes, Supplement No. 1, Part 1-2. Special Publication No. 25, The Chemical Society, London 1971.

/7/ Neretnieks, I. (1978): Transport of oxidants and radionuclides through a clay barrier. Kungl. Tekniska Högskolan, Stockholm, KBS Technical Report TR-79.

/8/ Bird, R.B., Stewart, W.E., Lightfoot, E.N. (1960): Transport phenomena. Wiley International Edition.

/9/ Poliwka, R.M., Wilson, E.L. (1976): Finite element analysis of nonlinear heat transfer problems. Dept. of Civ. Eng., Univ. of California, Berkeley, Report No. UC SESM 76-2.

/10/ Edwards, A.L. TRUMP (1969): A computer program for transient and steady state temperature distributions in multidimensional systems. National Technical Information Service, National Bureau of Standards, Springfield, Va.

/11/ FEMGEN USER MANUAL (1983) Version 8.2.

/12/ KEMAKTA Consultants Co, Stockholm, Personal Communication.

/13/ Lester, D.H., Jansen, G., Burkholder, H.C. (1975): Migration of radionuclide chains through an adsorbing medium. AIChE Symposium Series No. 152:71, 202.

/14/ Moore, W.J. (1974): Physical Chemistry, Fifth edition, Prentice Hall, Inc. Englewood Cliffs, New Jersey, USA.

/15/ Pourbaix, M. (1966): Atlas of electrochemical equilibria in aqueous solutions, Pergamon Press Ltd, London.

REFERENCES TO NGB- AND NTB-REPORTS

NGB 85-02 Radioactive waste: Properties and allocation to repository types.

NGB 85-06 Repository for low- and intermediate-level waste: Construction and operation.

NGB 85-07 Repository for low- and intermediate-level waste: Safety barrier system.

NGB 85-08 Repository for low- and intermediate-level waste: Safety report.

NTB 85-17 Gas formation in a Type B Repository and Gas transport in the Host-Rock; M. Wiborgh, L.O. Höglund, K. Pers, Kemakta Konsult, Schweden; in press.

NTB 85-18 Actinide Solubilities and Speciation in a Repository Environment; B. Allard, RCG Konsult, for Kemakta Consultants Co Schweden.

NTB 85-19 Organic Complexing Agents in Low and Medium Level Radioactive Waste; B. Allard, RCG Konsult, for Kemakta Consultants Co, Schweden.

NTB 85-21 Radionuclide Sorption in Concrete; B. Allard, RCG Konsult, for Kemakta Consultants Co, Schweden.

NTB 85-31 Three Dimensional Model Calculations of Groundwater flow at Oberbauenstock; B. Lindbom, A. Markström, B. Grundfelt, Kemakta Konsult, Schweden; in press.

NTB 86-15 Degradation of Concrete - Repository Type B; L.O. Höglund, KEMAKTA Consultants Co, Sweden, in press.

APPENDIX 1

SUBSTANCES CONSIDERED AND REACTION FORMULAE USED WHEN ESTABLISHING THE EQUILIBRIUM DIAGRAMS

1 INTRODUCTION

The electrochemical diagram of an element summarizes, in an extremely condensed form, the solution chemistry of the element.

For each of the elements, it is a question of characterization of the equilibrium conditions for systems whose constituent species are: the element in question and its ions in aqueous solution, water and its constituents (H^+ and OH^- ions, gaseous hydrogen and oxygen) and the products of the reactions of the element with these species (oxides, hydroxides, hydrides etc).

Solution reactions very often involve a transfer of electrons, e^-, from a reducing agent to an oxidizing agent. These so called redox-reactions or electrochemical reactions can be used together with the Nernst formula to calculate the limits of the domains of relative predominance of dissolved substances and the domains of relative stability of the elements and their oxides. For an arbitrary electrochemical reaction written in the form:

$$aA + cH_2O + ne^- = bB + mH^+$$

in which A is the oxidized form and B the reduced form of the element in question, the Nernst equation describing the condition for equilibrium at 25 °C will be of the form:

$$E_o = E_o - 0.0591\ m/n\ pH + 0.0591/n\ \log\ (ox)^a/(red)^b$$

If instead the reaction is a chemical reaction written in the form:

$$aA + cH_2O = bB + mH^+$$

in which B is the alkaline form and A is the acid form of the element in question, the condition for equilibrium will be of the form:

$$\log ((B)^b/(A)^a) = \log K + mpH$$

This expression can be derived from the general formula for chemical equilibria, which can be explained in the following way. When the equilibrium state of a chemical change is obtained at a given temperature and pressure, the algebraic sum of the logarithms of the fugacities and activities of the reacting substances is equal to a constant log K. The value of the constant depends only on the temperature and pressure and can be calculated from the values of the standard chemical potential of all the reacting substances in their standard reference state /14/.

2 CONSTRUCTION OF THE EQUILIBRIUM DIAGRAMS

If the electrode potential and the pH are considered as independent variables, logarithmic functions of the concentrations of the reacting substances (potential-pH-equilibrium diagrams) can be established.

The lines which express the reduction of water according to the reaction:

$$2H^+ + 2e^- = H_2$$

respectively, the oxidation equilibrium according to the reaction:

$$O_2 + 4H^+ + 4e^- = 2H_2O$$

can be constructed from the following expressions for 25 °C:

$$E_o = 0.000 - 0.0591\ pH \qquad (V)$$

and

$$E_o = 1.228 - 0.0591\ pH \qquad (V)$$

The drawing of lines expressing the conditions under which the activities of two dissolved substances are equal makes it possible to represent the domains of relative predominance of the dissolved species in question.

The drawing of lines which express the equilibrium conditions between two solid substances also makes it possible to represent the domains of relative stability of the solid substances in question.

The area under which a given solid substance and a given dissolved substance can be simultaneously stable can be calculated by the method described below:

By giving the activity of the dissolved substance a definite value in the equilibrium equation (e.g. 10^{-6} mole/l), it is possible to define a line which represents the conditions under which the dissolved form of the solid substance considered has this value. It is often useful to establish such lines for different solubility values. After combining some lines and omitting those lines or parts of a line which have no practical interest, the electrochemical equilibrium diagram for a specific element-water-system can be established. It is important to observe that such diagrams are valid only for the combinations of solution species and solid phase considered in their construction and can not be extrapolated beyond these bounds.

3 TIN

For tin the following substances have been considered:

$Sn(s)$, $Sn(OH)_2(s)$, $Sn(OH)_4(s)$, Sn^{2+}, Sn^{4+} and SnO_3^{2-}

and the following reactions and equations are the most important when establishing the Eh-pH-diagram for tin (Figure 3-3) /15/:

Sn^{2+}	$= Sn^{4+} + 2e^-$	$E_o=0.151+0.0295 \log (Sn^{4+})/(Sn^{2+})$
$Sn + 2\ H_2O$	$= Sn(OH)_2+2H^++2e^-$	$E_o = -0.091 - 0.0591\ pH$
$Sn(OH)_2+2H_2O$	$= Sn(OH)_4+2H^++2e^-$	$E_o = 0.075 - 0.0591\ pH$
$Sn^{2+} + 2\ H_2O$	$= Sn(OH)_2 + 2H^+$	$\log (Sn^{2+}) = 1.50 - 2\ pH$
$Sn^{4+} + 4\ H_2O$	$= Sn(OH)_4 + 4H^+$	$\log (Sn^{4+}) = -1.02 - 4\ pH$
$Sn(OH)_4$	$= SnO_3^{2-}+2H^++H_2O$	$\log (SnO_3^{2-}) = 24.50 + 2\ pH$
Sn	$= Sn^{2+} + 2e^-$	$E_o = -0.136 + 0.0295 \log (Sn^{2+})$
$Sn^{2+} + 4\ H_2O$	$= Sn(OH)_4+4H^++2e^-$	$E_o=0.120-0.1182\ pH-0.0295 \log(Sn^{2+})$
$Sn(OH)_2+H_2O$	$= SnO_3^{2-}+4H^++2e^-$	$E_o=0.791-0.1182pH-0.0295\log(SnO_3^{2-})$

4 TECHNETIUM

The following substances have been considered:

$Tc(s)$, $TcO_2(s)$, Tc^{2+} and TcO_4^-

and the following reactions and equations are the most important when establishing the Eh-pH-diagram for technetium (Figure 3-4) /15/:

Tc	$= Tc^{2+}+2e^-$	$E_o = 0.400 + 0.0295 \log (Tc^{2+})$
$Tc^{2+}+2H_2O$	$=TcO_2+4H^++2e^-$	$E_o = 0.144-0.1182\ pH-0.0295 \log (Tc^{2+})$
TcO_2+2H_2O	$=TcO_4^-+4H^++3e^-$	$E_o = 0.738-0.0788\ pH+0.0197 \log (TcO_4^-)$
$Tc+2H_2O$	$=TcO_2+4H^++4e^-$	$E_o = 0.272 - 0.0591\ pH$

5 PALLADIUM

The following substances have been considered:

Pd(s), PdO(s), Pd^{2+}, Pd_2H(s)

and the following reactions and equations are the most important when establishing the Eh-pH-diagram for palladium (Figure 3-5) /15/:

$Pd_2H = 2\,Pd + H^+ + e^-$	$E_o = 0.048 - 0.591\ pH$
$Pd + H_2O = PdO + 2H^+ + 2e^-$	$E_o = 0.897 - 0.0591\ pH$
$Pd^{2+} + H_2O = PdO + 2H^+$	$\log (Pd^{2+}) = -2.35 - 2\ pH$
$Pd = Pd^{2+} + 2e^-$	$E_o = 0.987 + 0.0295 \log (Pd^{2+})$

6 SELENIUM

The following substances have been considered:

Se(s), H_2Se, HSe^-, Se^{2-}, H_2SeO_3, $HSeO_3^-$ and SeO_3^{2-}

and the following reactions and equations are the most important when establishing the Eh-pH-diagram for selenium (Figure 3-6) /15/:.

$H_2Se = HSe^- + H^+$	$\log (HSe^-)/(H_2Se) = -3.74 + pH$
$HSe^- = Se^{2-} + H^+$	$\log (Se^{2-})/(HSe^-) = -14.01 + pH$
$H_2Se = Se + 2H^+ + 2e^-$	$E_o = -0.399 - 0.0591\ pH - 0.0295 \log (H_2Se)$
$HSe^- = Se + H^+ + 2e^-$	$E_o = -0.51 - 0.0295\ pH - 0.0295 \log (HSe^-)$
$Se^{2-} = Se + 2e^-$	$E_o = -0.924 - 0.0295 \log (Se^{2-})$
$Se+3H_2O=H_2SeO_3+4H^++4e^-$	$E_o = 0.741-0.0591\ pH+0.0148 \log (H_2SeO_3)$
$Se+3H_2O=HSeO_3^-+5H^++4e^-$	$E_o = 0.788-0.0739\ pH+0.0148 \log (HSeO_3^-)$
$Se+3H_2O=SeO_3^{2-}+6H^++4e^-$	$E_o = 0.875-0.0866\ pH+0.0148 \log (SeO_3^{2-})$
$Se^{2-}+3H_2O=SeO_3^{2-}+6H^+6e^-$	$E_o=0.276-0.0591\ pH+0.0098\log(SeO_3^{2-})/(Se^{2-})$

7 ZIRCONIUM

The following substances have been considered:

$Zr(s)$, $Zr(OH)_4(s)$, ZrO^{2+}, $HZrO_3^-$

and the following reactions and equations are the most important when establishing the Eh-pH-diagram for zirconium (Figure 3-7) /15/:

$Zr + 4\ H_2O = Zr(OH)_4 + 4H^+ + 4e^-$	$E_o = -1.456 - 0.0591\ pH$
$Zr + H_2O = ZrO^{2+} + 2H^+ + 4e^-$	$E_o = -1.570 - 0.0295pH + 0.0148\log(ZrO^{2+})$
$ZrO^{2+} + 3H_2O = Zr(OH)_4 + 2H^+$	$\log(ZrO^{2+}) = 7.7 - 2pH$
$Zr(OH)_4 = HZrO_3^- + H^+ + H_2O$	$\log(HZrO_3^-) = -12.25 + pH$
$Zr + 3H_2O = HZrO^- + 5H^+ + 4e^-$	$E_o = -1.276 - 0.074pH + 0.0148\log(HZrO_3^-)$
$ZrO^{2+} + 2\ H_2O = HZrO_3^- + 3H^+$	$\log(HZrO_2^-)/(ZrO^{2+}) = -19.95 + 3\ pH$

8 NICKEL

The following substances have been considered:

$Ni(s)$, $Ni(OH)_2(s)$, Ni^{2+}, $Ni(OH)_3^-$

and the following reactions and equations are the most important when establishing the Eh-pH-diagram for nickel (Figure 3-8) /15/:

$Ni + 2H_2O = Ni(OH)_2 + 2H^+ + 2e^-$	$E_o = 0.116 - 0.0591\ pH$
$Ni = Ni^{2+} + 2e^-$	$E_o = -0.250 + 0.0295\ \log(Ni^{2+})$
$Ni + 3H_2O = Ni(OH)_3^- + 3H^+ + 2e^-$	$E_o = 0.648 - 0.886pH + 0.0295\log(Ni(OH)_3^-)$
$Ni^{2+} + 2H_2O = Ni(OH)_2 + 2H^+$	$\log(Ni^{2+}) = 12.41 - 2\ pH$
$Ni(OH)_2 + H_2O = Ni(OH)_3^- + H^+$	$\log(Ni(OH)_3^-) = -17.99 + pH$
$Ni^{2+} + 3\ H_2O = Ni(OH)_3^- + 3H^+$	$\log(NiOH_3^-)/(Ni^{2+}) = -30.40 + 3\ pH$